NACA TN 4143 10480

TECH LIBRARY KAFB, NM
0067046

NATIONAL ADVISORY COMMITTEE FOR AERONAUTICS

TECHNICAL NOTE 4143

DEVELOPMENT OF A PISTON-COMPRESSOR TYPE LIGHT-GAS GUN FOR THE LAUNCHING OF FREE-FLIGHT MODELS AT HIGH VELOCITY

By A. C. Charters, B. Pat Denardo,
and Vernon J. Rossow

Ames Aeronautical Laboratory
Moffett Field, Calif.

Washington
November 1957

AFMDC
TECHN

TECH LIBRARY KAFB, NM

0067046

TABLE OF CONTENTS

	Page
SUMMARY	1
INTRODUCTION	1
SYMBOLS	6
DESCRIPTION OF GUN	9
Basic Elements of Light-Gas-Gun Operation	9
Construction Details of the Light-Gas Gun	13
Optimum Design Considerations	16
ANALYSIS	16
Basic Considerations	16
Launching Cycle	20
Pumping Cycle	24
Performance Charts	34
FIRING TRIALS	35
Calibrations	35
Experimental Apparatus and Measurements	37
Chronological Account of the Firings	40
Summary of Results	46
CONCLUDING REMARKS	47
APPENDIX A: EFFECTS OF AIR RESISTANCE AND BORE FRICTION	48
APPENDIX B: MODIFICATIONS TO PERFORMANCE CHARTS	49
Effect of Chamberage on Launching Cycle	49
Effect of Pump Pressure Override	52
APPENDIX C: COMPUTATIONAL PROCEDURE FOR PERFORMANCE OF PISTON-COMPRESSOR TYPE LIGHT-GAS GUN	58
REFERENCES	62
TABLE I	64
TABLE II	65
FIGURES 1 THROUGH 29	67

NATIONAL ADVISORY COMMITTEE FOR AERONAUTICS

TECHNICAL NOTE 4143

DEVELOPMENT OF A PISTON-COMPRESSOR TYPE LIGHT-GAS GUN FOR THE LAUNCHING OF FREE-FLIGHT MODELS AT HIGH VELOCITY[1]

By A. C. Charters, B. Pat Denardo,
and Vernon J. Rossow

SUMMARY

Recent interest in long-range missiles has stimulated a search for new experimental techniques which can reproduce in the laboratory the high temperatures and Mach numbers associated with the missiles' flight. One promising possibility lies in free-flight testing of laboratory models which are flown at the full velocity of the missile. In this type of test, temperatures are approximated and aerodynamic heating of the model is representative of that experienced by the missile in high-velocity flight.

A prime requirement of the free-flight test technique is a device which has the capacity for launching models at the velocities desired. In response to this need, a gun firing light models at velocities up to 15,000 feet per second has been developed at the Ames Aeronautical Laboratory. The design of this gun, the analysis of its performance, and the results of the initial firing trials are described in this paper.

The firing trials showed that the measured velocities and pressures agreed well with the predicted values. Also, the erosion of the launch tube was very small for the eleven rounds fired. The performance of the gun suggests that it will be a satisfactory launcher for high-velocity free-flight tests.

INTRODUCTION

With ever-increasing speeds of flight, it is clear that aerodynamic heating will be one of the most difficult problems to solve in the design of a high-speed missile (see refs. 1 and 2). The compression of the air due to the high velocity will raise the temperature of the flow over the missile thousands of degrees and will give rise to correspondingly large rates of heat transfer.

[1]Supersedes NACA RM A55G11 by A. C. Charters, B. Pat Denardo, and Vernon J. Rossow, 1955.

The designer's difficulties are compounded by a lack of knowledge of the aerodynamics of truly high-temperature, high Mach number flows. The extensive body of theory for supersonic flow may not be too much help in the present case because most of this theory is based on the assumption that fluid properties such as viscosity and thermal conductivity are constant or, at the most, change slowly. (See ref. 3.) The temperatures are so high that the phenomenon of dissociation may be of importance and the physical properties of the air may change by orders of magnitude in narrow regions (i.e., in the boundary layer). The theoretical treatment of this type of flow can hardly be considered adequate at present (see refs. 4, 5, and 6). Even such fundamental quantities as the Reynolds number of transition from laminar to turbulent flow in the boundary layer are largely a matter of conjecture.

The means that the designer will have to take to cool the missile may in themselves complicate the aerodynamics of the flow. For example, one method of counteracting the aerodynamic heating is to allow the surface of the missile to melt or sublime during the flight, thereby balancing the heat input with the heat of fusion or vaporization of the surface material. A difficulty may arise in the use of this method because many materials combine with oxygen and may burn instead of melting or subliming. If burning should take place in the boundary layer, the heat of combustion would add to the aerodynamic heating instead of counteracting it. This possibility cannot be predicted with any degree of certainty from the present state of knowledge, and the success or failure of this and other methods of cooling will undoubtedly have to be determined by experiment.

There is clearly a need for experiments carried out under conditions representative of high-speed, high-temperature flight. It will be appreciated that the combination of high temperature with high flow velocities makes it unusually difficult to produce the correct conditions in the laboratory. However, one promising approach is to extend the test range of the class of free-flight test facilities described in references 7 and 8. The method of testing in this class of facility is to launch a model at the desired velocity and allow it to fly freely through a long test chamber. Records of its flight are taken during its passage through the chamber and the aerodynamic quantities of interest are deduced from these records. Ordinarily, most of the records are made external to the model by apparatus placed in the chamber along its trajectory. Despite the fact that the measurements are indirect (drag, for example, being determined from deceleration), these facilities have been successful in obtaining reliable, accurate measurements of many aerodynamic quantities, as can be seen from references 7, 9, and 10. It appears entirely feasible to extend the region of testing in the free-flight test facility to velocities of 10,000 feet per second and above.

In view of the possibilities which are latent in the free-flight test facility, the Ames Laboratory has started a program to develop this facility into a new research tool for experimentation in the aerodynamics of

high-speed flight. One of the prime requirements of the new facility is a launching device capable of launching the model at full flight velocity. If the correct conditions of temperature and air flow are to be produced in the flight tests, it is necessary to fly the model at the same velocity as the full-scale missile, since the high temperature is the result of the high velocity. The results of the experiments must still be interpreted in the light of scaling laws, but the temperature, which is the most difficult quantity to reproduce in the laboratory, will have the right range of values. It is clear that the problem which must be solved at the outset of this initial phase is the method of launching the models at the high velocities required.

The launcher in common use in these facilities is a gun which uses the standard military type of nitrocellulose gun powder. In fact, the gun is normally a military weapon which has been modified to meet the particular demands of model launching. To be of use in the present case, the maximum velocity of the launcher must be as great as the flight speed of missiles having velocities of 20,000 ft/sec or more, since long-range ballistic missiles will re-enter the earth's atmosphere at nearly orbital velocities (26,000 ft/sec or greater), (refs. 1 and 2). This value is more than twice the maximum muzzle velocity that has ever been obtained from a military weapon, even in laboratory tests (around 10,000 ft/sec is the highest recorded muzzle velocity). A study of interior ballistics made by the authors showed that it would be difficult to design a gun giving the required muzzle velocity of 20,000 ft/sec as long as nitrocellulose gun powders were used as the propellant.

Nevertheless, a gun has many attractive features as a launching device. The tube contains the powder gases and there is no heavy rocket motor to jettison at the end of the launching run, as would be the case if a rocket were used to launch the model. The muzzle velocity can be changed easily by changing the amount of propellant used. The length of launching run is relatively short since the acceleration of the model can be made very high (an acceleration of 1,000,000 ft/sec^2 is common in small arms). If some technical modification could be found to increase its maximum velocity by a factor of 2, a gun would serve quite satisfactorily for the purpose at hand.

It is instructive to consider for a moment the causes which limit a gun's velocity. If a gun is reduced to its barest essentials, it consists of a long tube closed at one end. A projectile is located near the closed end and the region between the model and the closed end is filled with gas which is at high pressure (and usually at high temperature) at the start of the firing cycle. The gas expands thereby propelling both the projectile and itself down the tube. This is the physical model upon which LaGrange based his classical interior ballistic calculations.

The energy for the propulsion is stored in the potential energy of the gas. During the firing this energy is converted partly into the kinetic

energy of the projectile and partly into the kinetic energy of the gas itself. The division of energy between projectile and gas depends on the molecular weight of the gas, the weight of the projectile, and the projectile's velocity (or the distance traveled by the projectile, which is directly related to the velocity for a given set of firing conditions).

If the gun is infinite in length and such factors as heat loss to the gun and bore friction are negligible, the projectile will be accelerated by the gas until the pressure at its base is just balanced by the pressure acting against its head. In case the bore is filled with air, the projectile will accelerate until the base pressure equals the pressure behind the shock wave preceding the projectile down the bore. In case the bore is evacuated, the projectile will accelerate until it reaches the velocity of efflux of the gas into a vacuum (the velocity of efflux for a transient, centered expansion is $2a_o/(\gamma-1)$). For example, consider the limiting velocities when the propellant gas consists of the combustion products of nitrocellulose gun powder: If the tube ahead of the model is filled with air, the limiting velocity is about 10,000 ft/sec (see section 9.16 of reference 11, "The Maximum Possible Muzzle Velocity"); if the tube is evacuated, the limiting velocity is about 28,000 ft/sec.

In practice, two factors enter to limit the velocity to less than the theoretical maximum. First, the gun has a finite length so that the travel of the projectile is limited. Second, the gun has a finite strength, so that the maximum pressure and, hence, the potential energy is limited. The point of view taken here is that one is dealing with an actual gun whose physical dimensions are fixed. Should the reader be thinking of some existing gun and hold the opinion that certain modifications are desirable in order to improve its performance, then the modified and improved gun is the gun being considered in the present discussion.

It is evident that the highest velocities for a given gun of limited length and strength will be reached by reducing the weight of the projectile to a minimum and firing at the maximum allowable pressure. The maximum muzzle velocity will now be determined by the division of the kinetic energy between the projectile and the gas. However, since the projectile has been made as light as possible and, therefore, its weight is a fixed quantity, the muzzle velocity is determined solely by the molecular weight of the gas. The lighter the gas, the higher will be the muzzle velocity. If the gun is powered with nitrocellulose powder, the molecular weight of the combustion products will be approximately 28 (nearly that of air), which, of course, is quite heavy compared to the minimum molecular weight of 2 for hydrogen or even 4 for helium. The limit imposed on the muzzle velocity by the molecular weight of 28 for powder gas is borne out by experience. Firings in other laboratories indicate that the practical limit for a gun using nitrocellulose powder is around 10,000 ft/sec even though the bore is evacuated (if the bore is not evacuated, the limit is about 8,000 ft/sec).

One's imagination immediately suggests a solution, if only the chemistry could be brought under our control by some magical formula: Find a solid propellant whose gaseous combustion products have a low molecular weight. With this magical compound the gas will take up a far smaller share of the potential energy and the projectile will be driven to a correspondingly higher velocity. Despite the soundness of the physical basis on which it rests, this particular solution yet awaits the discovery of such a compound.

The idea of increasing a gun's velocity by decreasing the molecular weight of the propellant gases seems so straightforward that it must have been in the minds of interior ballisticians for years. Yet the first practical application known to the authors was made during the recent world war. A group at the New Mexico School of Mines developed a gun based on this principle. Hydrogen was used as the propellant, and the technical problem of bringing the hydrogen to high pressure at the start of the firing cycle was solved by adding a pump unit to the gun proper. The gun thus consisted of two parts: a gun tube proper and a pump tube, the two being placed end to end. The projectile was placed at the juncture of the gun and pump tubes and was held in position by a shear disk which was designed to rupture and release the projectile when the pressure in the hydrogen reached the full value desired at the start of the launching cycle. The hydrogen was injected into the pump tube at low pressure and was pumped to high pressure by the single, rapid stroke of a heavy piston. The piston, in turn, was propelled by the combustion of ordinary nitrocellulose gun powder. In a word, the pumping cycle is the mechanical analog of our magical compound and it served quite well to bring the hydrogen not only to high pressure, but also to high temperature, since the gas was compressed adiabatically in the rapid pumping stroke.

The principle of operation of the hydrogen gun was proved by firing light projectiles at velocities up to 13,000 ft/sec. In fact, it is believed that higher velocities still might have been obtained from the NMSM gun if lighter projectiles had been fired or if the bore had been evacuated, thereby eliminating air resistance ahead of the projectile during firing. Nevertheless, the NMSM gun clearly demonstrated the advantages of a gas of low molecular weight as a propellant.

Encouraged by the success of the NMSM gun, the authors undertook a study of the performance that might be expected from a light-gas gun similar in operation to the NMSM gun but different in design and in dimensions. The study showed that a light-gas gun of practical dimensions should be capable of firing aerodynamic models at velocities of 20,000 ft/sec or more. This result together with the New Mexico tests suggested that the light-gas gun would be a suitable launcher for high-velocity flight testing.

Requirements for a launcher for laboratory use are quite different from those for military service, and it was considered desirable to approach the design of a light-gas gun for use at the Ames Laboratory as an entirely new instrument, starting from the basic principles of operation. Thus, the design was preceded by a careful, thorough-going analysis of all phases of the gun's operation. Also, it was believed that the first gun to be constructed should be as small a unit as practical to work with. In this way, various features of the design could be evaluated by actual test, and modifications could be made easily as the need for them developed. The present light-gas gun can, in this respect, be regarded as a pilot model of a larger free-flight launcher having whatever caliber is desired for tests in an aerodynamics range. On the other hand, its size is large enough so that it can be used for many aerodynamic tests. Thus, in addition to being a pilot model for a larger gun, the present gun is suitable for use as a free-flight launcher for small-scale tests.

The purpose of this report is to describe the light-gas gun developed at the Ames Laboratory. Its design and the analysis of its performance will be presented, and the results of the first firing trials will be discussed. In addition, a few preliminary records will be included showing projectiles in flight at velocities between 10,000 and 15,000 ft/sec.

SYMBOLS

a	speed of sound
$\bar{a}$	$\frac{a}{\alpha_o}$
A_p	cross-sectional area of pump tube
A_v	cross-sectional area of valve tube
b	constant, a function of γ (See eq. (B4).)
c	constant involving geometry of system and masses of pistons (See eq. (39).)
C	constant involving geometry of system and masses of pistons (See eq. (44).)
d	diameter
D,E	constants in equation (B1)
L	length of launch tube

L_p	length of pump tube
m	mass
m_{s_F}	fictitious projectile mass
M	total mass of helium in pump tube
ΔM	mass of helium used in propelling projectile
p	light-gas (helium) pressure
$\bar{p}$	$\frac{p}{p_o}$
P	powder-gas pressure
R	perfect-gas constant
S	cross-sectional area of launching tube
t	time
$\bar{t}$	$\frac{p_o S t}{m_s \alpha_o}$
T	temperature
u	velocity
$\bar{u}$	$\frac{u}{\alpha_o}$
U	volume of powder gas chamber
v	specific volume
V	volume of powder gas at a given time
x	distance from end of pump tube to forward face of pump piston
y	distance traveled by valve piston
z	travel of projectile
$\bar{z}$	$\frac{p_o S z}{m_s \alpha_o^2}$
α_o	$\frac{2a_o}{\gamma-1}$ (See eq. (6).)

β	$\frac{2\gamma}{\gamma-1}$ (See eq. (6).)
γ	ratio of specific heats of light gas
Γ	ratio of specific heats of powder gas
ρ	density
σ	Riemann function (See eqs. (3) and (4).)
$\bar{\sigma}$	$\frac{\sigma}{\sigma_o}$
σ_o	α_o for a calorically and thermally perfect gas

Subscripts

o	conditions in reservoir
1	conditions at start of pump cycle
2	conditions at start of launching cycle
3	conditions at end of launching cycle
c	charge of powder
L	conditions at muzzle of launch tube
m	experimentally measured quantity
p	pump piston or tube
v	valve piston or tube
s	projectile or launch tube
s_{ac}	projectile for conditions with chamberage
s_{sc}	projectile for conditions without chamberage
T	Riemann function in pump tube
2D	design pressure
2R	shear-disk rupture pressure

Superscripts

$(\overline{\ })$ dimensionless quantity - used in equation (7) et seq. (Each dimensionless quantity is defined individually.)

$(\ )^*$ throat conditions

Note: All computations in this report were carried out with the dimensions of the quantities involved reduced to engineering units; that is, lengths in feet, times in seconds, masses in slugs, and forces in pounds. However, in the report itself the values of these quantities may be given in more familiar terms; for example, pressures are usually listed in pounds per square inch rather than in pounds per square foot. In all cases, the units are designated if a numerical value is quoted.

DESCRIPTION OF GUN

Basic Elements of Light-Gas-Gun Operation

The essential elements of the light-gas gun developed at the Ames Laboratory are shown in the sketch below.

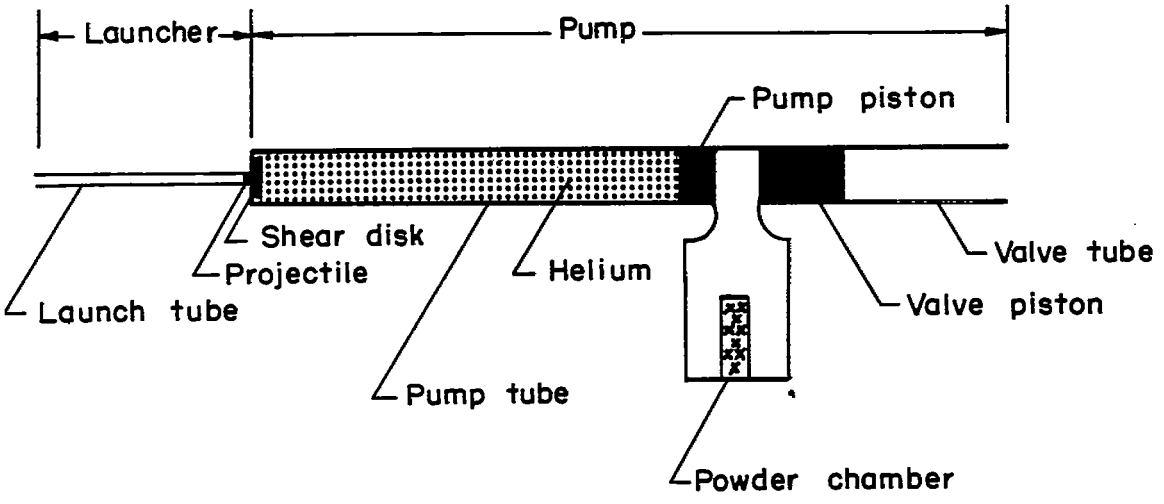

Sketch (a)

It will be recalled that the gun consists of two basic units, a launcher and a pump. If one compares the light-gas gun with a conventional gun, the launcher corresponds to the gun tube and the pump corresponds to the powder chamber. The launcher, in fact, is merely a long gun tube. The pump, on the other hand, is similar in function to the conventional gun's

powder chamber, since it is the unit in which the high-temperature, high-pressure propellant gas is generated.

The projectile is located at the juncture of launcher and pump and is held in position by a shear disk. The thickness of the shear disk is adjusted so that it withstands the pressure of the propellant gases until the pressure desired for launching is reached. At full launching pressure, the shear disk ruptures, releasing the projectile. The propellant gases then pour from the pump into the launcher and drive the projectile through the launch tube and out into flight.

The pump consists of a pump tube, a valve tube, and a powder chamber. The pump and valve tubes are coaxial but face in opposite directions, being placed breech to breech. The powder chamber is located to one side at the juncture of pump and valve tubes, as shown, and the port from the chamber leads into both tubes.

Helium is the light gas used. The use of hydrogen was considered and the performance of the gun was computed for a representative case with hydrogen as the light gas. The relative performance of the two gases depends, of course, not only on the difference of their molecular weights but also on the difference of their ratios of specific heats. It was found that the muzzle velocity with hydrogen was only 5 percent higher than with helium. Since helium is far safer to handle than hydrogen and its use eliminates any danger of explosion from the muzzle blast, helium was chosen in preference to hydrogen.

The helium is injected into the pump tube at relatively low pressure before firing and is compressed during the pumping cycle to the high pressures and temperatures desired for launching the projectile. The actual compression is done by a heavy piston which is driven by the combustion of the gun powder in the powder chamber.

The valve tube serves the function of a valve, as its name implies. It keeps the powder gases contained in the pump during the compression stroke of the pump piston and releases them after the compression stroke is completed. It also provides an avenue of escape for the pump piston, as will be explained in detail later on. Its action is accomplished by the movement of a heavy piston.

The functioning of each part and its relation to the gun as a whole can be seen if one follows through the sequence of events that take place when the gun is fired. The condition of the gun just prior to firing is shown in sketch (a) (above). The projectile-shear-disk unit is in position at the juncture of pump and launcher. Pump and valve pistons are located at the breeches of their respective tubes and are held in place initially by shear disks. The launch tube has been evacuated to minimize air resistance and the pump tube has been filled with helium. The powder chamber is loaded.

The events during firing are illustrated in sketches (b) through (e) (below). In these sketches the arrows indicate roughly the relative velocities of pistons and projectile at various times. The firing starts with the ignition of the powder. The powder burns and the gases drive the pistons in opposite directions. The pump piston compresses the helium, being accelerated by the powder gases in the first part of the compression stroke and decelerated by the increasing helium pressure in the last part. The situation part way through the compression stroke is shown in sketch (b).

Sketch (b)

The pressure in the helium rises steadily during the compression stroke until the full pressure desired for launching is reached. At this pressure, the shear disk ruptures, and the projectile starts its launching run, as shown in sketch (c).

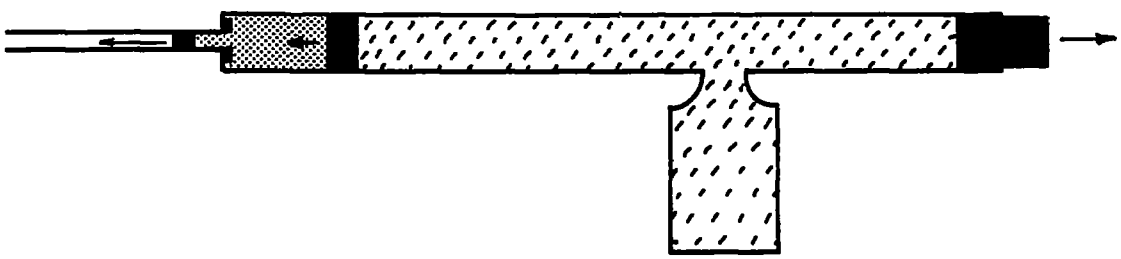

Sketch (c)

The loading conditions are adjusted so that three things take place during the time the projectile traverses the launcher:

1. The pump piston continues to move forward at the mean velocity necessary to hold the pressure of the helium in the pump tube roughly constant at launching pressure.

2. At the instant that the projectile leaves the muzzle of the launcher, the helium pressure brings the pump piston to a stop a short distance from the end of the pump tube.

3. At this same instant the valve piston leaves the end of the valve tube.

The situation at the time that the projectile leaves the launcher muzzle is shown in sketch (d). It is evident that this time marks the start of the projectile's flight and the end of the compression cycle.

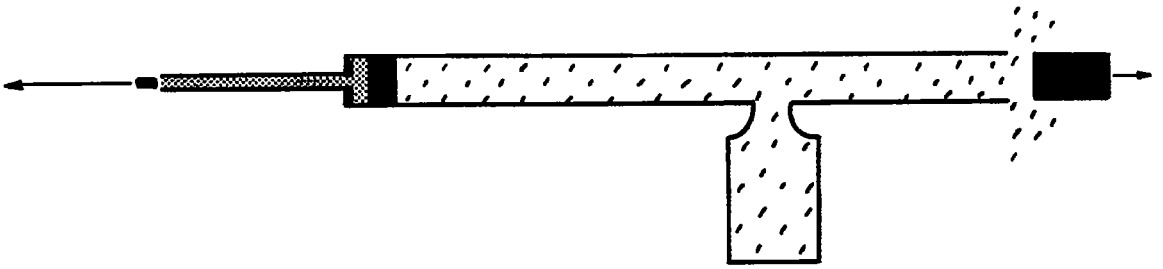

Sketch (d)

At the end of the compression cycle the projectile has been launched and the gun has thus completed its primary task. However, one event has yet to take place before the firing is finished. Sketch (d) shows that there remains a buffer of helium at high pressure between the pump piston and the end of the pump tube; also, the pump unit is filled with powder gas when the compression stroke ends. It is now necessary to dissipate the energy remaining in these two regions of gas, and this action is accomplished by the valve piston leaving the end of the valve tube. The valve tube thus becomes a port through which the powder gases pour out into the room. The pressure in the helium buffer is much greater than in the powder gases and the buffer reverses the direction of the pump piston and drives it back down the pump tube, as shown in sketch (e). Since gas

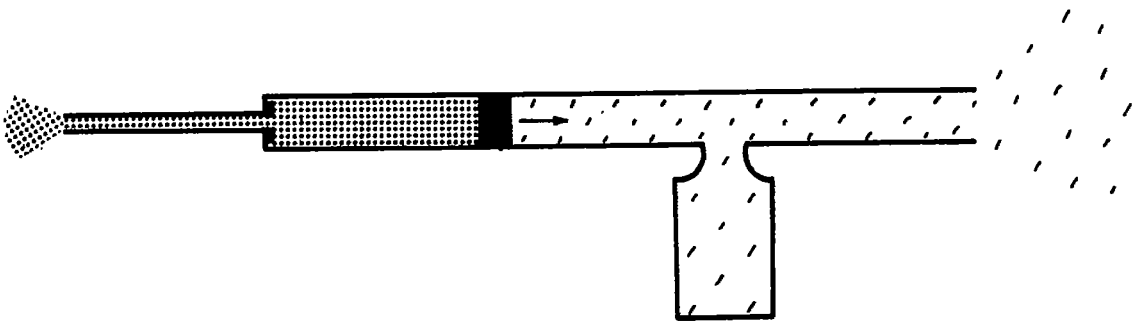

Sketch (e)

pressure only weakly opposes the motion of the pump piston as it returns, it may traverse both pump and valve tubes and leave the gun, thus completing the firing. However, if the pressures in the helium buffer and the powder gases are balanced just right in this last phase of the operating cycle, the pump piston may come to rest in the pump tube instead of being driven out of the gun.

Construction Details of the Light-Gas Gun

A photograph of the light-gas gun is shown in figure 1. The principal components of the gun, the launcher and pump units, are designated in the photograph. The two units are joined together by a coupling, as shown. The entire assembly is mounted on a very rigid steel beam which, in turn, is supported by five stands spaced along its length. Three pieces of auxiliary equipment, a vacuum tank, recoil supports, and a catcher, are also shown in the photograph. All of the components will now be described in detail. For reference purposes a list of all dimensions of the Ames gun and of certain other quantities which have fixed values in the operation of the gun is given in table I.

Figure 2 shows a photograph of the launcher together with a sketch giving the details of its construction. Actually, other units of the gun are shown in figure 2 for the purpose of visual continuity, but these will be described later. The essential element of the launcher is a 0.22-caliber rifle barrel. The launcher was constructed from two rifle barrels coupled end to end and placed inside a 4-inch-diameter tube which alined and supported the two barrels. (Two barrels coupled end to end were used in preference to a single, long barrel because, in this way, the launch tube was made from standard, rifle barrels at far less expense and time than would have been involved in the manufacture of a single, long barrel.) The total length from breech to muzzle is about 4 feet. The barrels were smooth-bored after assembly and thus have a uniform bore of diameter a little less than 1/4 inch.

A sketch of the pump giving the details of its construction is shown in figure 3. The pump consists of three main subunits: the pump tube, the valve tube, and the powder chamber. The pump and valve tubes are constructed from standard smooth-bore, 20-mm test barrels. The pump tube is made from two barrels coupled end to end. (The reason for this type of construction is the same as for the launch tube.) The total length of the pump tube is about 9 feet and of the valve tube about 5 feet. The bore diameter of the pump tube is the standard 20 mm, but the bore of the valve tube has been enlarged slightly. The powder chamber is bored from a 6-inch-diameter steel forging (AISI No. 4340, heat treated to a Rockwell hardness of C38) and its internal dimensions are a diameter of 3 inches and length of 8 inches. The chamber is closed by a breech of special design whose only feature pertinent to the present discussion is that it supports and fires a 37-mm percussion-type primer. The pump tube, valve tube, and powder chamber are coupled by a heavy forging, shown in figure 3 as the T-connector, and the unit is balanced in rotation about the pump-valve tube axis by a counterweight.

The pistons used in the pump and valve tubes are shown in figure 4. Each piston is a right, circular cylinder of metal with the center relieved to insure proper bearing support and to provide a labyrinth seal. An

additional groove is machined in each end section of the pump piston to improve the sealing. The end sections are made of half-hard brass to avoid seizure with the steel bore surface and are machined to a sliding fit with the bore, allowing a diametral clearance of about 0.001 inch. The center section is made of either brass or steel, depending on the pressures involved. A thin flange is machined on the end of the pump piston facing the powder chamber. This flange bears against a sealing ring in the T-connector and serves to seal this end of the pump tube as it is pressurized with helium in preparation for firing (the pressures in the helium run from 100 to 1,000 psi, depending on the firing conditions). It also provides a weak shear disk that the powder pressure must rupture before the pump piston can move, and for this reason a similar flange is machined on the valve piston in order to insure that both pistons start moving at the same instant.

The method of loading the gun powder in the powder chamber deserves a brief mention. Both the pressures and the densities of loading are very low compared to normal gun practice, and it is difficult to produce good ignition and repeatable burning of the powder under these conditions. The scheme used is shown in figure 5. The powder is held around the primer by a cardboard tube taped to the face of the breech. It is thus saturated at once by the fire from the primer, and the entire charge of powder appears to ignite nearly simultaneously. The uniformity of the action of the propellant from round to round is further enhanced by the shot-starts on the pump and valve pistons. Neither piston can move until the powder pressure reaches approximately 2,000 psi and, consequently, any irregularities in the burning of the powder up to this pressure do not affect the action of the propellant in the pumping stroke.

A cross section of the coupling between the pump and launcher units is shown in figure 6. A model, sabot, and shear disk are also shown in position, and the outlines of two of the pressure-gage units are sketched in. The design of the projectile-shear-disk unit shown is the final design developed during the firing trials.

The sabot and shear disk are machined as an integral piece from a rod of nylon; the ring is made of steel. The units used in the first few rounds did not contain the steel ring, and it was found that the disk ruptured along a ragged, roughly conical surface and that pieces of the disk around the hole broke out after the main plug had sheared and were apparently driven down the bore of the launcher close behind the sabot. The steel ring is made a close fit with the disk so that there is little leakage of helium between the two, and the front face of the ring is pressed firmly against the rear face of the disk by the pressure of the helium. The disk is thus squeezed between opposing faces of ring and launch tube and ruptures cleanly along a cylindrical surface joining the hole in the ring with the bore of the launch tube.

In the design just described the sabot is formed in part from the cylindrical plug sheared out of the disk. Since the plug is bore diameter, it assists in supporting and guiding the model during the launching. In fact, the sabot of high-velocity rounds consists almost entirely of this plug from the shear disk.

The type of seals which are in evidence in the coupling cross section (fig. 6) deserve to be mentioned in passing. The light-gas gun is a composite structure made of many parts and the joints between these parts must be sealed in order to contain the gases in the interior of the gun. Certain of the seals must withstand very high pressures (of the order of 100,000 psi) and all must seal very tightly. Even a small amount of leakage makes the operation quite uncertain. Acting on the advice of the Naval Ordnance Laboratory,[2] the authors found that the synthetic rubber O-ring in common industrial use fulfilled the sealing requirements of the light-gas gun exceptionally well. Synthetic rubber O-rings are designed for pressures up to a few thousand pounds per square inch; but, if the clearances between mating parts are kept to the order of 0.001 inch or less and the O-ring grooves are made to close tolerances, the O-rings will seal against the transient pressures acting in the coupling as high as 100,000 psi and possibly higher.[3]

The pieces of auxiliary equipment shown in figure 1 are a vacuum tank, recoil supports, and a catcher. The vacuum tank is attached to the muzzle of the launch tube by a sliding, vacuum-tight seal. Its function is to collect and contain the helium as it pours out of the launch tube behind the projectile and thereby to protect the instrumentation along the trajectory from the blast and flash of the propellant gas. It also acts as a ballast in the vacuum system.

The recoil supports take up the axial loads which occur during the firing. They are rigid members running from the T-connector to the walls of the range and transmit the stresses in the gun directly into the building structure. The gun is held rigidly in place and not allowed to recoil during firing, so the term "recoil support" is perhaps a misnomer, although these members replace the usual recoil system.

The catcher serves to stop and hold the valve and pump pistons after they leave the valve tube. It is composed of a heavy steel box with a port

---

[2]The authors are indebted to the staff of the Hyperballistics Division of the Aeroballistics Research Department, U. S. Naval Ordnance Laboratory, and particularly to Mr. B. M. Shepard of this division, for their assistance in the design of O-ring seals.

[3]Some of the O-rings may extrude a little into the joints and have to be replaced each round. Since O-rings are relatively inexpensive, it is standard practice to replace all seals that might have been damaged in firing.

facing the valve tube. The front part of the box (the end facing the port) is filled with sand or slabs of fiberboard and the rear part contains a heavy slab of reinforced concrete. The pistons are actually stopped by the concrete block, and the sand (or fiberboard) serves primarily to prevent the pistons or fragments of concrete from ricocheting back out through the port. Consequently, both pistons are expended on each round. However, they are simple in design and inexpensive to build and their loss is unimportant.

Optimum Design Considerations

It may be appropriate to conclude this section by remarking that the gun described in this report does not in any way represent the optimum design of light-gas gun. In fact, it is not clear at the present time just how to derive firm engineering criteria for the design of the optimum light-gas gun. If the length of the pump tube is increased, the compression ratio is increased for a specified pressure at the end of the compression stroke. As a result, the density of the gas will be less, the gas will require a smaller share of the potential energy for its acceleration, and the muzzle velocity of the projectile will be increased. Similarly, if the length of the launch tube is increased, the projectile will be accelerated by the gas for a longer length of time, and the muzzle velocity will be increased. Of course, these changes will be counteracted in due course by effects such as friction between the projectile and the bore of the launch tube or the loss of heat from the gas to the pump and launch tubes. At best, it is believed that the dimensions chosen for the Ames gun are still far from the balance point. The lengths of launch and pump tubes, the volume of the powder chamber, and other dimensions were chosen because previous experience indicated that they were reasonable. The results of the firing trials have shown that the choices made have, in fact, produced a workable unit.

ANALYSIS

Basic Considerations

Let us start the analysis by considering certain basic factors which control the functioning of the gun. The purpose of the gun is to impart the highest possible muzzle velocity to the projectile. Since the projectile is accelerated by the helium pressure on its base, the gun should be designed to function so that the helium pressure at the projectile's base is maintained at the highest possible value throughout the launching cycle. At the start of the launching run, the requirement of maximum base pressure is quite simple: The helium pressure in the pump tube should be as high as

the strength of the gun will allow. During the launching run, however, the requirement of maximum base pressure becomes more complex and it is necessary to examine in some detail the conditions of gas flow from pump tube to projectile base.

As the projectile traverses the launch tube, the helium pressure at its base diminishes because a pressure drop is required to accelerate the helium from very low velocity in the pump tube to the velocity of the projectile at its base in the launch tube. This pressure drop is proportional to the kinetic energy which must be imparted to the helium as it accelerates, and, consequently, the drop is minimized by keeping the density of the helium to a minimum. The point of view taken here is that the dimensions of the gun are fixed initially. Hence, it is clear that the density of the helium will be a minimum at all times only if the amount of helium loaded initially into the pump tube is kept to the bare minimum required to launch the projectile.

The total amount of helium required for launching is determined by the pressure in the pump tube during the launching cycle. At the start the pressure is fixed by the maximum value allowed by the gun. During the first part of the cycle the pressure should be held at this maximum value since a decrease in pump tube pressure causes a corresponding decrease in base pressure while the projectile's velocity is still low. However, as the projectile travels along the launch tube and its velocity increases, an interval of time is required for an expansion wave caused by a decrease in pump tube pressure to reach the projectile's base and this time increases steadily the further the projectile travels. A certain time is finally reached beyond which a decrease in pump tube pressure cannot be transmitted to the projectile before it arrives at the muzzle and completes its launching run. The two requirements of (1) keeping the total amount of helium to a minimum and (2) holding the pump tube pressure at maximum during the first part of the launching cycle necessitate a careful adjustment of the loading conditions in order to obtain the best possible performance from the gun.

An approach to the optimum rather than a design for the optimum itself was considered satisfactory for the first firing trials and an arbitrary choice was made between the two requirements stated above. It was decided to adjust the loading conditions so that the pressure in the pump tube would be held at the full maximum value during the entire launching cycle. This interval of time is undoubtedly longer than necessary for optimum performance, but it insures that there will be an adequate supply of helium to propel the projectile; also, the choice of this particular interval greatly simplifies the analysis of the gun's operation.

The question immediately arises: Is it possible to design the pumping stroke so that the pressure in the pump tube will remain constant during the launching cycle, as desired? The answer is that it is possible to do so only approximately. A certain amount of helium will flow out of the

pump tube into the launch tube during the launching cycle. Now, if the mass and velocity of the pump piston are adjusted so that it will move just the distance required to make up for the loss of helium, then the pressure in the pump tube at the end of the launching cycle will be the same as at the start. Since the end points are the same, it seems reasonable to assume that the variation in the pressure over this interval will also be small. Unfortunately, the very physical nature of the process makes it difficult to keep the pressure constant over the entire interval. At the start of the launching cycle, the velocity of the pump piston is high while the velocity at which the helium flows out of the pump tube is low. At the end of the launching cycle, the state of affairs is just reversed; the velocity of the pump piston is low and the flow velocity of the helium is high. Consequently, the pressure rises too high at the start of the launching cycle and falls too low at its end. In practice, the velocity and mass of the pump piston are adjusted so that the pressure remains roughly constant during the first part of the launching cycle. The fall-off in pressure toward the end of the cycle actually causes very little loss in muzzle velocity.

The first part of the launching cycle is the important part insofar as the muzzle velocity is concerned, and, since it is possible to hold the pressure approximately constant over this part, the analysis will be based on the assumption of constant pressure in the pump tube throughout the launching cycle. In concert with the assumption of constant pressure it will also be assumed that the velocity of flow of helium out of the pump tube is also constant during the launching cycle. This second assumption is a very rough approximation indeed to the actual physical situation, and the results of the analysis are somewhat in error as a consequence. Fortunately, it is possible to use the results of the analysis in such a manner that the errors introduced by these assumptions are compensated for to a large extent. The over-all result is that the measured performance is found to agree satisfactorily with that predicted.

The first two assumptions on which the analysis is based may be summarized as follows:

1. The pressure in the pump tube is constant during the launching cycle.

2. The velocity of the helium flowing out of the pump tube into the launch tube springs immediately to the local speed of sound at the entrance of the launch tube and remains at this value throughout the launching cycle.

The physical model underlying the flow of helium from pump to launch tube is assumed to consist of a sequence of two events: (1) The projectile accelerates to the sonic velocity of the helium in a negligibly short time; (2) the helium flows into the launch tube starting immediately at the

steady-state value, the local velocity of sound, and continues to flow into the entrance of the launch tube at this value throughout the launching cycle.

The assumption of steady-state sonic flow into the entrance of the launch tube effectively separates the pumping cycle from the launching cycle, just as the sonic flow in the throat of a wind tunnel prevents conditions in the supersonic flow downstream of the throat from affecting the subsonic flow upstream. This situation is a marked simplification over the normal interior ballistic problem in which the volume opened up by the movement of the projectile has a strong influence over the pressure-time history. The only connection between launching and pumping cycles is through the time t_L that the pump is called upon to supply flow to the launcher, and in practice the two cycles may be analyzed independently.

Three other assumptions are made in analyzing the flow of gases in both pumping and launching cycles:

3. The equations of state involved are assumed to be those of perfect gases.

4. All thermodynamic processes are assumed to take place adiabatically and isentropically.

5. The pressures of the powder gas and of the helium are assumed to be constant throughout their respective volumes at any instant of time, although these pressures may vary with time (i.e., P and p are functions of t only).

Undoubtedly, these conditions only approximate the true physical processes taking place. The covolume of the helium has been neglected in the equation of state. Shock waves set up in the compression stroke, heat loss to the pump and launch tubes, and skin friction of the helium flow are all ignored. On the other hand, the temperature of the helium increases along with its density as it is compressed, so the covolume effects may not be too serious; the velocities involved in the compression are low compared to the speed of sound in the helium (and in the powder gas, which drives the pump piston); studies made in references 12, 13, and 14 suggest that the losses involved in heat transfer to the tubes and in skin friction are negligible compared to the primary changes of energy taking place in the very short times of the pumping and launching cycles. It is believed that these assumptions are consistent with the level of engineering approximation expected from the complete analysis.

Two further approximations of importance are made:

6. The friction between the projectile and the launch tube is neglected.

7. The launch tube is assumed to be evacuated ahead of the projectile.

The bore friction in many guns significantly decreases the muzzle velocity. However, nylon is used as the sabot material in the gun developed at Ames and its bore friction is so small, based on other tests at this laboratory, that the retardation accumulated over the 4-foot length of launch tube is believed to be very small. The resistance of the air ahead of the projectile is an important factor in many guns, and the present gun is no exception in this regard. The acceleration of the projectile is so rapid that a shock wave forms in the air in the bore shortly ahead of the projectile and creates a back pressure which opposes the driving pressure of the propellant gases. In practice the problem is avoided by evacuating the launch tube and hence eliminating the air resistance. The effects of bore friction and air resistance are discussed further in Appendix A.

Launching Cycle

In starting the analysis of the launching cycle, one should recall the first assumption of the preceding section; namely, that the motion of the pump piston is adjusted to hold the pressure of the helium in the pump tube approximately constant during the launching cycle. The pump tube is related to the launch tube as the chamber of a conventional gun is related to the bore of the gun tube, and the maintenance of constant pressure corresponds to the chamber having infinite cross-sectional area and volume. Consequently, the analysis of the launching cycle is, in essence, the analysis of the flow of gas in a gun with an infinite chamber.

The interior ballistics of the infinite-chamber gun have been studied in detail. A method of computation has been worked out based on the well-known method of characteristics (see ref. 15), and excellent agreement has been obtained with experiment. However, the method requires rather lengthy numerical calculations, and a simpler formulation of the ballistics was sought. The problem was discussed with ballisticians[4] at the U. S. Naval Ordnance Laboratory and they suggested that the analysis be based on the ballistics of a gun having a chamber of bore diameter and infinite length, rather than infinite diameter and infinite volume. The muzzle velocities thus obtained can be corrected to the true conditions of "chamberage"[5] through multiplication by a constant factor.

---

[4]The authors are indebted to the staff of the Hyperballistics Division of the Aeroballistics Research Department, and in particular to Dr. A. E. Seigel of this division, for their assistance in this phase of the analysis.

[5]"Chamberage" is a ballistic term and ordinarily refers to the reduction in area from the chamber to the bore of the gun. If the chamber has the same diameter as the bore, the gun is said to have no chamberage.

In accordance with the NOL suggestion, the analysis of the launching cycle is carried out with the pump tube replaced by an infinitely long tube having the same bore diameter as the launch tube. The helium in this tube is assumed to have the same pressure, density, and temperature at the start of the launching cycle as in the pump tube (i.e., p_2, ρ_2, and T_2). The situation is portrayed in the following sketch. The modifications of

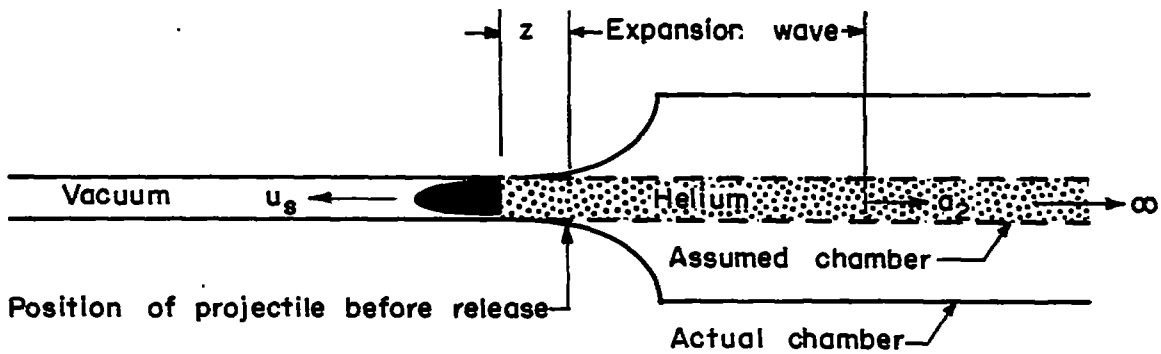

Sketch (f)

the analysis which are needed to account for the effects of chamberage are discussed in Appendix B.

The launching cycle starts with the shear disk rupturing and releasing the projectile. The chamber behind the projectile is assumed to be filled with helium at rest at pressure p_2, density ρ_2, and speed of sound a_2. The bore ahead of the projectile is evacuated. The projectile is accelerated by the pressure[6] at its base, p_s, and starts to move. As it moves with ever increasing velocity, it sends out expansion waves into the helium which decrease the pressure at its base. The trade of pressure for velocity is determined by the acoustic impedance ρa, that is

$$dp = - \rho a \, du \tag{1}$$

For the particular circumstances assumed to exist here, the pressure at the projectile's base is always related to the projectile's velocity by the following equation (see refs. 12 through 15):

$$u_s + \sigma_s = \sigma_o \tag{2}$$

where σ is the Riemann function, defined by

[6]The subscript s designates conditions at the base of the projectile. The letter is derived from the British term for projectile, "shot," and is used to avoid confusion with the subscript p which designates conditions in the pump tube.

$$\sigma = \left(\int_0^p \frac{dp}{\rho a}\right)_{\text{entropy=constant}} \tag{3}$$

Since the entire flow is isentropic, σ is given by

$$\sigma = \frac{2}{\gamma - 1} a \tag{4}$$

and the pressure ratio p/p_o is given by the Riemann function ratio σ/σ_o as follows:

$$\frac{p}{p_o} = \left(\frac{\sigma}{\sigma_o}\right)^{\frac{2\gamma}{\gamma-1}} \tag{5}$$

If two new symbols are introduced, as defined by the following equations

$$\left.\begin{aligned} \alpha_o &= \frac{2}{\gamma - 1} a_o \\ \beta &= \frac{2\gamma}{\gamma - 1} \end{aligned}\right\} \tag{6}$$

and dimensionless notation[7] is introduced, as defined in the list of symbols, with the dimensionless quantity denoted by a bar over the quantity, equation (2) becomes

$$\bar{u}_s + \bar{\sigma}_s = 1 \tag{7}$$

and equation (5) becomes

$$\bar{p}_s = \bar{\sigma}_s{}^{\beta} \tag{8}$$

where the initial conditions are given by

[7]The notation for dimensionless quantities used herein is similar to that in reference 14.

$$\left.\begin{array}{lll} p_{s_o} = p_o = p_2 & a_{s_o} = a_o = a_2 & \sigma_{s_o} = \alpha_o \\ \bar{t}_o = \bar{z}_o = \bar{u}_{s_o} = 0 & \bar{p}_{s_o} = \bar{\sigma}_{s_o} = 1 & \end{array}\right\} \tag{9}$$

and hence the limits of $\bar{u}_s$ and $\bar{p}_s$ are

$$0 \leq \bar{u}_s \leq 1 \qquad\qquad 1 \geqq \bar{p}_s \geqq 0$$

It should be noted that the differential equations defining the dimensionless and dimensional velocities are the same; namely,

$$\bar{u}_s = \frac{d\bar{z}}{d\bar{t}} \tag{10}$$

The acceleration of the projectile is related to the pressure acting on its base by

$$\frac{d\bar{u}_s}{d\bar{t}} = \bar{p}_s \tag{11}$$

If equations (7) and (8) are substituted into equation (11) and the resulting equation is integrated, one obtains the following equation for distance and velocity

$$\bar{z} = \frac{\gamma - 1}{2}\left\{\left[\frac{\frac{2}{\gamma + 1} - (1 - \bar{u}_s)}{(1 - \bar{u}_s)^{\frac{\gamma+1}{\gamma-1}}}\right] + \frac{\gamma - 1}{\gamma + 1}\right\} \tag{12}$$

the following equation for velocity and time

$$\bar{u}_s = 1 - \left(1 + \frac{\gamma + 1}{\gamma - 1}\,\bar{t}\right)^{-\frac{\gamma-1}{\gamma+1}} \tag{13}$$

and the following equation for distance and time

$$\bar{z} = \frac{\gamma - 1}{2}\left[1 + \frac{2}{\gamma - 1}\bar{t} - \left(1 + \frac{\gamma + 1}{\gamma - 1}\bar{t}\right)^{\frac{2}{\gamma+1}}\right] \tag{14}$$

The muzzle velocity, $\bar{u}_{s_L}$, is given by equation (12) and the time of traverse of the launch tube, t_L, by equation (14) with $\bar{z}$ set equal to its value at the muzzle, that is with $\bar{z} = \bar{z}_L = p_oSL/m_s\alpha_o^2$. Graphs of $\bar{u}(\bar{z})$ from equation (12) and of $\bar{t}(\bar{z})$ from equation (14) are shown in figures 7 and 8. These graphs are the interior ballistic charts and will be referred to as such in the remainder of the analysis.

Pumping Cycle

Two requirements have already been imposed on the pumping cycle, namely (reference is made to sketch (g) below),

(1) The helium must be compressed to a specified pressure, p_2.

(2) The pump piston must move the correct distance $(x_2 - x_3)$, to maintain a constant pump-tube pressure, p_2, during the time of the launching cycle, t_L.

Two additional requirements will now be imposed on the pumping cycle, namely,

(3) The pump piston shall complete its compression stroke and shall come to rest at position x_3 just as the projectile leaves the muzzle at time t_L.

(4) A buffer of gas of prescribed length, x_3, shall remain in the pump tube at the end of the compression stroke.

Condition (3) insures that the kinetic energy of the pump piston is completely used up in compressing the helium and that the piston has no forward motion after it has done its work of maintaining the pump pressure constant during the launching cycle. After the compression stroke is completed, the piston is driven back down the pump tube and out of the valve tube by the buffer of helium. Condition (4) is purely a safety factor to protect the breech of the launch tube from being rammed by the pump piston before it is completely stopped by the helium pressure. It is the design feature included to account for the approximations of the analysis and the faults of the operation. In the initial firing trials, x_3 was arbitrarily given the value of 0.2 foot. However, it should be noted that the buffer of gas increases the initial load of helium and hence falls into the category of a necessary evil. As the gun is used and its actual performance becomes better known, the length of the buffer should be reduced accordingly.

The following sketch portrays the sequence of events taking place during the pumping cycle. Position 1 marks the start of the pumping

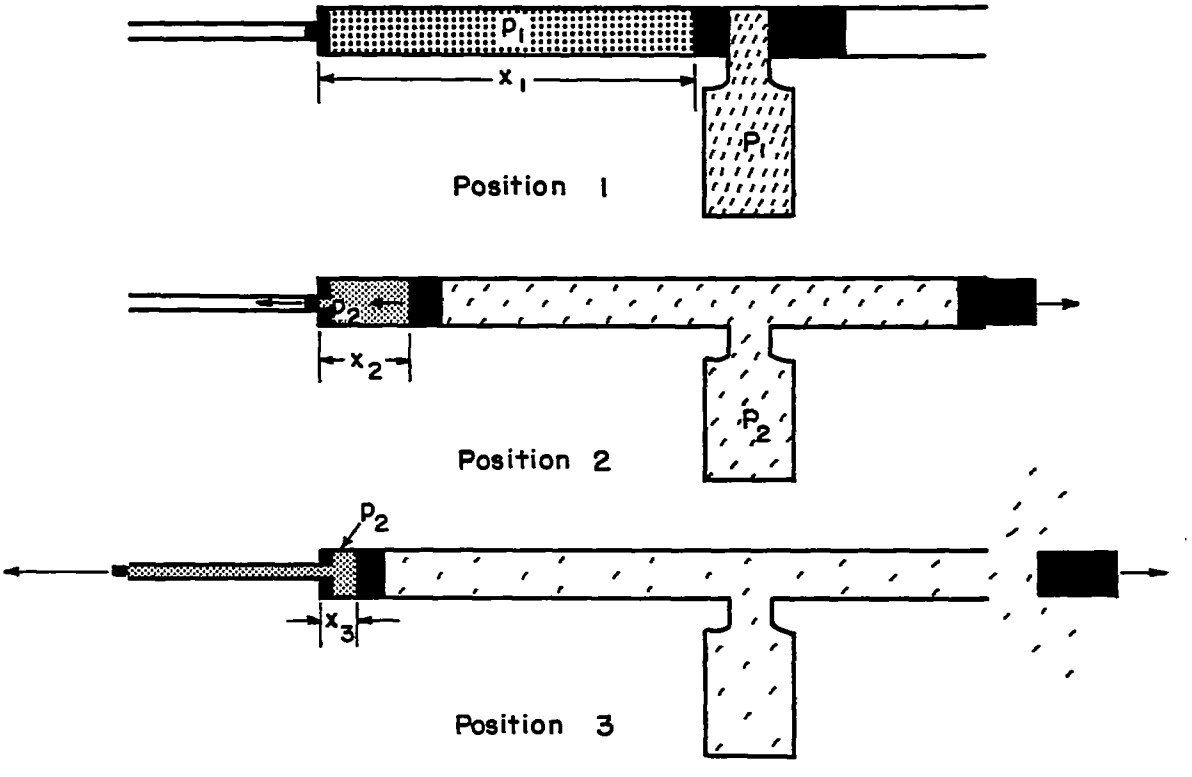

Sketch (g)

cycle. Position 2 marks the start of the launching cycle; that is, the position of the pump piston when the helium pressure has just reached the design value, p_2, and the shear disk has just ruptured releasing the projectile. Position 3 marks the end of both pumping and launching cycles; that is, the stop position of the piston at the end of the compression stroke and the time when the projectile leaves the launch tube.

The requirements imposed on the pumping cycle determine the loading conditions of the gun. By the loading conditions one means the shear-disk thickness, the initial helium pressure, the pump piston mass, and the powder charge. These conditions are uniquely determined by the mass of the projectile and the launch velocity desired (it is assumed that the dimensions of the gun are fixed).

The over-all purpose of the analysis is to enable one to compute the loading conditions which are necessary for the gun to function as required and to launch a projectile of a given mass at a given velocity. The analysis of the launching cycle has already produced the interior ballistic charts (see figs. 7 and 8) and these charts enable one to compute the launching pressure of the helium at the end of the compression stroke, p_2, and the time taken by the launching run, t_L, from the projectile mass, m_s, and the desired muzzle velocity, u_{s_L}. However, this computation requires a value for the speed of sound, a_2, in the helium in the pump tube during the launching cycle. Now the quantity, a_2, is determined from the requirements of both launching and pumping cycles taken together. Clearly, the first step to take in the analysis of the pumping cycle is to determine a_2.

The mass of the helium loaded initially into the pump tube is the quantity connecting the pumping and launching cycles, since this mass must be sufficient to supply the flow into the launcher during the launching cycle and to provide a buffer remaining in the pump tube at the end of the compression stroke. The mass of helium flowing into the launch tube during the launching cycle is given by

$$\Delta M = a^*\rho^* S t_L \tag{15}$$

The mass of helium to be delivered by the pump tube, assuming that p_2 and ρ_2 are constant, is given by

$$\Delta M = A_p \rho_2 (x_2 - x_3) \tag{16}$$

Equating the two masses and relating quantities in the entrance of the launch tube to quantities in the pump tube gives

$$A_p \rho_2 (x_2 - x_3) = a_2 \rho_2 S t_L \frac{a^*}{a_2} \frac{\rho^*}{\rho_2} \tag{17}$$

Consequently, the position of the pump piston at the start of the launching cycle, x_2, is given by

$$x_2 = x_3 + a_2 t_L \frac{S}{A_p} \frac{a^*}{a_2} \frac{\rho^*}{\rho_2} \tag{18}$$

Now, the ratios a^*/a_2 and ρ^*/ρ_2 are functions of the γ of helium, since isentropic flow is assumed, according to

$$\frac{a^*}{a_2} = \left(\frac{2}{\gamma + 1}\right)^{\frac{1}{2}} \tag{19}$$

$$\frac{\rho^*}{\rho_2} = \left(\frac{2}{\gamma + 1}\right)^{\frac{1}{\gamma-1}} \tag{20}$$

If equations (19) and (20) are substituted into equation (18), the formula for x_2 becomes

$$x_2 = x_3 + a_2 t_L \frac{S}{A_p}\left(\frac{2}{\gamma + 1}\right)^{\frac{\gamma+1}{2(\gamma-1)}} \tag{21}$$

The compression ratio, x_2/x_1, is determined by equation (21) once the initial conditions and a_2 are specified. On the other hand, a_2 is determined by the compression ratio, since the helium is loaded into the pump tube at room temperature and the compression is assumed to be isentropic, the formula being

$$a_2 = a_1\left(\frac{x_1}{x_2}\right)^{\frac{\gamma-1}{2}} \tag{22}$$

Consequently, the relations which must be satisfied simultaneously by a_2 are equations (21) and (22) and the interior ballistic charts of figures 7 and 8.

The computation is made by an iterative procedure. A value is assumed for a_2, and x_2 is computed from equation (21) and the interior ballistic charts using this assumed value. The value of x_2 thus obtained is used to compute a new value of a_2 from equation (22). This new value is then used to recompute x_2 from equation (21) and the interior ballistic charts, and the process is repeated. Experience has shown that it is rapidly convergent and three or four iterations are sufficient to give a_2 as accurately as the approximations of the analysis justify.

Once x_2 has been determined, the initial helium pressure may be computed using the compression ratio, x_2/x_1, and the design pressure, p_2, the formula being

$$p_1 = p_2\left(\frac{x_2}{x_1}\right)^{\gamma} \tag{23}$$

The next step in the analysis is to determine two quantities: (1) the mass of the pump piston; (2) the velocity required of the pump piston at position x_2 so that it will hold the mean pressure constant during the launching cycle and come to rest at position x_3 at precisely time t_L, the end of the launching run. The velocity u_p is related to the distance x by

$$u_p = -\frac{dx}{dt} \tag{24}$$

The piston is decelerated by the differential in pressure $(p - P)$. Now, p is assumed to be constant over the interval 2 - 3 and P is nearly constant also, since the volume opened up by the piston in this interval is small compared to the total volume occupied by the powder gas at this time. Consequently, the differential in pressure may be taken to be the constant value $(p_2 - P_2)$, and the deceleration is also constant, according to

$$m_p \frac{du_p}{dt} = -A_p(p_2 - P_2) \tag{25}$$

The piston stops at position 3; hence, the boundary conditions are

$$\left.\begin{array}{ll} \text{(1) at } x = x_2 & u_p = u_{p_2},\ t = 0 \\ \text{(2) at } x = x_3 & u_p = u_{p_3} = 0,\ t = t_L \end{array}\right\} \tag{26}$$

The velocity, u_{p_2}, is determined from the first integral of equation (25) and the boundary conditions given by equations (26), as follows:

$$u_{p_2} = \frac{A_p(p_2 - P_2)t_L}{m_p} \tag{27}$$

The mass, m_p, is determined from the second integral of equation (25) and the boundary conditions of equations (26) and (27) as follows:

$$m_p = \frac{A_p(p_2 - P_2)(t_L)^2}{2(x_2 - x_3)} \tag{28}$$

All of the quantities in equations (27) and (28) are known at this point except the pressure of the powder gas, P_2. However, P_2 is an order of magnitude smaller than p_2 and may be neglected in making the initial

calculations of u_{p_2} and m_p. If subsequent calculations indicate that P_2 is more than a few percent of p_2, it may be included in the computation of u_{p_2} and m_p as an iterative correction.

The final step of the analysis is to determine the correct powder charge which will give the pump piston of mass m_p the velocity u_{p_2} at x_2 specified by equation (27). A fairly fast powder (e.g., IMR 4227) is used, and, in order to simplify the analysis, it is assumed that the powder burns completely before the pump and valve pistons have moved an appreciable distance. Consequently, the powder is assumed to burn in a closed chamber, and the pressure of the powder gas at the end of burning is given by its equation of state

$$Pv = RT \tag{29}$$

Powder burns at practically constant temperature independent of the pressure and hence RT is a constant for any particular powder. The quantity RT is called the force constant of the powder; a typical value is 70 long tons/sq in. × cc/gram (see Chapter Three: "The Thermochemistry of Propellants" of ref. 11). Once P_1 is known, the powder charge may be computed from

$$m_c = \frac{P_1 U}{RT} \tag{30}$$

The experiments have shown that the assumption of instantaneous burning is not too good an approximation by itself. The pistons move an appreciable distance in the time of burning, and, furthermore, the force constant, RT, and the ratio of specific heats of the powder gas Γ are customarily considered to be empirical constants which must be evaluated for the particular circumstances of each firing. It is standard practice to calibrate the powder under the actual conditions of firing rather than in a closed chamber. In the present gun the essential operation required of the powder is to propel the pump piston to the velocity u_{p_2} at precisely the position x_2. The calibration follows standard practice and is based on a measured velocity corresponding to u_{p_2} rather than on a measurement of the peak powder pressure, which would correspond to P_1. The calibration is carried out under conditions simulating as closely as possible the actual compression stroke. The procedure followed and the method of applying the results to the analysis of the pumping cycle are described at the end of this section.

The pumping cycle starts with the ignition of the powder in the powder chamber. Since the powder is assumed to burn instantaneously, the chamber is assumed to be filled at the start of the cycle with a gas at pressure P_1 and having a ratio of specific heats, Γ. The gas expands isentropically, driving the pump and valve pistons in opposite directions. The

motion of the pump piston is opposed by the helium pressure, p. The valve piston acts against the pressure of the air in the bore of the valve tube; but, since the velocity of the valve piston is less than the speed of sound in air, this resistance may be safely neglected compared with the driving force of the powder gas pressure. The equation for the acceleration of the pump piston is

$$m_p \frac{du_p}{dt} = A_p(P - p) \tag{31}$$

It is more convenient to take the distance x that the pump piston moves rather than time as the independent variable since the problem centers on the value of the piston velocity at the particular distance x_2. The transformation from time to distance is given by

$$\frac{du_p}{dt} = \frac{dx}{dt}\frac{du_p}{dx} = - u_p \frac{du_p}{dx} \tag{32}$$

and equation (31) becomes

$$m_p u_p \frac{du_p}{dx} = - A_p(P - p) \tag{33}$$

The helium pressure, p, is a function of the distance moved by the pump piston, according to

$$p = p_1\left(\frac{x_1}{x}\right)^{\gamma} \tag{34}$$

The powder gas pressure is a function of the distances moved by the valve and pump pistons, according to

$$P = P_1\left(\frac{U}{V}\right)^{\Gamma} \tag{35}$$

where V is given by

$$V = U + A_p(x_1 - x) + A_v y \tag{36}$$

The analysis is complicated by the introduction of the new variable, y, the distance moved by the valve piston, and it is necessary to find a relation between x and y in order to solve the problem. An exact equation giving y as a function of x would be difficult to derive in a

convenient form; but, fortunately, a study of the physical situation suggests that an approximate equation may be entirely adequate. At the start of the cycle the helium pressure, p, is much smaller than the powder gas pressure, P, and may be neglected in solving for the motion of the valve and pump pistons. Near the end of the pumping cycle the motion of the valve piston is relatively independent of the motion of the pump piston. In addition, the volume opened up by the motions of the pump and valve pistons during this part of the cycle is small compared to the total volume of the powder gas (at this time), so that errors in the motion of the valve piston will have little effect on the powder gas pressure. As a result, the motion of the valve piston may be related with sufficient accuracy to that of the pump piston by neglecting the action of the helium in retarding the latter. Since the same pressure, P, accelerates both pistons if the helium pressure, p, is neglected, their motions are related by

$$y = \frac{m_p}{m_V} \frac{A_V}{A_p} (x_1 - x) \tag{37}$$

The volume of the powder gases may now be given as a function of the distance traveled by the pump piston only, by substituting equation (37) into equation (36), as follows:

$$V = U\left[1 + c\left(1 - \frac{x}{x_1}\right)\right] \tag{38}$$

where the presentation is made more succinct by introducing a new constant which is defined by

$$c = \frac{A_p x_1}{U} \left[1 + \frac{m_p}{m_V} \left(\frac{A_V}{A_p}\right)^2\right] \tag{39}$$

Finally, one obtains the following equation for the powder gas pressure by substituting equation (38) in equation (35)

$$P = \frac{P_1}{\left[1 + c\left(1 - \frac{x}{x_1}\right)\right]^{\Gamma}} \tag{40}$$

Since p and P are given as functions of x by equations (34) and (40), equation (33) may be integrated to obtain u_{p_2} at x_2. The quantity

desired is P_1 since all other quantities are specified to a first approximation at this point, and the integral of equation (33) written in this form is as follows:

$$P_1 = \frac{c(\Gamma - 1)\left\{\frac{m_p u_{p_2}^2}{2A_p x_1} + \frac{p_1}{(\gamma - 1)}\left[\left(\frac{x_1}{x_2}\right)^{\gamma - 1} - 1\right]\right\}}{1 - \frac{1}{\left[1 + c\left(1 - \frac{x_2}{x_1}\right)\right]^{\Gamma - 1}}} \tag{41}$$

The use of equation (41) involves three quantities whose values have not been specified previously, namely, Γ, A_v/A_p, and m_v/m_p. A value of 1.3 was selected for Γ after a study of reference 11. The value of A_v/A_p is 1.09 in the present gun. The valve pistons were arbitrarily made 3.15 times heavier than the pump pistons so that $m_v/m_p = 3.15$. The mass of the valve piston should be adjusted to keep the valve tube closed during the pumping stroke of the pump piston and to open it just after the stroke is completed, but the exact value is not critical. A preliminary analysis indicated that a mass ratio of 3.15 would work satisfactorily, and subsequent tests bore out this prediction.

The values of m_p and u_{p_2} used in equation (41) were obtained from equations (27) and (28), neglecting the quantity P_2, and it may be desirable to repeat the calculation at this stage including the value of P_2. Since the compression is assumed isentropic, P_2 may be computed from P_1 and the compression ratio x_2/x_1 as follows:

$$P_2 = \frac{P_1}{\left[1 + c\left(1 - \frac{x_2}{x_1}\right)\right]^{\Gamma}} \tag{42}$$

If P_2 is appreciable compared to p_2, it should be treated as an iterative correction to m_p, u_{p_2}, and P_1.

This step of the analysis could be concluded by computing the powder charge from equation (30), but, as mentioned previously, it has been found that closed-chamber calibrations do not predict satisfactorily the performance of the powder in actual gun firings (e.g., see Chapter Two: "Gun Propellants" of ref. 11). The calibration should duplicate as closely as possible the conditions under which the powder operates. In the light-gas gun the essential function of the powder is to impart a specified velocity, u_{p_2}, to a piston of given mass, m_p, at a particular position, x_2. Now, if the launch tube and coupling were removed from the end of the pump

tube and the pump piston were fired from the open-ended pump tube as a projectile is fired from a conventional gun, the powder charge corresponding to P_1 would give the piston a certain velocity u_{p_L} at the muzzle of the open pump tube. If the value of u_{p_L} is determined by an analysis similar to that which has already been carried out for the compression stroke, the u_{p_L} corresponding to P_1 will be given by

$$u_{p_L}^2 = \frac{2A_pL_pP_1}{m_pC(\Gamma - 1)}\left[1 - \frac{1}{(1 + C)^{\Gamma-1}}\right] \tag{43}$$

where the factor C is defined by the equation

$$C = \frac{A_pL_p}{U}\left[1 + \frac{m_p}{m_v}\left(\frac{A_v}{A_p}\right)^2\right] \tag{44}$$

(It should be noted that, in general, c will differ numerically from C because x_1 differs from L_p due to the lengths of the pump piston and the coupling.) The quantity u_{p_L} can serve to calibrate the powder equally as well as the quantity P_1, and represents much more closely the performance expected of the powder than the closed-chamber pressure, P_1.

The powder is calibrated by firing the gun with the pump tube open; that is, with the coupling and launch tube removed, as postulated above. (The valve tube remains in position, of course, and the valve piston is launched simultaneously with the pump piston so that the volume opened up by the movement of the pistons in the calibration firing simulates as closely as possible the volume opened up during the compression stroke.) The masses of the pump piston and powder charge are both varied systematically and the muzzle velocity is measured. The results of the calibration are plotted as a graph of u_{p_L} versus m_c with m_p as a parameter (see fig. 9).

In utilizing the powder calibration, the quantity P_1 is computed as one of the parameters in the over-all performance required of the gun. The quantity u_{p_L} is computed from equation (43) using this value of P_1. The powder charge is read from the calibration chart using the values of u_{p_L} and m_p. Thus the last quantity required for the pumping cycle is determined by this procedure.

Performance Charts

The preceding analysis is summarized in a set of four performance charts which are shown in figures 10, 11, 12, and 13. The usual problem of operating the gun may be stated as follows: Given the projectile mass and the muzzle velocity desired, determine the initial helium pressure, the mass of the pump piston, the powder charge, and the shear-disk thickness. Accordingly, one enters the chart of figure 10 with u_{s_L} and m_s and determines p_2. The loading conditions p_1, m_p, and m_c are given by the charts of figures 11, 12, and 13 using m_s and the value of p_2 just obtained. The quantity p_2 also determines the thickness of the shear disk (see fig. 6). However, it will be recalled that the central plug sheared out of the shear disk on the release of the projectile travels with the projectile and, hence, its mass must be added into the projectile's mass. Consequently, several iterations may be necessary in order to obtain a firm value of m_s and, in turn, the loading conditions.

The performance charts may be said to represent an ideal operating cycle of the gun, and two modifications should be made in their use in order to account for the approximations of the analysis. The actual muzzle velocity desired of the projectile should be reduced in determining the u_{s_L} of the charts to account for the effects of chamberage. The p_2 used in charts of figures 11, 12, and 13 should be diminished from the rupture pressure of the shear disk given by the chart of figure 10 in order to compensate for override of the pressure in the pump tube during the first part of the launching cycle. These changes are discussed in detail in Appendix B. They are pointed out in this section on the use of the operating charts since they must be taken into account if one is to predict accurately the real performance of the light-gas gun. The modifications may be summarized succinctly in the following two rules on the use of the charts:

1. Take u_{s_L} as 0.9 times the desired muzzle velocity to enter the chart of figure 10.

2. Take $p_{2D} = p_{2R} - 10{,}000$ psi.

In order to clarify the use of the performance charts, the pressure p_2 of the chart of figure 10 is designated by p_{2R} and the pressure p_2 of the charts of figures 11, 12, and 13 is designated by p_{2D}.

The performance charts of this report are based on the use of helium. On the other hand, the reader may wish to evaluate the performance of a similar gun using hydrogen or some other gas as the light gas. Perhaps he may wish to explore the possibilities of a larger light-gas gun or one of different proportions. In order to assist him in this task the analysis has been summarized in a computing procedure in Appendix C. This procedure gives him a step-by-step account of the computations he must perform in order to determine the performance of his light-gas gun.

FIRING TRIALS

Calibrations

Before the gun could be fired, it was necessary to calibrate (1) the rupture strength of the shear disk and (2) the interior ballistics of the powder charge. The shear disk was calibrated by hydraulic test, as illustrated in the following sketch. The cross section of the disk was made

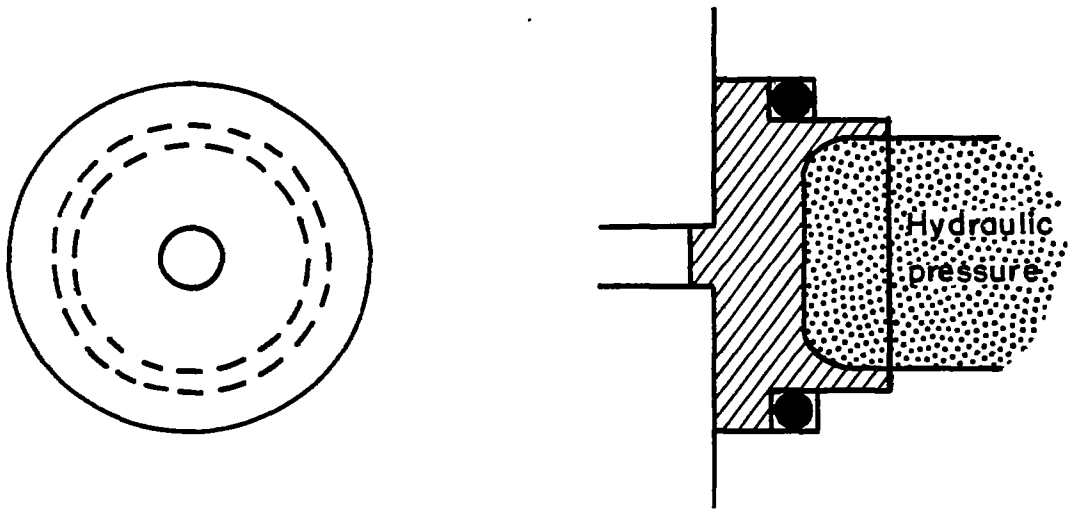

Sketch (h)

as shown in the sketch. The steel ring, which can be seen placed behind the disk in figure 6, was not present in these tests but was later found necessary in order to insure clean rupture during actual firing conditions. The procedure was straightforward; the hydraulic pressure was increased slowly until the disk ruptured. On rupture, a central plug of nearly bore diameter sheared out cleanly, which, of course, is the type of break that had been hoped for.

A series of disks were tested with systematically increasing thickness. The results are plotted in figure 14 as a graph of rupture pressure against shear-disk thickness. The shear stress at failure was computed and is shown as the dashed curve in figure 14. As can be seen, the shear stress has a constant value of 10,000 psi up to a disk thickness of 1/8 inch, after which it increases slowly. The rupture pressure curve of figure 14 was used throughout the firing trials to compute the thickness of the shear disk required for rupture at the firing pressure, p_2, specified by the performance chart of figure 10.

The method of calibrating the powder has already been described. The test setup is shown in the following sketch. A fine wire grid made

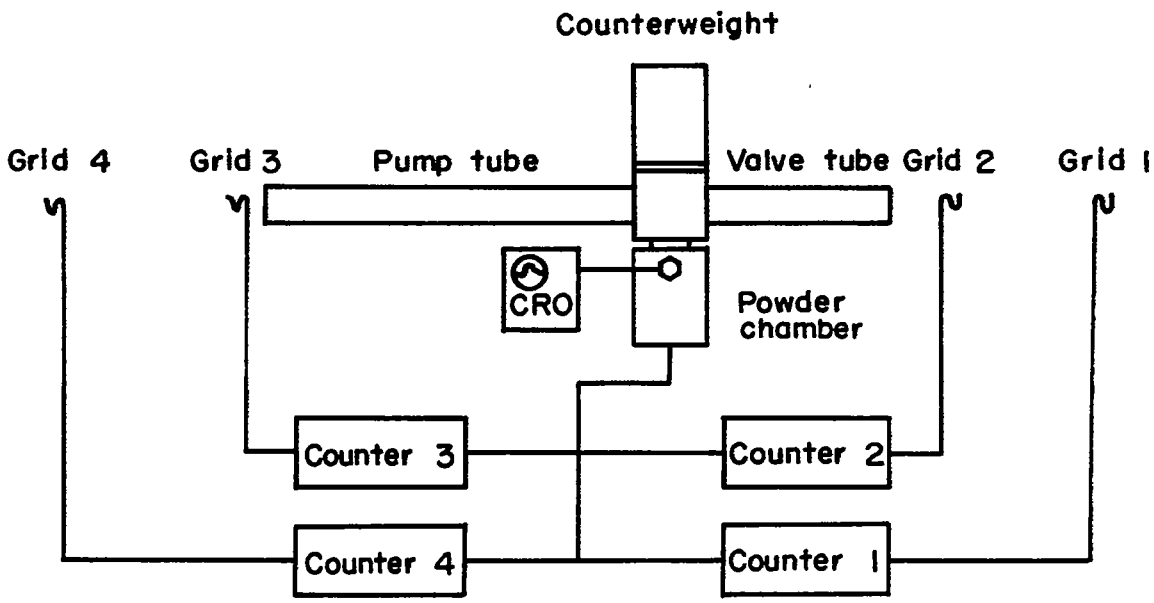

Sketch (i)

from copper wire 0.002 inch in diameter was placed close to the muzzle of the pump tube. A second grid was placed on the trajectory about 3-1/2 feet out from the muzzle of the pump tube. Two more grids were similarly placed adjacent to and out from the muzzle of the valve tube. Each of the grids was connected to the stop gate of a 1.6-megacycle counter chronograph. All four cycle counters were started by a signal from a switch which was closed as the firing pin was struck; each counter was stopped in turn as one of the pistons perforated the grid connected to it. In addition to the timing records, a piston-type strain gage was placed in the powder chamber and its output recorded on a cathode ray oscilloscope.

The muzzle velocities of each of the pistons were determined from the time differences of the counters and the spacings of the grids. The piston strain gage was calibrated and the cathode-ray trace gave the time history of the powder pressure. A typical powder pressure record is shown in figure 15.

The results of the firings are plotted in figure 9 as curves of muzzle velocity against powder charge with the mass of the pump piston as a parameter. The individual points are not shown, but the scatter was

quite small throughout. As mentioned previously, the method of loading the powder produced consistent, reproducible results.

In this test, the only datum of direct concern to the powder calibration was the muzzle velocity of the pump piston. However, the muzzle velocity of the valve piston and the time history of the powder pressure gave additional evidence as to whether the powder acted in the way it was assumed to act in the performance analysis. It was found that the measured powder pressure was always lower than the computed powder pressure, P_1, which indicates that the pistons were accelerated during the burning of the powder as well as by the expansion of the gases afterwards. This inference is substantiated by the pressure record of figure 15. An average figure for the total pumping time is 10 milliseconds, and it is evident that the burning of the powder as shown by the rise time of the pressure takes an appreciable fraction of this interval.

A further check on the process was made by integrating the powder pressure curve to obtain the muzzle velocity of the valve piston, assuming that the pressure was constant throughout chamber, pump, and valve tubes, as in the performance analysis. The computed velocity was 476 ft/sec which agrees favorably with the measured value of 484 ft/sec. Here also the validity of the assumptions on which the performance is based is borne out by the results of the tests.

Experimental Apparatus and Measurements

The experimental setup which was used in carrying out the firing trials is shown in figure 16. Gages were placed in the gun to record pressures. Chronographs were used to time the motion of the projectile along its trajectory. Although the primary interest was in the gun's performance, the flight was recorded by a spark station and two still cameras.

Two types of pressure gages were used: (1) a special adaption of the standard copper crusher gage (see section 81 of ref. 16, "The Crusher Gage"); (2) the piston strain gage developed at the Ames Laboratory (ref. 17). The gages were used in parallel and served to check each other, although it should be noted that the piston strain gage gives a complete history of the variation of pressure with time while the crusher gage records only the peak pressure. The output of each piston strain gage was recorded on a cathode-ray oscilloscope. The gage was first calibrated on a dead-weight testing machine to determine its gage factor. The over-all response of the gage-oscilloscope circuit was then calibrated by shunting the gage with a known resistance and noting the deflection of the cathode-ray beam. The crusher gage measures the pressure through the permanent deformation of a small copper cylinder. These deformations were measured by micrometer measurement of the cylinders before and after test and were converted to pressures by a tarage table furnished with the copper cylinders.

One pair of gages was placed in the powder chamber to record the powder pressure. A second pair of gages was placed in the coupling at the high-pressure end of the pump tube to record the helium pressure at this point. Actually, the second pair consisted of one piston strain gage and two crusher gages, since it is customary to use two copper crusher gages for each measurement in order to minimize the errors inherent in this instrument. Also, the output of the piston strain gage at the coupling was recorded by two oscilloscopes, one with a relatively slow sweep rate to give the complete pressure history and the other with a relatively fast sweep rate to give a detailed record of the pressure variation in the pump tube during the launching cycle.

A photograph of the three oscilloscope records for a representative round (round number 10) is shown in figure 17. All traces sweep from left to right. The traces for the powder pressure and slow sweep helium pressure were started by a signal from the switch on the firing pin, and it is interesting to note that an appreciable delay occurs between the time the firing pin is struck and the time the gas pressure from the combustion of the powder starts to rise. The trace for the fast sweep helium pressure was triggered by an internal signal and started when the pressure reached a certain value (a few thousand psi). This record contains a small amplitude, high-frequency oscillation superimposed on the main pressure variation, but this secondary oscillation should be disregarded in interpreting the record. It is believed that the secondary oscillation comes from a mechanical resonance of the gage itself and is not due to an oscillation in the helium pressure, since the frequency agrees with that computed from the dimensions of the gage. It is felt that an improved design of gage would have given a record free from this secondary oscillation. Despite this difficulty, calibrations before and after pressure measurements and agreement between independent gages measuring the same pressure indicate that the accuracy of the gage records is 5 percent or better.

The flight of the projectile was timed by the same method used in the powder calibration firings. Fine wire grids were placed at the muzzle of the gun, at the exit port of the vacuum tank, and on the trajectory 2 feet out in the room from the tank. Each grid was connected to the stop circuit of a 1.6 megacycle counter chronograph. All counters were started by a signal from the firing pin switch and were stopped successively as the projectile broke each grid in turn. The exit port of the vacuum tank was sealed by a thin cellophane diaphragm and the tank and launch tube were evacuated before firing. Consequently, the projectile traversed the tank in a near vacuum and the muzzle velocity was computed directly from the time difference across the tank, since its retardation in the vacuum tank was negligibly small. The accuracy with which the velocity is measured is better than 1 percent. After perforating the diaphragm at the exit port, the projectile traversed the next timed interval through the air of the open room, and its retardation was substantial. As a result, the velocity computed from the time difference across this second interval

was considerably lower than the velocity across the vacuum tank. However, it should not be concluded that the decrease in the velocity over the second interval is a correct measure of the retardation of the projectile as fired from the gun. Impact with grids and diaphragm have fragmented the nylon portion, and, hence, the retardation over the second interval is representative of a group of small fragments flying close together (similar to a shotgun charge) rather than the projectile flying as a structurally sound unit. Consequently, the velocity from the second interval served mainly as a check on the tank velocity.

A spark photography station was located at the position of the third grid, 2 feet out from the vacuum tank. Referring to figure 16, one sees the spark located on one side of the trajectory and the photographic plate placed opposite. In the actual setup the line from spark to film was approximately horizontal and the two were positioned about 2 feet away from the trajectory on opposite sides. The spark was triggered by a signal from the third grid and recorded a silhouette of the projectile after it had passed a fraction of an inch or so beyond the grid. A typical spark photograph (round number 3) is shown in figure 18. The projectile has been partly broken up by impacts with the three wire grids and the cellophane diaphragm, and the silhouettes of the main projectile and the fragments surrounding it are clearly evident. The heavy lines and the filigree patterns sweeping back from the projectile and its fragments trace out the shock waves and wakes, the disturbances in the surrounding air that characterize flight at supersonic speeds. The dark vertical lines are the shadows of the grid wires.

The projectile traversed some 10 feet of open air in the firing range before being stopped by a butt. Its flight path was recorded by two still cameras, one placed near the butt facing along the flight path toward the gun and the other placed near the spark unit facing across the flight path toward the photographic plate. The significance of the camera records is perhaps best explained by describing the procedure followed in operating the photographic apparatus. Before a round was fired, the range was darkened. The film was placed in the spark station and the shutters of the cameras were opened. The round was then fired. Next, the film of the spark station was removed and the shutters of the cameras were closed. After these operations were completed, the range was lighted again. Consequently, any light that appears on the camera records must have been generated during the flight of the projectile. Examples of these camera records will be described subsequently.

One additional measurement not indicated in figure 16 was made during the firing. A rough indication was obtained of the stop position of the pump piston as it completes its compression stroke and reverses direction. On the first three rounds small pieces of scotch tape 1/16 inch square were stuck to the surface of the bore of the pump tube. They were placed in a line along the length of the bore about 1/4 inch apart and covered the last 4 inches of the pump tube at its high-pressure end (extending into

the coupling; see fig. 6). The piston scraped off those pieces encountered in the length of its stroke. The pieces located beyond the excursion of the piston were untouched, although a trifle scorched by the hot helium. Thus, the pieces remaining recorded the forwardmost position of the piston to within 1/4 inch.

On each of these rounds it was noticed that the piston's stop position was marked by a ring around the bore which seemed to be caused by a thin deposit of some dark substance on the surface of the bore. It was thought that the heat of compression evaporated a small amount of nylon from the exposed face of the shear disk which decomposed and deposited itself on the bore surface. However, the piston scraped off this deposit during its forward stroke, and, although a little more may have been deposited on the return stroke, the contrast between the heavy and light deposits generated the ring. The occurrence of the ring at the stop position as determined by the scotch tape suggested that the ring itself would be adequate for this record, although, in the authors' opinion, this ring is not so reliable an indication of the stop position of the piston as the scotch tape. Nevertheless, the ring was used to indicate the stop position on all subsequent rounds, since considerable care was required to place the scotch tape properly and time was a factor in carrying out the firing trials due to the press of other tests for the use of the firing range.

Chronological Account of the Firings

The analysis gave a certain degree of confidence in the performance expected of the gun. Nevertheless, it seemed prudent to start the trials with a low helium pressure, p_2, and to increase this value gradually to the maximum pressure that the strength of the gun would allow; also, the loading conditions were not adjusted to minimize the pressure override on the first five rounds. The possibility of the override was recognized from the start, of course, but it was believed desirable to establish its magnitude experimentally before attempting a correction. Accordingly, the first round was loaded for a p_{2D} of 20,000 psi. The projectile was a nylon proof slug 2 calibers long weighing 0.31 gram (including the central plug sheared out of the disk) and the velocity predicted was 8,700 ft/sec (without correction for chamberage).

The first round[8] was perhaps typical of first rounds in that almost none of the electronic instrumentation functioned properly. Consequently, no velocity records or piston-strain-gage pressure records were obtained and the spark was not triggered at the right time to silhouette the projectile. On the other hand, the copper crusher measurement of the peak

[8]The reader may be assisted in following the chronological account of the firings presented in this section by making reference to table II, which summarizes the results of the firing trials.

helium pressure and scotch tape record of the stop position of the pump piston showed that the gun had functioned very much as expected. Also, the still-camera photographs showed a bright streak along the trajectory. The results of this first round were encouraging, to say the least.

The second round was a repeat of the first. This time the electronic instrumentation functioned satisfactorily and the records of this round gave the first real confirmation that the gun functioned successfully. The peak helium pressure was 29,000 psi, a value that one might expect due to the pressure override. The muzzle velocity was 9,870 ft/sec. The increase over the predicted velocity is about right to account for the effects of chamberage. The spark station operated at the right time; however, the spark photograph showed that the nylon slug had been fragmented by its successive impacts with grids and diaphragms. Again the pump piston stopped and reversed its direction close to the design position x_3, and the still-camera records showed streaks of light along the trajectory.

An unexpected feature of the performance was disclosed by these first two rounds, which proved to be characteristic of all the rounds, with only one exception. The pump piston came to rest in the pump tube instead of crossing the T-connector and leaving the gun via the valve tube. Its rest position varied from round to round and in some rounds the piston was found in the coupling adjacent to the shear disk. On the other hand, there was no evidence that the piston had struck the end of the tube (the face of the shear disk) with any appreciable force. It is surmised that the balance between the helium buffer, the powder pressure, and the valve piston timing is such that the piston is stopped on its return stroke by the residual pressure of the powder gases and either stopped somewhere along the length of the pump tube or shoved slowly back up the tube into the coupling. Actually, the termination of the pumping cycle in this manner did not impair the gun's performance in any way, although a return of the piston all the way into the coupling destroys the scotch tape record of the piston's stop position. If it is desired that the pump piston leave the gun on its return stroke, this action can probably be achieved by lightening the valve piston so that it opens sooner and reduces the powder pressure during the return stroke. Under different circumstances it might be desirable to bring the pump piston to rest in the pump tube, that is, purposefully rather than accidentally as in the present firings. This performance can undoubtedly be realized by the correct balance between powder charge, valve action, and helium buffer. In fact it might be possible to replace the valve tube and valve piston altogether by a nozzle, and to design the pump so that it will function in a manner similar to a recoilless gun, thereby eliminating the necessity of stopping pistons fired to the rear. If a military weapon were ever designed around the principle of the light-gas gun, this modification would surely enhance its utility.

The next three rounds were spent working out two difficulties which are characteristic of the gun, namely, the shear-disk break and the

pressure override. The problem of the shear-disk break is illustrated by figure 19. It was found that the original design of shear disk did not break out cleanly as it had in the hydraulic tests but fragmented all around the central hole leaving a ragged edge, as may be seen in the top photograph of this figure (the shear disk from round number 3). Whenever this type of break occurred, the muzzle velocity was less than the theoretical value, that is, less than the velocity predicted by the analysis increased by 10 percent to account for the effect of chamberage. The cause of the loss in velocity is not known, but it is suspected that the flow of helium in the launch tube is impeded by the fragments which have broken away from the edges of the hole. Looking at the phenomena from another standpoint, one might say that part of the energy of the propellant gases has gone into the acceleration of the fragments instead of the projectile. In any case, it is necessary to design the shear disk so that it will rupture cleanly if the full potential of the gun is to be realized.

At first it was thought that the entire projectile might have fractured upon rupture of the shear disk instead of being broken by impact with the grids and diaphragm (see fig. 18, which is the spark photograph for round number 3). To test this theory a round (number 4) was fired with the grid at the gun muzzle and the grid and diaphragm at the tank port removed. The spark station was moved as close as possible to the tank port, and its grid was left in place so that a silhouette of the model would be obtained and thereby determine its condition in flight. A second grid was placed 2 feet farther along the trajectory from the spark station for a measurement of the flight velocity. The tank and launch tube were filled with helium (at atmospheric pressure, of course) in order to alleviate the effects of air resistance during launching insofar as possible. The spark photograph of this round is shown in figure 20. It is evident that the entire projectile consisting of sabot and central plug is quite intact, has the shape intended, and was not damaged during rupture and launching, although the shear disk of this round fragmented in the same manner as the previous rounds. Apparently the central plug shears out of the disk cleanly, but the region of the disk around the hole fragments and breaks away afterwards.

This difficulty was cured by placing a steel ring behind the shear disk, as shown by the sketch in the lower half of figure 19. The ring presses so firmly against the disk that the interface is effectively sealed from the helium. Thus the helium pressure squeezes the disk between the ring and the breech of the launch tube. When it is compressed in this manner, the disk shears out cleanly and the edges of the hole do not fragment, as can be seen from the photograph in the lower half of figure 19 (shear disk from round number 6).

The difficulties associated with the pressure override and the method of minimizing the override are discussed in Appendix B. The analysis indicates that the override will be relatively ineffective in increasing the muzzle velocity, but it was thought desirable to fire one round to test

this conclusion. In order to exaggerate the override for the round in question, round number 5, the shear disk was designed to rupture at 20,000 psi but was loaded for a design pressure, p_{2D}, of 40,000 psi; this provided a thorough test of the theory. Actually, the pressure rose to a peak of 56,000 psi or nearly three times the rupture pressure. If the rupture pressure is controlling, the muzzle velocity should be 9,600 ft/sec, but, if the design pressure is controlling, the muzzle velocity should be 11,700 ft/sec (the chamberage factor was taken to be 1.1). The measured muzzle velocity was 9,000 ft/sec. A comparison of predicted and measured velocities suggests that the rupture pressure is, in fact, the controlling quantity. Unfortunately the experimental evidence is not as clear cut as desired, since the shear disk ruptured in a ragged hole and the muzzle velocity was thus lower than it would have been with a clean break by an unknown amount. At best one can say that the experimental results tend to support the contentions of the theory.

The method chosen for minimizing the pressure override was to reduce the design pressure, p_{2D}, by 10,000 psi from the shear-disk rupture pressure, p_{2R}, as described in the analysis section and Appendix B. This modification to the loading was put into effect for all rounds starting with round 6, with the exception of round number 9. However, a slight variation in carrying out this correction had to be made in loading the rounds for the firing trials reported herein. The pump and valve pistons for all 11 rounds of the shoot had been manufactured before starting the firings and circumstances made it desirable to use these rather than construct new pistons of a lighter mass. On the other hand, the initial helium pressure and powder charge could be varied at will, and, taking advantage of the parameters at our control, we adopted the following procedure:

1. The rupture pressure, p_{2R}, of the shear disk was specified in advance for all of the rounds, since all shear disks had been manufactured ahead of time. The muzzle velocity, u_{s_L}, was predicted from p_{2R} and the actual mass of the projectile m_s using the chart of figure 10.

2. The design pressure, p_{2D}, used in the remaining performance charts was taken to be (p_{2R} - 10,000 psi).

3. The design pressure, p_{2D}, and the actual mass of the pump piston, m_p, were used in the chart of figure 12 to determine a fictitious projectile mass, m_{s_F}.

4. The fictitious projectile mass, m_{s_F}, and the design pressure, p_{2D}, were used to determine the initial helium pressure, p_1, from the chart of figure 11 and the powder charge, m_c, from the chart of figure 13.

The effect of this variation in modifying the loading specified by the performance charts was to reduce the pressure override, as the results of the remaining rounds will show. However, the velocities were probably lower than they would have been if there had been time to manufacture lighter pistons. The heavy piston produced the same variation in pressure as the light piston would have but held the pressure at its peak value longer, since the fictitious mass was greater than the actual mass and hence demanded a longer launching cycle than was actually needed.

Another result of interest came from round 5, in addition to the test of pressure override. This round differed from all the rest in that the entire projectile-shear-disk unit was made from a magnesium alloy. When the gun was disassembled after firing, it was found that a large part of the shear disk exposed to the hot helium had melted away. This result is not too surprising if one considers the high heat conductivity and low melting point of magnesium alloy. In contrast to the magnesium, the nylon withstands the exposure to the hot helium probably because its conductivity is so low that only a thin layer of the surface is affected in the millisecond or so that the temperature is high, despite its relatively low temperature of decomposition. Molten magnesium can hardly improve the propulsive properties of helium, and for this reason, among others, nylon has been used almost exclusively as the material for sabots and shear disks.

The first fully successful round fired at high pressure was round number 6. The techniques employed in this round have been used in all subsequent rounds, and so round 6 may be considered to be representative. The projectile was similar to the proof slugs of the previous rounds with the difference that a small duraluminum sphere (1/8-inch diameter) was seated in the front of the nylon cylinder. Thus the nylon serves as a sabot in this round and the configuration is similar to that which will be used in aerodynamic tests.

The design pressure for loading was 40,000 psi. The rupture pressure of the shear disk was 50,000 psi. The peak pressure rose to 56,000 psi, as expected. This result substantiated the procedure for controlling the pressure override. The pressure records are similar to those shown in figure 17 for round 10 (the records of round 10 were chosen because the densities of the negatives were more suitable for illustration). The rupture pressure of the shear disk is marked on the helium pressure record from the oscilloscope with the fast sweep, and it can be seen that the pressure remained almost constant at this value for 1/3 millisecond (it will be recalled that the secondary oscillation is believed to be a mechanical resonance of the gage and not a pressure fluctuation). The time of the launching cycle is 1/2 millisecond. Consequently, the pump piston moved the right distance in the right time to hold the helium pressure in the pump tube at the shear-disk rupture pressure and a little above for two-thirds of the time of the launching cycle. Also, the pump piston stopped and reversed its direction 3 inches from the end of the

pump tube, just short of the distance specified in the analysis of 2-1/2 inches. These results are both in accord with the predictions of the analysis.

Two pictures taken by the still camera placed near the butt and looking along the trajectory are shown in figure 21. The picture on the left was taken before the round was fired and shows the orientation of the apparatus in the field of view. The face and exit port of the vacuum tank are seen on the right and the framework of the spark station and the plywood surface for mounting the photographic plate, in the center. The picture on the right was taken during the firing, and it will be recalled from the description of the firing routine that all of the exposure in this photograph comes from light generated during the flight of the projectile (subsequent tests have shown that the vacuum tank contains the blast of helium from the launch tube and that little light comes from this source). The trajectory of the projectile is marked out by a bright streak. A brilliant burst of light occurs as the projectile impacts the diaphragm and grid at the tank port and again as it impacts the grid at the spark station. The streak persists at full intensity for some 6 feet from the tank and then fades out toward the end of the trajectory.

The spark photograph of round 6 is shown in figure 22. The dural sphere is surrounded by the fragments of the nylon sabot which partly obscure it, and only the round contour of the sphere's leading surface can be distinguished from the overlapping shadows cast by sphere and fragments. The fine, dark lines radiating out in front of the sphere are the wakes of tiny particles of copper coming from the grid wires. The impact of the projectile with the wire is so violent at these speeds that the wire disintegrates into small particles which are hurled ahead with roughly twice the velocity of the projectile itself. It should be noted that this spark photograph was taken in the presence of all the light visible in figure 21, which was bright enough to produce an image in the still camera record of the spark photographic plate itself. Fortunately, the light from the spark is intense and photographically active, since much of it is in the ultraviolet, and the contrast on the spark photograph is satisfactory despite the diffuse illumination coming from the light along the trajectory.

The streak photograph suggests that objects flying through the air at speeds above 10,000 ft/sec will be subject to much the same conditions as meteors entering the earth's atmosphere at velocities far greater than this. (Meteor velocities range from 25,000 ft/sec to 240,000 ft/sec; see refs. 18 and 19.) Their flight will be characterized by high temperatures and high rates of heating. On the other hand, the evidence from the streak photographs of the present firing trials may be quite misleading because the impacts with the grids and diaphragm may be the controlling factor in the phenomena which are observed in these tests. The critical experiment will come when the projectile is launched into flight without encountering any obstacles along its flight path.

Eleven rounds in all were fired in the present firing trials. The gun functioned satisfactorily from round 6 on, with the single exception of round 9 in which a new design of ring and shear disk was tried that failed to give a clean break. The pressure was gradually increased until a peak of 109,000 psi was reached, which is believed to be close to the maximum pressure that the strength of the gun will allow. On the last round the projectile's mass was reduced to a minimum by making the projectile merely the central plug sheared out of the disk. This round gave the highest velocity of the test, 15,400 ft/sec.

The firing trials disclosed an important difference in the operating quality of the light-gas gun from conventional high-velocity weapons. Erosion of the bore is characteristic of nearly all high-velocity guns. In fact, some high-velocity guns erode so rapidly that their useful life is limited to a few rounds. In contrast to the conventional behavior, the light-gas gun eroded very little. Its bore was enlarged by 0.0001 inch at the breech of the launch tube, but otherwise the dimensions of the bores of the pump and launch tubes were unchanged. It is evident, of course, that the low rate of erosion in the gun greatly enhances its utility even as a laboratory instrument.

Summary of Results

The results of the firing trials are summarized in table II. A study of the experimental data made it clear that the rounds should be divided into two categories, those with clean shear breaks and those with ragged shear breaks. It is felt that only those rounds with clean shear breaks are truly representative of the performance which may be expected of the light-gas gun. Accordingly, only those rounds (2, 6, 7, 8, 10, and 11) were included in the final analysis of results which follows.

In the over-all picture of aerodynamic testing, the basic function of the gun is to launch a given projectile at a specified velocity. The criterion for evaluating its performance is thus the comparison of measured muzzle velocity with predicted muzzle velocity for a variety of launching conditions. This comparison is attempted for the limited range of launching conditions covered in the present firing trials by plotting the ratio of the measured velocity to the predicted velocity (based on the shear-disk rupture pressure), u_m/u_{s_L}, against the shear-disk rupture pressure, p_{2R}, in figure 23.[9] It can be seen that a ratio of 1.1,

[9]It will be recalled that the shear-disk rupture pressure is determined by the thickness of the shear disk and the hydraulic calibration curve of figure 14. The pressure at which the shear disk actually ruptured was not measured. Consequently, p_{2R} is a design rather than a measured quantity, and its true value may differ somewhat from the value given in table II and figure 23. Variation in the actual value of p_{2R} from the design value may account for part of the scatter evident in figure 23.

indicated by the dashed line, represents the test data fairly well. Thus an empirical factor of 1.1 is adequate to account for the increase in muzzle velocity due to chamberage and the departures of the actual physical situation from the physical model assumed. There is some scatter about the 1.1 line, but the variation in muzzle velocity is probably small enough to be acceptable for launching free-flight models.

CONCLUDING REMARKS

The firing trials have demonstrated that the piston compressor type of light-gas gun is a workable unit. Operating techniques have been developed which give reliable results whenever the gun is fired. Good agreement has been obtained between the predictions of the performance charts and the experimental data for all quantities which were measured. The erosion of the barrels for the 11 rounds fired has been negligible. It appears safe to conclude that the gun will be suitable for launching models at high velocity in an aerodynamics range.

On the other hand, it may be appropriate to conclude by mentioning that the development of the gun described in this report was controlled in part by the availability of materials and by a desire to produce a simple unit which would serve to test the gun's functioning. Compromises in design were made at some sacrifice in performance and suitability as a launcher for aerodynamic models. If a new gun were to be constructed, it would be desirable to redesign, placing proper emphasis on these two factors of performance and suitability rather than building a scaled replica of the unit described herein.

Furthermore, it should be mentioned that certain pieces of apparatus auxiliary to the gun must be developed and put into operation before the gun can be used to launch free-flight models. The flight records of the present firing trials show clearly that the wire grids must be replaced by some sensing device such as a photoscreen which does not interfere with the model's flight. In the same category, some mechanism must be introduced to remove the diaphragm at the exit port of the vacuum tank just prior to the passage of the projectile through this port. It may also be desirable to take a spark photograph of the projectile before it leaves the vacuum system in order to establish its structural integrity just before it starts its flight through the air, and also to separate the sabot from the model in the interval between the gun's muzzle and the exit from the vacuum system. However, the development of this auxiliary equipment, important as it is, lies beyond the scope of the work reported herein.

Ames Aeronautical Laboratory
National Advisory Committee for Aeronautics
Moffett Field, Calif., July 11, 1955

APPENDIX A

EFFECTS OF AIR RESISTANCE AND BORE FRICTION

The desirability of evacuating the launch tube can be illustrated by estimating the effect of the air resistance on the muzzle velocity of a typical light-weight round. The example chosen is a projectile weighing 0.15 gram and fired at a rupture pressure of 50,000 psi (this is the same example which is illustrated in Appendix B, "Modifications to the Performance Charts"). Calculations based on the method of characteristics show that this round will have a muzzle velocity of 17,000 ft/sec if the bore is evacuated. On the other hand, if the bore is filled with air at ordinary room conditions, the back pressure[1] will just balance the driving pressure at a velocity of 12,000 ft/sec and hence, the muzzle velocity will be less than this value. Consequently, the air resistance will reduce the muzzle velocity of this round by 30 percent or more.

It should also be noted that, in general, the importance of the bore friction is determined by the length of the gun. If the length is increased sufficiently, the bore friction will eventually balance the accelerating force of the propellant even though the gun tube is evacuated. The balance point will be determined by the value of the friction, and the smaller the friction the longer the length of gun before the balance point is reached. Although it is thought that the length of the gun is far from this balance point, tests will have to be carried out before it is firmly established that the bore friction can, in fact, be neglected.

---

[1]The back pressure can be estimated from the formula

$$p = 1.72(u/a)^2$$

where p is the back pressure in atmospheres, u is the velocity of the projectile, and a is the velocity of sound in the undisturbed air. This formula is accurate to 2 percent for u/a greater than 5. A general equation for very high values of u/a is

$$\frac{p}{p_o} = \frac{\gamma(\gamma + 1)}{2}\left(\frac{u}{a}\right)^2$$

where p_o is the pressure in the bore before firing.

APPENDIX B

MODIFICATIONS TO PERFORMANCE CHARTS

Effect of Chamberage on Launching Cycle

The muzzle velocity, u_{s_L}, must be corrected for the effects of chamberage because the analysis is based on a bore-diameter, infinite-length chamber; whereas, the gun acts as if it had an infinite-area, infinite-volume chamber. The reduction in area in going from the chamber to the gun bore (i.e., the chamberage) generates compression waves, and these waves act to increase the pressure over that of the simple, constant-area expansion wave assumed in the analysis. In other words, the actual pressure at the base of the projectile will be higher for each value of the projectile's velocity than the pressure predicted by equations (2) or (7).

The flow of gas in an infinite-area, infinite-volume gun can be analyzed by the method of characteristics. One example was worked out by the method of characteristics and did include the effects of chamberage. The pump tube pressure was taken as 50,000 psi and was assumed to be held constant during the launching cycle. The speed of sound in the helium in the pump tube was assumed to be 10,000 ft/sec. The mass of the projectile was taken to be 0.15 gram.

The results are shown in figures 24 and 25, which give the velocity of the projectile and the pressure at its base as functions of the distance traveled along the bore. The severe decrease in base pressure with distance seen in figure 25 emphasizes the critical role played by the kinetic energy of the propellant gas. It is of interest to note that the muzzle velocity obtained by the method of characteristics for this example, 17,000 ft/sec, agrees well with the muzzle velocity predicted by the approximate formulae which are to be developed shortly; namely, 17,400 ft/sec.

An approximate method for computing the effects of chamberage was devised, which is believed to be sufficiently accurate for the engineering estimates required here (based on the results of experiments carried out at the Naval Ordnance Laboratory). The essence of the approximation is contained in the generalization of equation (7) for the relation between $\bar{u}_s$ and $\bar{\sigma}_s$. The complete excursion of $\bar{u}_s$ is divided into two regions, the first extending from 0 to $(\gamma - 1)/2$ and the second from $(\gamma - 1)/2$ to $\sqrt{(\gamma + 1)/2}$.[1] In region 1, $\bar{\sigma}_s + \bar{u}_s$ is assumed to increase

[1]Experience suggests that the juncture should depend on γ, and it was estimated that a juncture at $\bar{u}_s = \frac{\gamma - 1}{2}\left(= \frac{1}{3}\right)$ would represent the characteristic data. A check was made with one characteristic solution and the estimated value of $\frac{\gamma - 1}{2}$ was borne out by a satisfactory fit to the data.

linearly with $\bar{u}_s$, that is,

for $0 \leq \bar{u}_s \leq \frac{\gamma - 1}{2}$

$$\bar{\sigma}_s + \bar{u}_s = D + E\bar{u}_s \tag{B1}$$

In region 2, $\bar{\sigma}_s + \bar{u}_s$ is assumed to have the constant value equal to $\sqrt{(\gamma + 1)/2}$, that is,

for $\frac{\gamma - 1}{2} \leq \bar{u}_s \leq \sqrt{\frac{\gamma + 1}{2}}$

$$\bar{\sigma}_s + \bar{u}_s = \sqrt{\frac{\gamma + 1}{2}} \tag{B2}$$

At this point it should be noted that the maximum value of $\bar{u}_s$ has been increased from 1 to $\sqrt{(\gamma + 1)/2}$. The physical significance of this increase is connected with the change in the acceleration of the flow to sonic velocity produced on the one hand by a constant-area expansion wave and on the other hand by a variable-area steady flow. The same maximum value ($\sqrt{(\gamma + 1)/2}$) is obtained if the flow in the launch tube is assumed to consist of (1) a steady-state flow going from the chamber into the entrance of the tube at sonic velocity and (2) an expansion wave from the sonic flow at the entrance to the base of the projectile. It seems clear that the flow will approach this model as a limit at infinite time.

Returning to a consideration of equation (B1), one can immediately place limits on the values of $\bar{\sigma}_s$ at the boundaries of region 1. The quantity $\bar{\sigma}_s$ must start with the value of unity (at $\bar{u}_s = 0$), since the pressure at the base of the projectile is equal to the pressure in the pump tube at the start of the launching cycle; at the $\bar{u}_s = (\gamma - 1)/2$ boundary $\bar{\sigma}_s$ must have the value given by equation (B2) for the start of region 2, since the pressure must be continuous from one region to the next. These limits prescribe the values of the constants in equation (B1), which becomes, after the limits have been imposed

for $0 \leq \bar{u}_s \leq \frac{\gamma - 1}{2}$

$$\bar{\sigma}_s + \bar{u}_s = 1 + \frac{2}{\gamma - 1}\left(\sqrt{\frac{\gamma + 1}{2}} - 1\right)\bar{u}_s \tag{B3}$$

The acceleration of the projectile is given by equation (11), and the relation between $\bar{p}_s$ and $\bar{\sigma}_s$ by equation (8). If equation (B3) is substituted into equation (8) for region 1, equation (B2) is substituted into

equation (8) for region 2, and equation (11) is integrated using equation (8), the following formulae are obtained for the velocity - travel history of the projectile:

For region 1: $0 \leq \bar{u}_s \leq (\gamma - 1)/2$

$$\bar{z} = \frac{1}{(\beta - 2)b^2}\left[\frac{\frac{\beta - 2}{\beta - 1} - (1 - b\bar{u}_s)}{(1 - b\bar{u}_s)^{\beta-1}}\right]_0^{\bar{u}_s} \tag{B4}$$

where

$$b = 1 - \left[\frac{2}{\gamma - 1}\left(\sqrt{\frac{\gamma + 1}{2}} - 1\right)\right]$$

For region 2: $\frac{\gamma - 1}{2} \leq \bar{u}_s \leq \sqrt{\frac{\gamma + 1}{2}}$

$$\bar{z}=(\bar{z})_{\bar{u} = \frac{\gamma-1}{2}} + \frac{1}{\beta - 2}\left[\frac{\frac{\beta - 2}{\beta - 1}\sqrt{\frac{\gamma + 1}{2}} - \left(\sqrt{\frac{\gamma + 1}{2}} - \bar{u}_s\right)}{\left(\sqrt{\frac{\gamma + 1}{2}} - \bar{u}_s\right)^{\beta-1}}\right]_{\frac{\gamma-1}{2}}^{\bar{u}_s} \tag{B5}$$

where $(\bar{z})_{\bar{u}=(\gamma-1)/2}$ = value of $\bar{z}$ at $\bar{u}_s = (\gamma - 1)/2$ from region 1.

Comparison of the two curves in figure 26 shows the increase in velocity due to chamberage.[2] A graph of the increase, represented by the quantity $(\bar{u}_{s_{ac}} - \bar{u}_{s_{sc}})/\bar{u}_{s_{sc}}$, is shown in figure 27. For the present gun most of the firings are covered by a range in $\bar{z}$ from 0.2 to 4.0, and it can be

[2]In the notation of figures 26 and 27, the subscript ac (i.e., avec chambrage) denotes the infinite-area, infinite-volume chamber, and the subscript sc (i.e., sans chambrage) denotes the bore-area, infinite-length chamber.

seen that the velocity increase changes but little over this interval. Consequently, the actual muzzle velocity can be computed from the chart velocity of figure 10 by multiplying the chart velocity, u_{s_L}, by a constant factor, as was suggested by the ballisticians of the NOL. However, it would be misleading to determine this factor as accurately as figure 27 might indicate. The theory gives a value for this factor of 1.2, but the experimental data show that this value is too high, which may be the accumulated result of errors in the various assumptions on which the analysis is based. The results of the present firing trials cluster about a value of 1.1 for the ratio of measured velocity to predicted velocity (see fig. 23), and it is believed that this figure represents the best value to take at the present time to obtain the increase in muzzle velocity above the theoretical value predicted for the gun with the bore-area, infinite-length chamber.

The modification to the use of the performance charts which accounts for the chamberage may be summarized in the following rule of thumb:

Take u_{s_L} as 0.9 times the desired muzzle velocity to enter figure 10.

It should be noted that the muzzle velocity depends critically on the pressure at which the shear disk breaks. In fact, the shear-disk break pressure controls almost completely the acceleration of the projectile during the first part of its motion, since changes in pressure in the pump tube after the rupture of the shear disk are so slow compared to the time scale of the projectile's motion that they have little effect on the projectile's velocity. Now, the pressure at rupture may vary somewhat from round to round since the strength of the shear disk may vary due to inhomogeneities in the material, manufacturing tolerances, and so forth. Also, the central plug may not break out of the shear disk cleanly on all rounds with the result that extra mass may be added to the projectile and ragged edges in the hole in the disk may partially obstruct the flow of helium into the launch tube. These factors will diminish the muzzle velocity. However, experience with the gun to date indicates that the muzzle velocity nearly always lies between u_{s_L} and $1.2 \times u_{s_L}$. This variation in muzzle velocity is ordinarily tolerable when the gun is used to launch models in a free-flight, aerodynamics range.

Effect of Pump Pressure Override

The performance charts are based on the assumption that the helium starts flowing into the launch tube at sonic velocity immediately. Actually, the flow velocity is zero to start with and increases toward sonic velocity as a limit. Consequently, the helium does not leave the pump tube as fast as assumed and the pressure increases beyond or overrides the design value, as indicated in the following sketch:

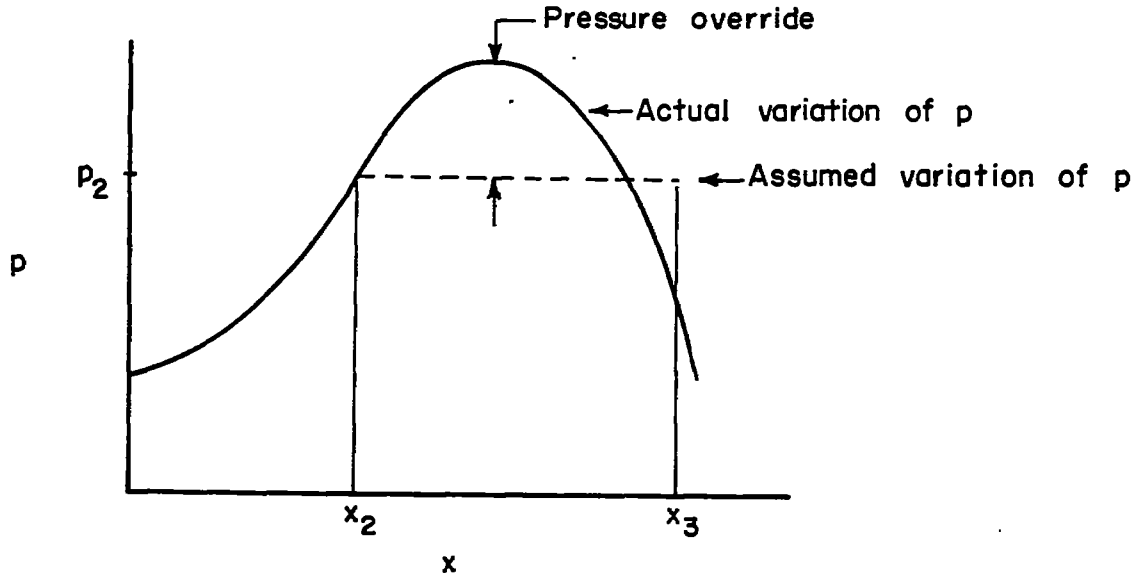

Sketch (j)

The pressure override was first discovered when the flow of helium in the pump tube during the pumping and launching cycles was studied for one specific case by the method of characteristics. The example chosen had the following loading conditions: $m_s = 0.15$ gram; $m_p = 171$ grams; $P_1 = 6{,}850$ psi; $p_1 = 248$ psi; $p_{2R} = 50{,}000$ psi = rupture pressure of the shear disk (m_s and p_2 are the same as for the example presented in the previous section). The helium pressure and the velocity of the pump piston are graphed for this case as functions of the distance moved by the pump piston in figures 28 and 29. Figure 28 shows that the pressure rises beyond the rupture pressure of 50,000 psi to a peak of 73,000 psi. Consequently, the override amounts to 23,000 psi, or nearly 50 percent in this case. The magnitude of this override is representative of the pressure history which will result if the performance charts are used without modification.

It is important to deviate from the subject of this section for a moment to mention one result obtained from this analysis. It was found that the pressure in the helium at any given instant of time during the compression stroke did not vary appreciably over the length of the pump tube. This result places the assumption of isentropic compression on a firm basis and justifies the assumption that the helium pressure prior to release of the projectile is a function solely of the position of the pump piston.

It might be supposed that the override is not particularly detrimental to the gun's performance, since the acceleration of the projectile is related, of course, to the pressure in the pump tube during the launching

cycle. However, two effects enter into this relation between pump pressure and projectile acceleration which render the override largely ineffective in increasing the acceleration. Both effects stem from the rapid rise in the projectile's velocity compared to the rate of pressure increase in the pump tube. The first effect, the time required for a pressure increase in the pump tube to reach the base of the projectile, is illustrated in the following sketch taken from the characteristic diagram.

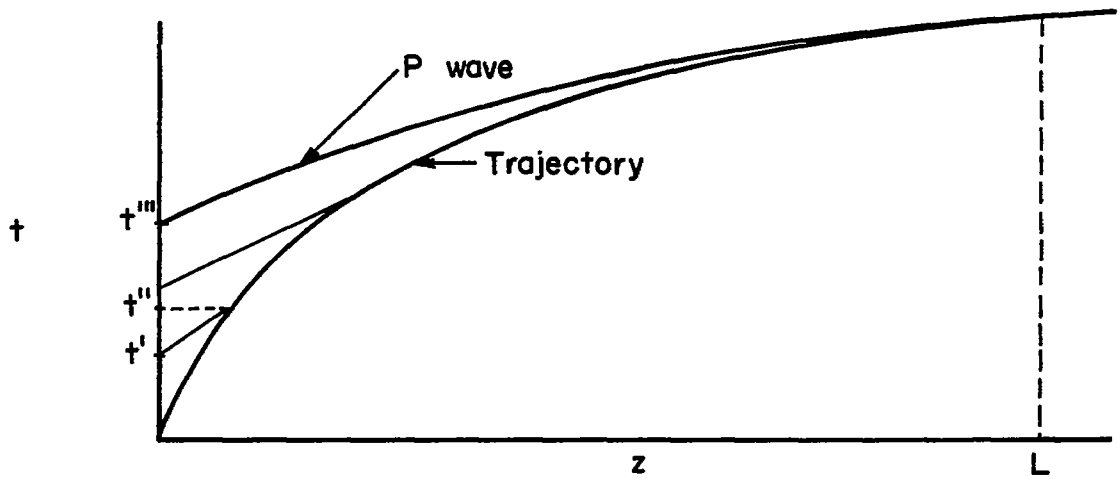

Sketch (k)

Pressure impulses coming from the pump tube are transmitted along the so-called P waves of the flow, and, referring to the sketch, one sees that an impulse starting at t' reaches the base of the projectile at a later time t''. Consequently, only part of the pressure rise taking place in any interval of time after the release of the projectile acts to accelerate the projectile. The transmission time steadily increases as the projectile moves out along the bore, and, in fact, there is a time t''' beyond which no further pressure changes in the pump tube will reach the projectile before it leaves the muzzle.

The second effect is the reduction in the magnitude of an increment in pressure that takes place as it traverses the flow from the nearly still helium in the pump tube to the rapidly moving helium adjacent to the projectile's base. Referring to the above sketch, one recalls that the characteristic quantity $(\bar{u} + \bar{\sigma})$ is transmitted unchanged along P waves, that is

$$\bar{u} + \bar{\sigma} = \bar{\sigma}_T \tag{B6}$$

where the subscript T denotes quantities in the pump tube. As the pressure in the pump tube is changed the quantity $\bar{\sigma}_T$ will change, and, if the effects of chamberage are ignored (for the sake of simplicity), the corresponding change in the value of $\bar{\sigma}_S$ when the wave reaches the

projectile's base, will be the same as the change in $\bar{\sigma}_T$, since the projectile's velocity does not vary in the instant that the wave strikes the base. This equality is evident on inspection of equation (B6) and may be written as follows:

$$\Delta\bar{\sigma}_s = \Delta\bar{\sigma}_T \tag{B7}$$

Since all changes in the flow are assumed to be isentropic, $\bar{p}$ and $\bar{\sigma}$ are related everywhere by an equation similar to equation (8); namely,

$$\bar{\sigma} = \bar{p}^{\frac{1}{\beta}} \tag{B8}$$

If the variation in pressure is considered to consist of a succession of small increments $\Delta\bar{p}$, the corresponding increment in $\bar{\sigma}$ is given by the differential of equation (B8) as follows:

$$\Delta\bar{\sigma} = \frac{\bar{p}^{-\frac{\beta-1}{\beta}}}{\beta} \Delta\bar{p} \tag{B9}$$

The increment in pressure at the base of the projectile caused by an increment in pressure in the pump tube is determined by substituting equation (B9) in equation (B7), multiplying by $\beta p_o^{1/\beta}$ (p_o is the reference pressure on which all isentropic calculations are based), and collecting terms, thereby obtaining

$$\Delta p_s = \left(\frac{p_s}{p_T}\right)^{\frac{\beta-1}{\beta}} \Delta p_T \tag{B10}$$

The exponent $(\beta - 1)/\beta$ has the value 4/5 for helium, and consequently the increment in pressure is reduced very nearly in proportion to the pressure itself, as can be seen from equation (B10). As a result, those pressure increases which reach the projectile after it has accelerated to an appreciable velocity are substantially reduced from their original value. They also act for a shorter time and these two factors make them very much less effective than they would have been if they had acted from the start of the motion.

The loss in effectiveness of the override may be illustrated by following a pressure increase from the pump tube to the base of the projectile. The same case that was treated in the preceding section

(m_s = 0.15 gram, p = 50,000 psi) will be taken as the example here (see figs. 24 and 25). Consider first a pressure pulse that reaches the projectile 80 microseconds after release, which is the time required for the pressure in the pump tube to rise from 50,000 psi to 60,000 psi. At this time the projectile has moved 5 inches, its velocity is 9,000 ft/sec, and the pressure at its base is 19,000 psi. If the pulse started with a magnitude of 100 psi, it will have a magnitude of only 40 psi as it reaches the projectile. Consider next the last pressure pulse that can act on the projectile, the one that reaches it right at the muzzle. Here the velocity is 17,000 ft/sec and the pressure is 3,500 psi. If the pulse was again 100 psi to start with, it will be only 10 psi as it reaches the projectile.

The foregoing discussion makes it clear that the pressure override decreases the maximum muzzle velocity that can be obtained for a fixed maximum allowable pressure. Of course, some override is necessary to insure rupture of the shear disk and to hold the pump pressure at or above the design value during the first part of the launching cycle. However, the rupture pressure should be close to the peak pressure for optimum performance within a given pressure limit.

Undoubtedly the final solution to the override problem will be found in a revision of the analysis to account correctly for the flow of helium out of the pump tube. However, an interim solution has been found in a modification to the use of the performance charts which, in practice, gives the desired results. The revised procedure to be followed in the use of the charts is this:

The design value of pressure, p_{2D}, used in the charts of figures 11, 12, and 13 is the shear-disk break pressure p_{2R} from the chart of figure 10 reduced by 10,000 psi. Stating the rule as a formula one obtains

$$p_{2D} = p_{2R} - 10{,}000 \text{ psi} \tag{B11}$$

The effect of this modification is to reduce the override to around 10,000 psi for projectiles weighing about 0.30 gram and shear-disk break pressures running around 50,000 psi. The reasons for the reduction in override are clear if one explores the changes in the pumping cycle brought about by the new loading conditions. The initial helium pressure, the powder charge, and the mass of the pump piston are all reduced, as can be seen from figures 11, 12, and 13. The velocity of the pump piston at station 2 is also reduced, as may be determined from calculations based on equations (41) and (43) and the powder charge calibration of figure 9 (e.g., if u_{p_2} is computed for the case treated in the preceding section, its value is reduced from 800 ft/sec to 700 ft/sec). Consequently, at the start of the launching cycle the pump piston is lighter and is traveling slower than called for by the analysis. (The helium is also a little hotter, since the compression ratio is greater.) As a result, the volume of the pump tube is not reduced as rapidly at the time that the pump piston

reaches station 2 as it would be with the unmodified loading conditions, and the pressure override is reduced proportionally.

A secondary effect of the modification in loading conditions is to reduce the time during which the pressure is held above the rupture value. The pump pressure probably falls below the shear-disk break pressure in the latter part of the launching cycle. On the other hand, a loss in pump pressure toward the last of the launching cycle probably has little effect on the muzzle velocity for the very same reasons that the pressure override is ineffective. As sketch (k) illustrates, any change in pump pressure after time t''' cannot reach the projectile before it leaves the muzzle.

It is well to conclude this section on the pressure override with a note of caution. The rule given by equation (B11) is a purely empirical one and the value of 10,000 psi is quite arbitrary. It is fairly firm for projectile masses and rupture pressures close to the values quoted (0.30 gram and 50,000 psi). On the other hand, if the masses and pressures differ markedly from these values, the override may well become excessive.

The rule of equation (B11) will require further modification in order to adapt it to the full range of operating conditions. At present, great caution should be exercised in operating the gun at high pressure. The helium pressure in the coupling should be measured on every round. The loading conditions should be varied in small steps. Only in this way will it be possible to obtain the highest velocities from the gun within the limits of pressure set by its strength.

APPENDIX C

COMPUTATIONAL PROCEDURE FOR PERFORMANCE OF PISTON-COMPRESSOR TYPE LIGHT-GAS GUN

In outlining the computational procedure to be followed in computing the performance of a light-gas gun of the piston-compressor type, it is considered that the dimensions of the gun and the light gas to be used have been chosen and are fixed quantities at the start of the computation. The initial conditions for the computation are the projectile mass, m_s, and the muzzle velocity, u_{s_L}. The steps of the computation are given in sequence in the following outline. It will be recalled that the states designated by the subscripts 0 and 2 are the same in this application of the analysis (i.e., $p_0 = p_2$).

1. Assume a value for a_2; (if helium is used, a representative value is 10,000 ft/sec).

2. Compute $\bar{u}_s$ and α_0 from u_s, a_2, and γ.

3. Compute $\bar{z}$ from the following equation:

$$\bar{z} = \frac{\gamma - 1}{2}\left\{\left[\frac{\left(\frac{2}{\gamma + 1}\right) - (1 - \bar{u}_s)}{(1 - \bar{u}_s)^{\frac{\gamma+1}{\gamma-1}}}\right] + \frac{\gamma - 1}{\gamma + 1}\right\} \tag{C1}$$

4. Compute $\bar{t}$ from the following equation:

$$\bar{t} = \frac{\gamma - 1}{\gamma + 1}\left[(1 - \bar{u}_s)^{-\frac{\gamma+1}{\gamma-1}} - 1\right] \tag{C2}$$

5. Compute p_2 from $\bar{z}$ of step 3, and compute t_L from p_2 of this step and $\bar{t}$ of step 4.

6. Compute x_2 from

$$x_2 = x_3 + a_2 t_L \frac{S}{A_p}\left(\frac{2}{\gamma + 1}\right)^{\frac{\gamma+1}{2(\gamma-1)}} \tag{C3}$$

7. Compute a_2 from

$$a_2 = a_1\left(\frac{x_1}{x_2}\right)^{\frac{\gamma-1}{2}} \tag{C4}$$

8. Iterate, starting with the value of a_2 from step 7 in step 1 and repeating steps 1 through 7 until the values of a_2 from steps 1 and 7 agree within the desired accuracy. Experience has shown that the process is rapidly convergent and agreement within 1 percent is usually obtained with three or four iterations. One-percent accuracy is probably all that is justified considering the uncertainties in the basic assumptions of the analysis.

9. Compute $\bar{u}_s$ using the final value of a_2 from step 8.

10. Compute $\bar{z}$ and $\bar{t}$ from equations (C1) and (C2) using $\bar{u}_s$ from step 9.

11. Compute p_2 using $\bar{z}$ from step 10. The value of p_2 obtained in this step is to be used in all subsequent calculations.

12. Determine the thickness of the shear disk from p_2 of step 11. For the Ames gun, the relation between shear-disk thickness and rupture pressure (p_2 of step 11) was determined by experiment (see fig. 14).

13. Compute the initial helium pressure, p_1, from

$$p_1 = p_2\left(\frac{x_2}{x_1}\right)^{\gamma} \tag{C5}$$

14. Compute t_L from $\bar{t}$ of step 10.

15. Compute the mass of the pump piston, m_p, from the following equation, setting $P_2 = 0$:

$$m_p = \frac{A_p(p_2 - P_2)t_L^2}{2(x_2 - x_3)} \tag{C6}$$

16. Compute u_{p_2} from the following equation, setting $P_2 = 0$:

$$u_{p_2} = \frac{A_p(p_2 - P_2)t_L}{m_p} \tag{C7}$$

17. Compute P_1 from

$$P_1 = \frac{c(\Gamma - 1)\left\{\frac{m_p u_{p_2}^2}{2A_p x_1} + \frac{p_1}{\gamma - 1}\left[\left(\frac{x_1}{x_2}\right)^{\gamma-1} - 1\right]\right\}}{\left\{1 - \frac{1}{\left[1 + c\left(1 - \frac{x_2}{x_1}\right)\right]^{\Gamma-1}}\right\}} \tag{C8}$$

where c is given by

$$c = \frac{x_1 A_p}{U}\left[1 + \frac{m_p}{m_v}\left(\frac{A_v}{A_p}\right)^2\right] \tag{C9}$$

18. Compute P_2 from

$$P_2 = \frac{P_1}{\left[1 + c\left(1 - \frac{x_2}{x_1}\right)\right]^{\Gamma}} \tag{C10}$$

19. Repeat steps 15 through 18 using the value of P_2 from step 18 and continue the iteration until the values of P_2 from successive iterations agree within the desired accuracy. Usually three or four iterations are sufficient to obtain agreement within 1 percent.

20. Compute m_p, u_{p_L}, and P_1 using the final value of P_2 from step 19.

21. The last part of the calculation is to compute the powder charge, m_c. A choice is involved here depending on whether or not firings have been carried out with the open-ended pump tube to calibrate the powder (see the section in this report: "ANALYSIS: Pumping Cycle"). If a powder-calibration firing has not been carried out, the powder charge may be computed from the following equation:

$$Pv = RT \tag{C11}$$

where RT is called the force constant of the powder (a typical value is 70 long tons/sq in. × cc/gram - see Chapter Three: "The Thermochemistry of Propellants" of ref. 15), or the charge may be computed from more exact interior ballistic methods (see ref. 11).

22. If powder-calibration firings have been carried out, (a) compute u_{p_L} from the following equation using the values of P_1 and m_p from step 20.

$$u_{p_L}{}^2 = \frac{2A_pL_pP_1}{m_pC(\Gamma - 1)}\left[1 - \frac{1}{(1 + C)^{\Gamma-1}}\right] \tag{C12}$$

where the factor C is defined by the following equation:

$$C = \frac{A_pL_p}{U}\left[1 + \frac{m_p}{m_v}\left(\frac{A_v}{A_p}\right)^2\right] \tag{C13}$$

(b) and use the results of the calibration firings to obtain m_c from u_{p_L} of step 21(a) and m_p of step 20 (for an example of a charge calibration chart see fig. 9).

REFERENCES

1. Allen, H. Julian, and Eggers, A. J., Jr.: A Study of the Motion and Aerodynamic Heating of Missiles Entering the Earth's Atmosphere at High Supersonic Speeds. NACA TN 4047, 1957. (Formerly NACA RM A53D28)

2. Eggers, A. J., Jr., Allen, H. Julian, and Neice, Stanford E.: A Comparative Analysis of the Performance of Long Range Hypervelocity Vehicles. NACA TN 4046, 1957. (Formerly NACA RM A54L10)

3. Sibulkin, M.: Heat Transfer Near the Forward Stagnation Point of a Body of Revolution. Jour. Aero. Sci., vol. 19, no. 8, Aug. 1952, pp. 570-571.

4. Ivey, H. Reese, and Cline, Charles W.: Effect of Heat-Capacity Lag on the Flow Through Oblique Shock Waves. NACA TN 2196, 1950.

5. Moore, L. L.: A Solution of the Laminar Boundary Layer Equations for a Compressible Fluid With Variable Properties, Including Dissociation. Jour. Aero. Sci., vol. 19, no. 8, Aug. 1952, pp. 505-518.

6. Heat Transfer - A Symposium held at the University of Michigan, 1952. Engineering Research Institute, Univ. of Michigan, 1953.

7. Seiff, Alvin, James, Carlton S., Canning, Thomas N., and Boissevain, Alfred G.: The Ames Supersonic Free-Flight Wind Tunnel. NACA RM A52A24, 1952.

8. Charters, A. C.: Some Ballistic Contributions to Aerodynamics. Jour. Aero. Sci., vol. 14, no. 3, Mar. 1947, pp. 155-166.

9. Canning, Thomas N., and Denardo, Billy Pat: Investigation of Lift and Center of Pressure of Low-Aspect-Ratio, Cruciform, Triangular, and Rectangular Wings in Combination With a Slender Fuselage at High Supersonic Speeds. NACA RM A52C24, 1952.

10. Murphy, C. H.: Data Reduction for the Free Flight Spark Ranges. BRL Rep. No. 900, Aberdeen Proving Ground, Feb. 1954.

11. Corner, J.: Theory of Interior Ballistics of Guns. John Wiley and Sons, Inc., New York, 1950.

12. Seigel, Arnold E.: A Study of the Applicability of the Unsteady One-Dimensional Isentropic Theory to an Experimental Gun. NAVORD Rep. 2692, U. S. Naval Ordnance Lab., White Oak, Md., July 15, 1952.

13. Seigel, Arnold E.: An Experimental Solution to the Lagrange Ballistic Problem. NAVORD Rep. 2693, U. S. Naval Ordnance Lab., White Oak, Md., Sept. 1, 1952.

14. Seigel, Arnold E.: The Rapid Expansion of Compressed Gases Behind a Piston. Ph.D. Thesis, Univ. of Amsterdam, Jan. 23, 1952.

15. Courant, R., and Friedrichs, K. O.: Supersonic Flow and Shock Waves. Interscience Publishers, Inc., New York, 1948.

16. Hayes, Thomas J.: Elements of Ordnance. John Wiley and Sons, Inc., New York, 1938.

17. Dimeff, J., Carson, J. A., and Charters, A. C.: A Piston-Type Strain Gage for Measuring Pressures in Interior Ballistics Research. Review of Scientific Research, Sept. 1955.

18. Thomas, Richard N., and Whipple, Fred L.: The Physical Theory of Meteors. II. Astroballistic Heat Transfer. The Astrophysical Journal, vol. 114, no. 3, Nov. 1951, pp. 448-465.

19. Allen, William A., Rinehart, John S., and White, W. C.: Phenomena Associated With the Flight of Ultra-Speed Pellets. Part I. Ballistics. Jour. Appl. Phys., vol. 23, no. 1, Jan. 1952, pp. 132-137.

TABLE I.- FIXED QUANTITIES FOR THE LIGHT-GAS GUN

Launch tube	
Length, L, ft	4.40
Diameter, d_s, in.	0.229
Pump tube	
Length, L_p, ft	9.24
Diameter, d_p, in.	0.786
Pump piston stop-reverse position, x_3, ft	0.2
Powder chamber	
Volume, U	54.0 in.^{3} = 0.0313 ft^3
Valve tube	
Length, L_v, ft	4.66
Diameter, d_v, in.	0.822
Ratio of piston masses, m_v/m_p	3.15
Ratio of specific heats	
Powder gas, Γ	1.300
Helium, γ	1.667

TABLE II.- SUMMARY OF FIRING DATA

Round No.	Projectile design	m_p,[a] grams	Type of shear-disk break	Design pressure, p_{2D}, psi	Rupture pressure, p_{2R}, psi	Peak pressure, p_2, psi	x_s,[b] ft	p_v,[c] mmHg	u_{s_L},[d] ft/sec	u_m,[e] ft/sec	$_2u_s$,[f] ft/sec	$\frac{u_m}{u_{s_L}}$ [g]
1	Nylon cylinder	0.311	Ragged	20,000	20,000	17,800	0.23	24	8,900	- - -	- - -	- - -
2	Nylon cylinder	.311	Clean	20,000	20,000	29,000	.22	26	8,900	9,870	9,700	1.11
3	Nylon cylinder with 0.003 in. thick brass cap on front	.311	Ragged	30,000	30,000	39,000	.24	22	10,000	10,600	9,700	1.06
4	Nylon cylinder	.311	Ragged	30,000	30,000	40,000	.26	He @ 760	10,000	- - -	6,960	- - -
5	Magnesium cylinder	.311	Eroded-Melted	40,000	20,000	56,000	.12	27	8,900	9,000	8,400	1.01
6	Nylon cylinder and 1/8 in. diam. 75 - S-T sphere	.311	Clean	40,000	50,000	56,000	.25	30	11,400	12,000	11,600	1.05
7	Nylon cylinder	.221	Clean	40,000	50,000	54,000	.27	42	12,350	12,600	11,800	1.02
8	Nylon cylinder	.311	Clean	50,000	60,000	72,000	.04	31	11,900	12,800	11,800	1.08
9	Nylon cylinder	.192	Ragged	60,000	61,000	109,000	.23	34	13,400	12,100	11,600	.90
10	Nylon cylinder	.311	Clean	60,000	70,000	84,000	.07	40	12,370	12,100	11,600	.98
11	Nylon cylinder	.211	Clean	60,000	70,000	84,000	- - -	8	13,450	15,400	12,100	1.15

(a) m_p = projectile mass
(b) x_s = stop reversal position of pump piston
(c) p_v = pressure in vacuum tank
(d) u_{s_L} = muzzle velocity predicted (fig. 10) based on p_{2R}
(e) u_m = measured muzzle velocity
(f) $_2u_s$ = mean velocity measured between second and third grids
(g) u_m/u_{s_L} = ratio of measured muzzle velocity to predicted muzzle velocity

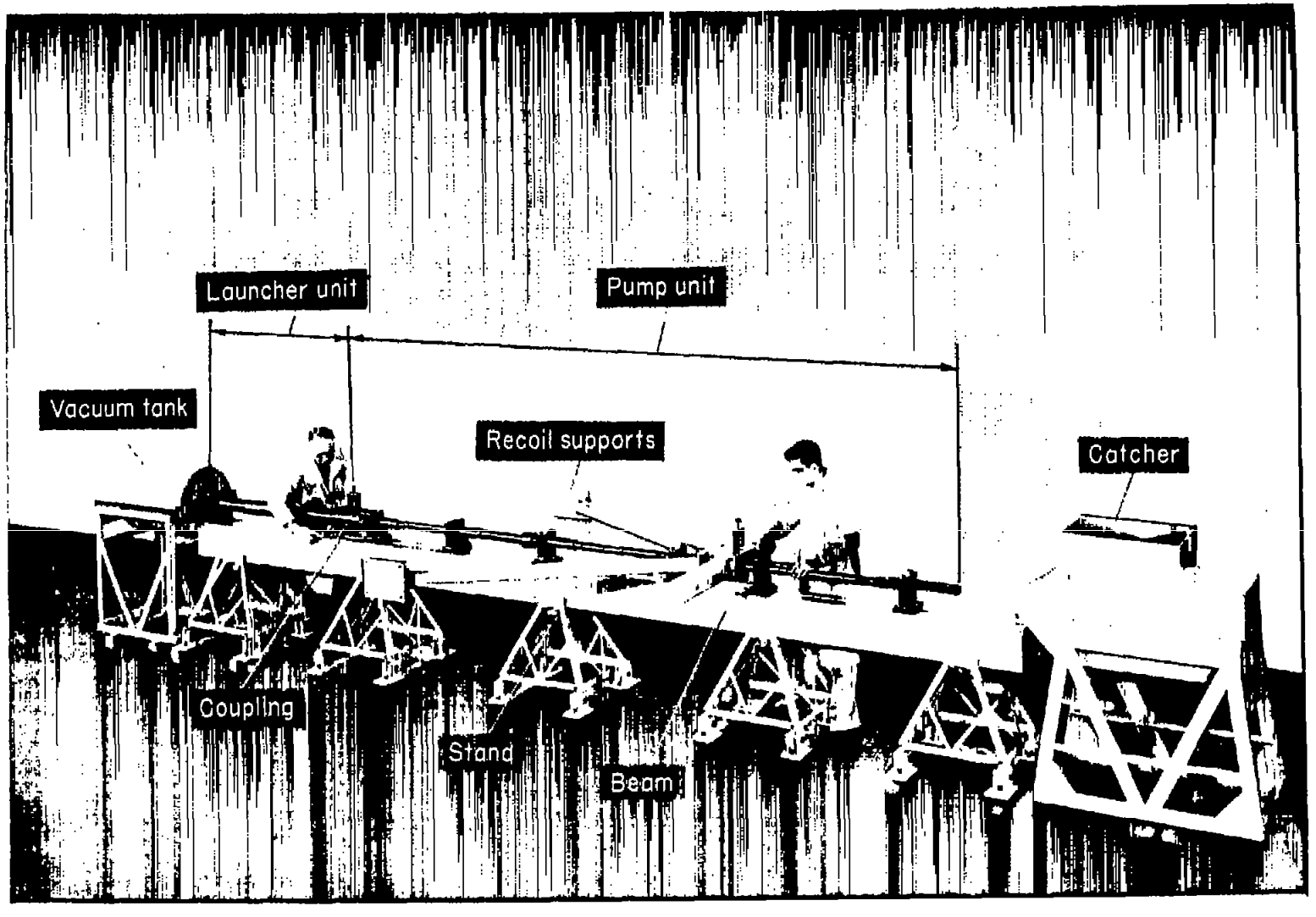

Figure 1.- The light-gas gun.

A-18764.1

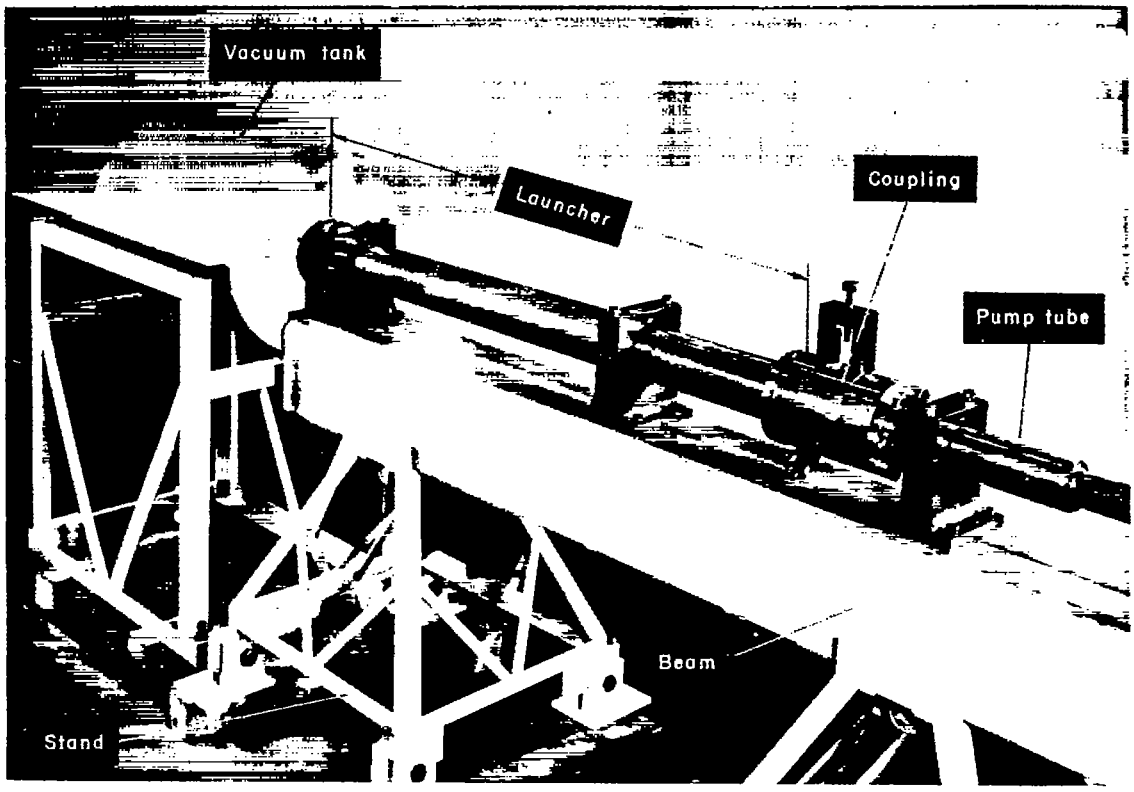

A-18761.2

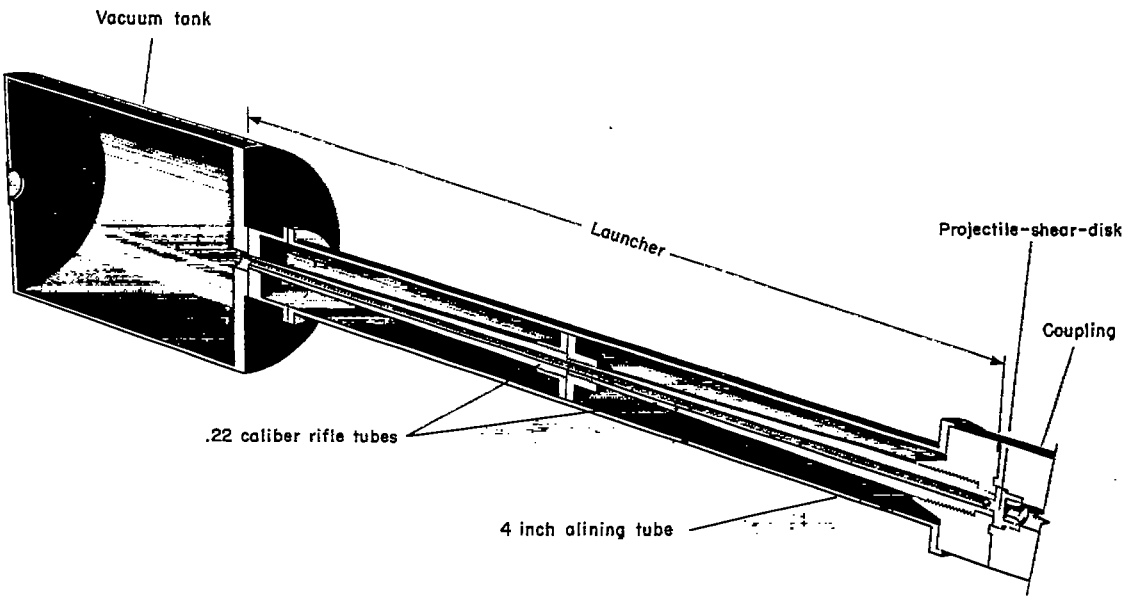

Figure 2.- The launcher unit.

A-19998

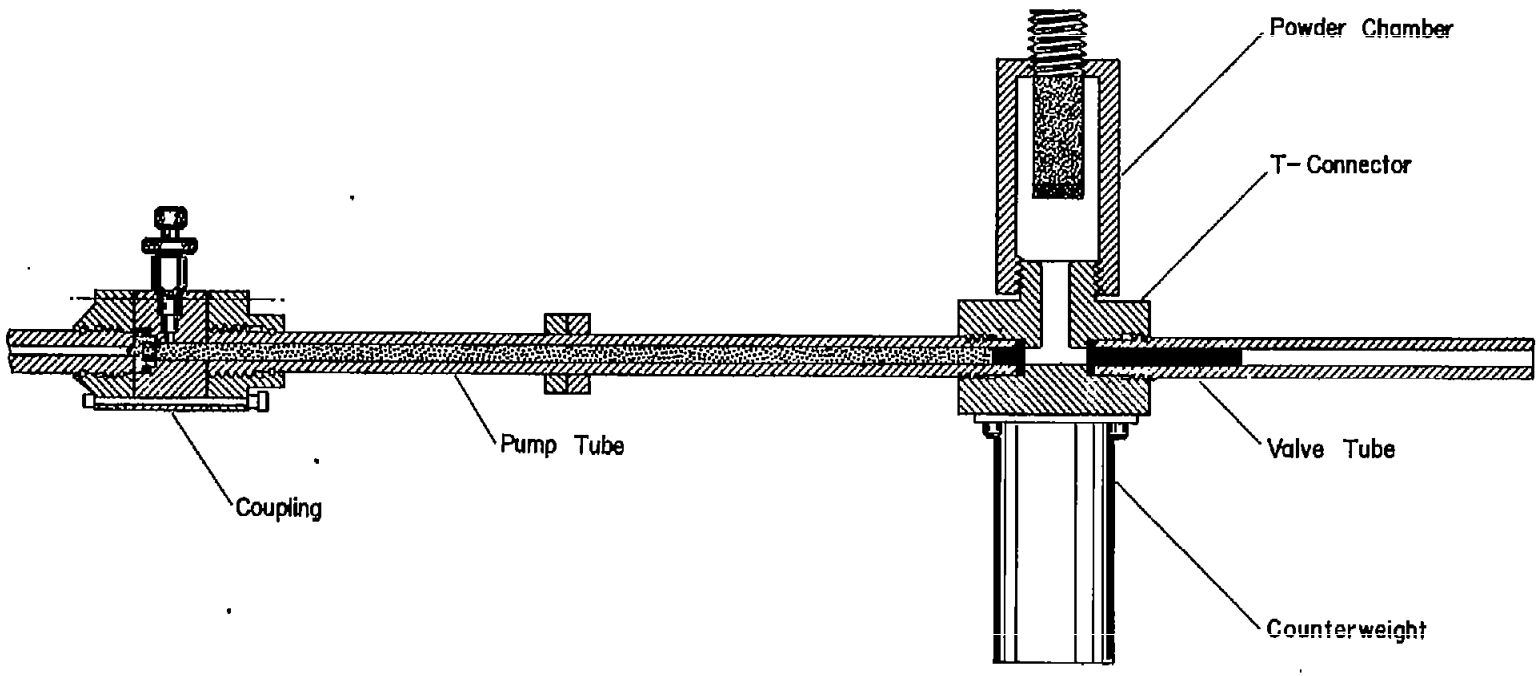

Figure 3.- The pump unit.

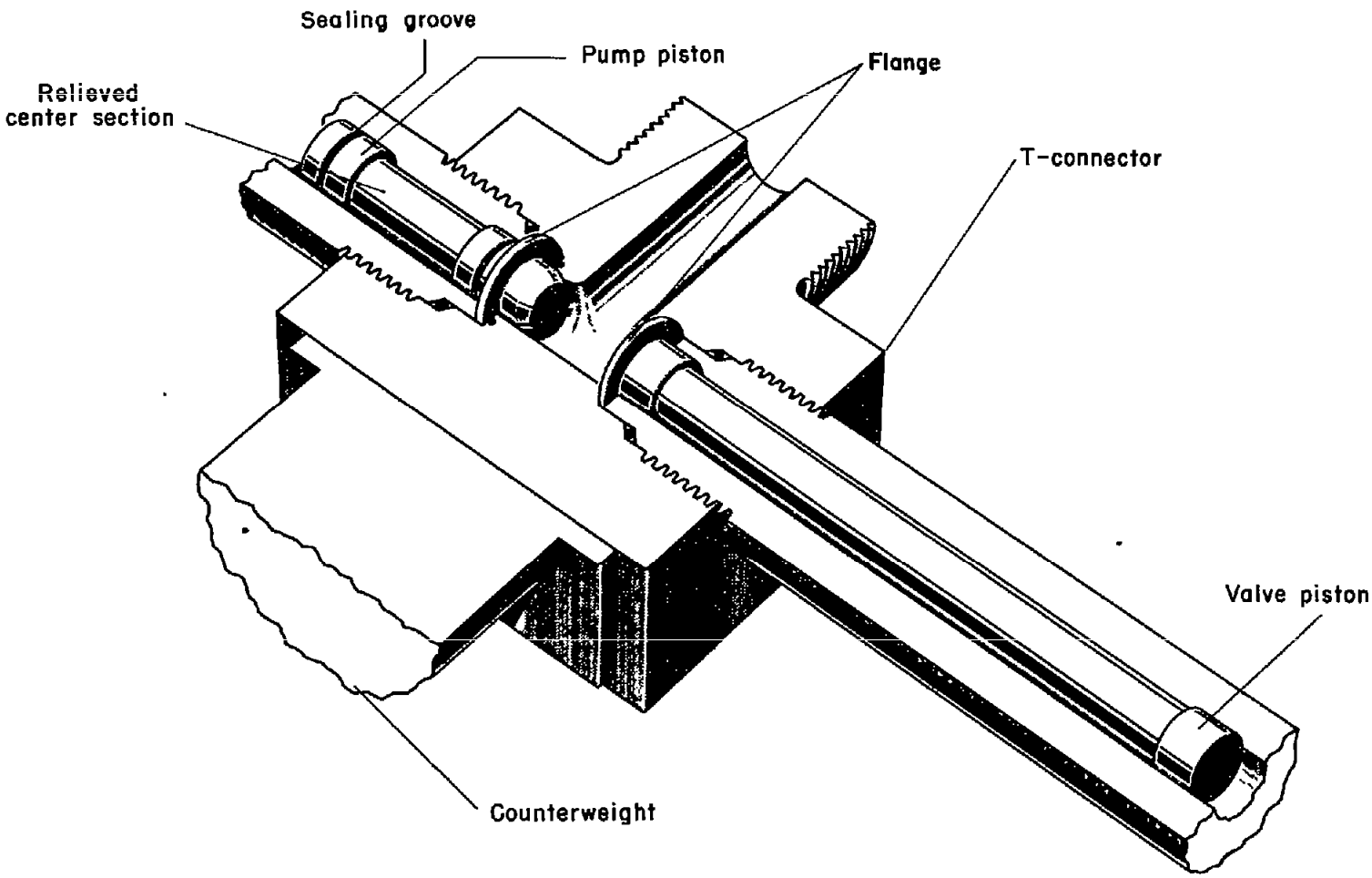

Figure 4.- Loading positions of pump and valve pistons.

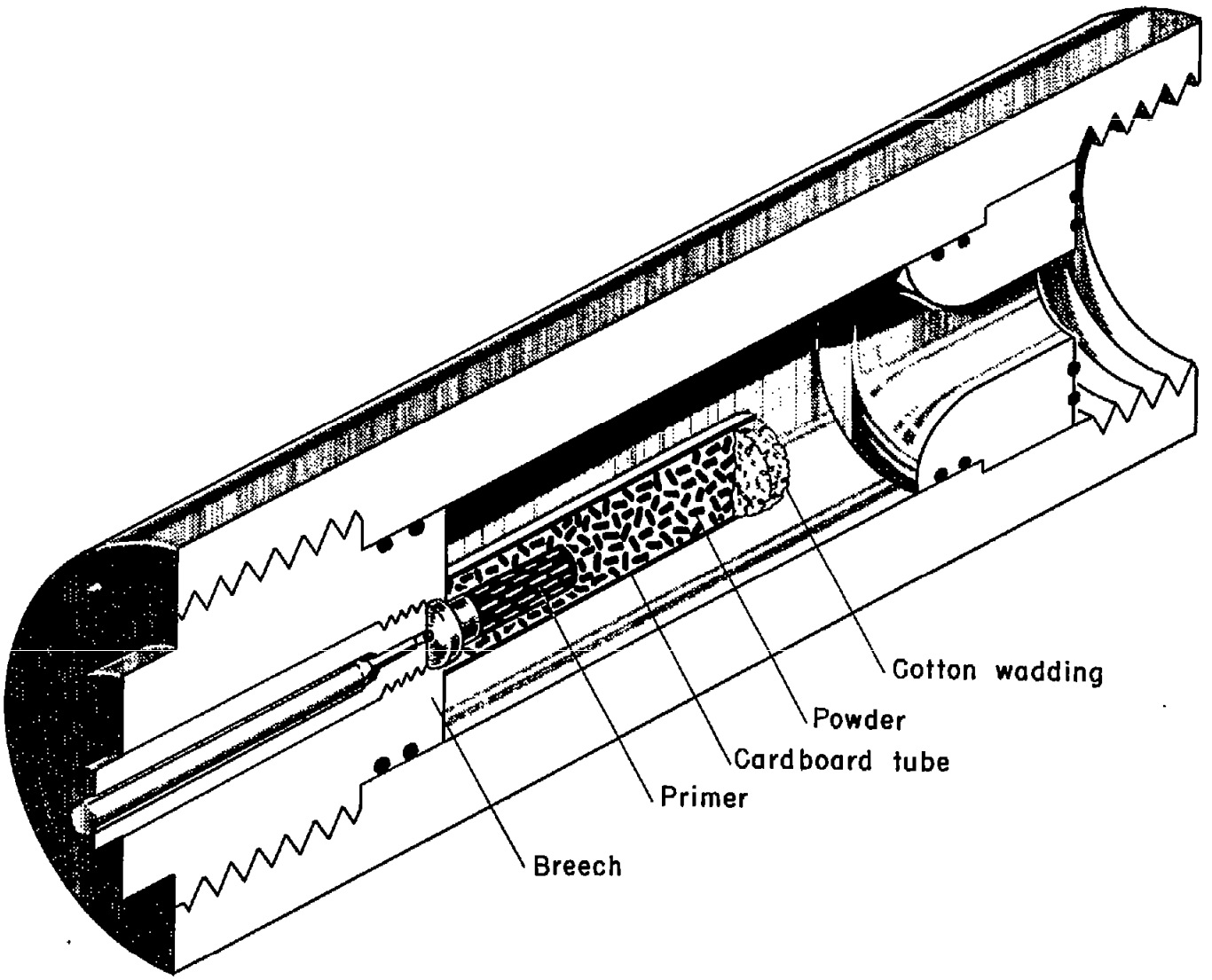

Figure 5.- The powder chamber.

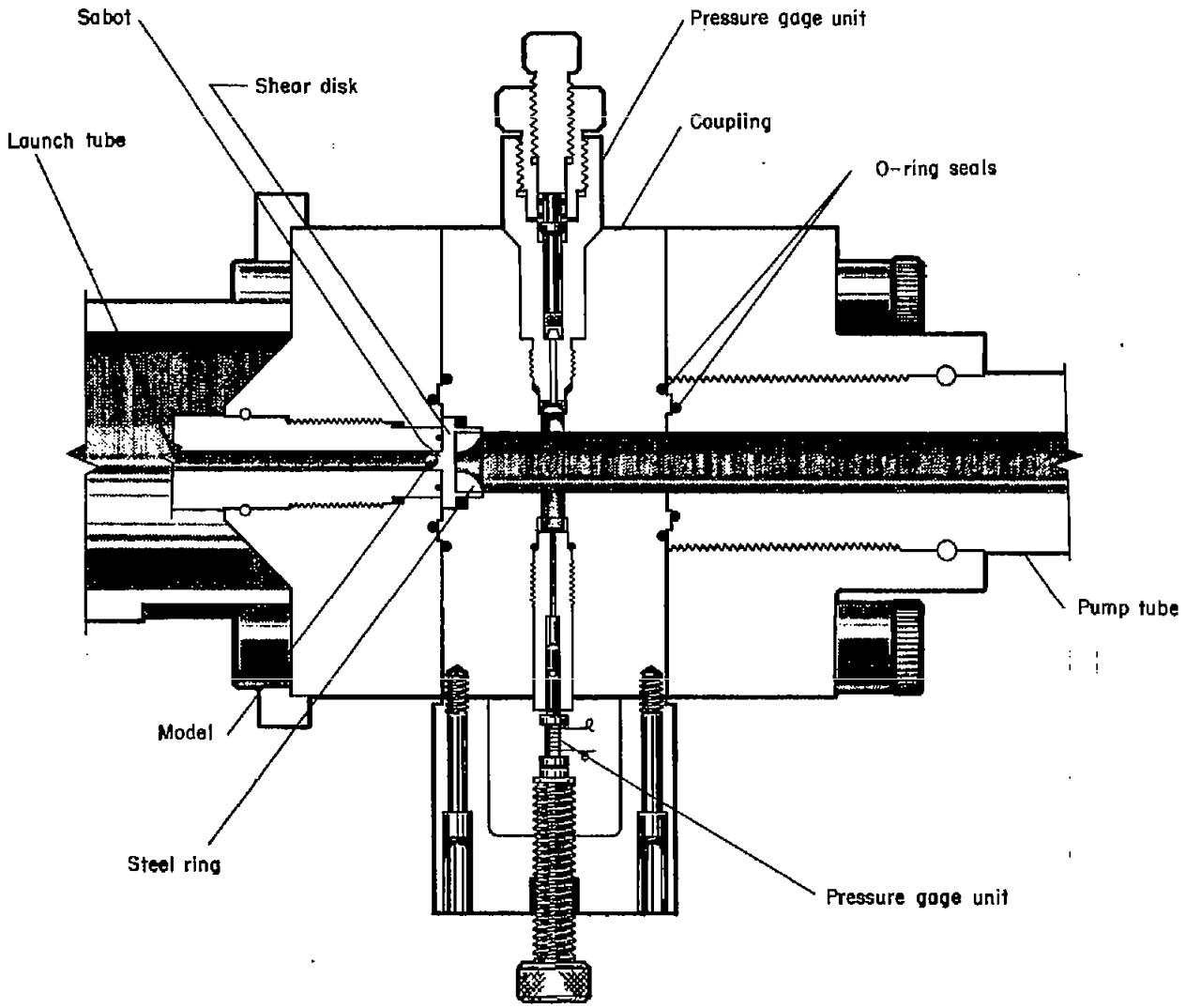

Figure 6.- The coupling.

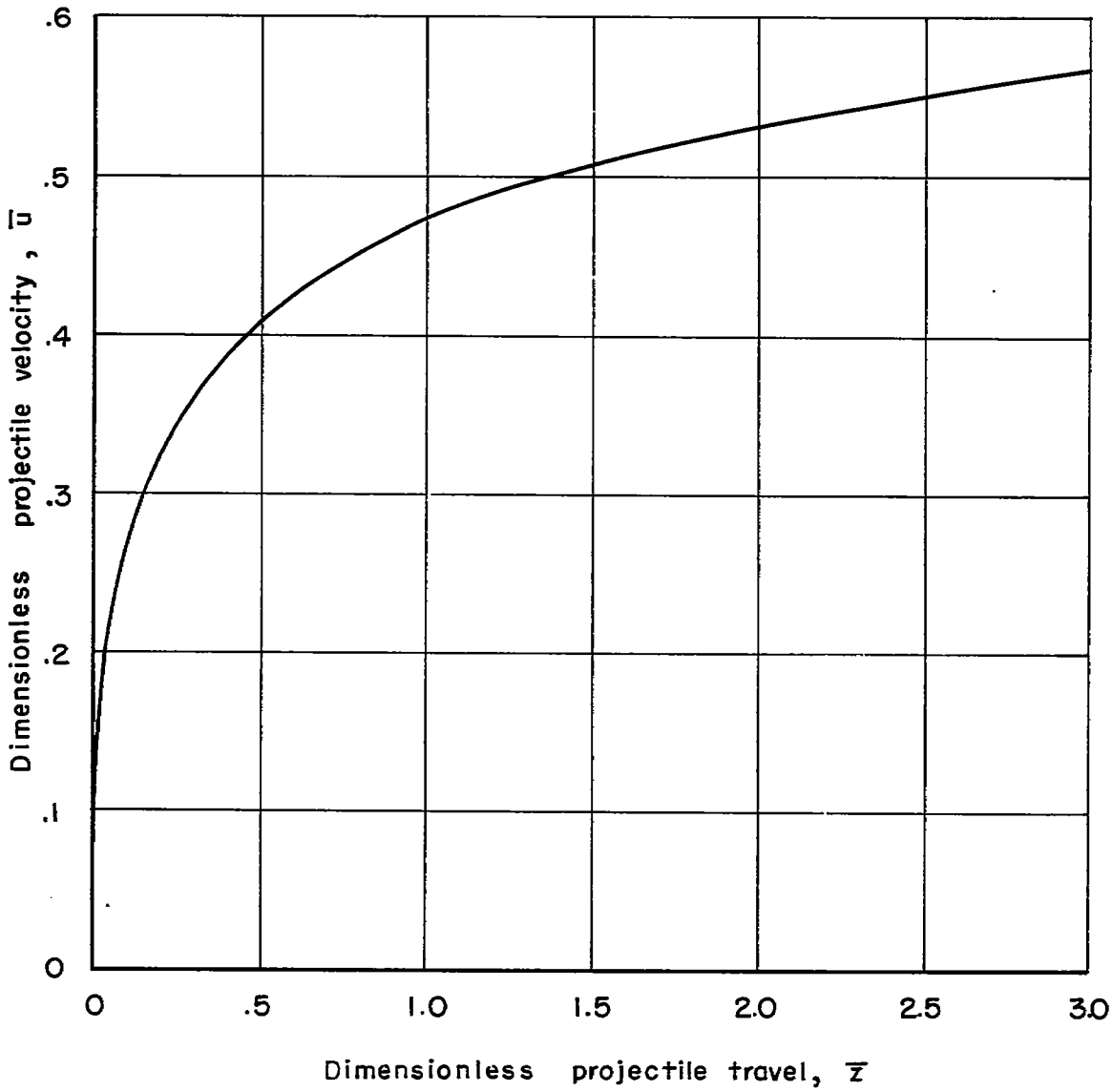

Figure 7.- Interior ballistic chart: variation of velocity with distance for γ = 5/3 (helium).

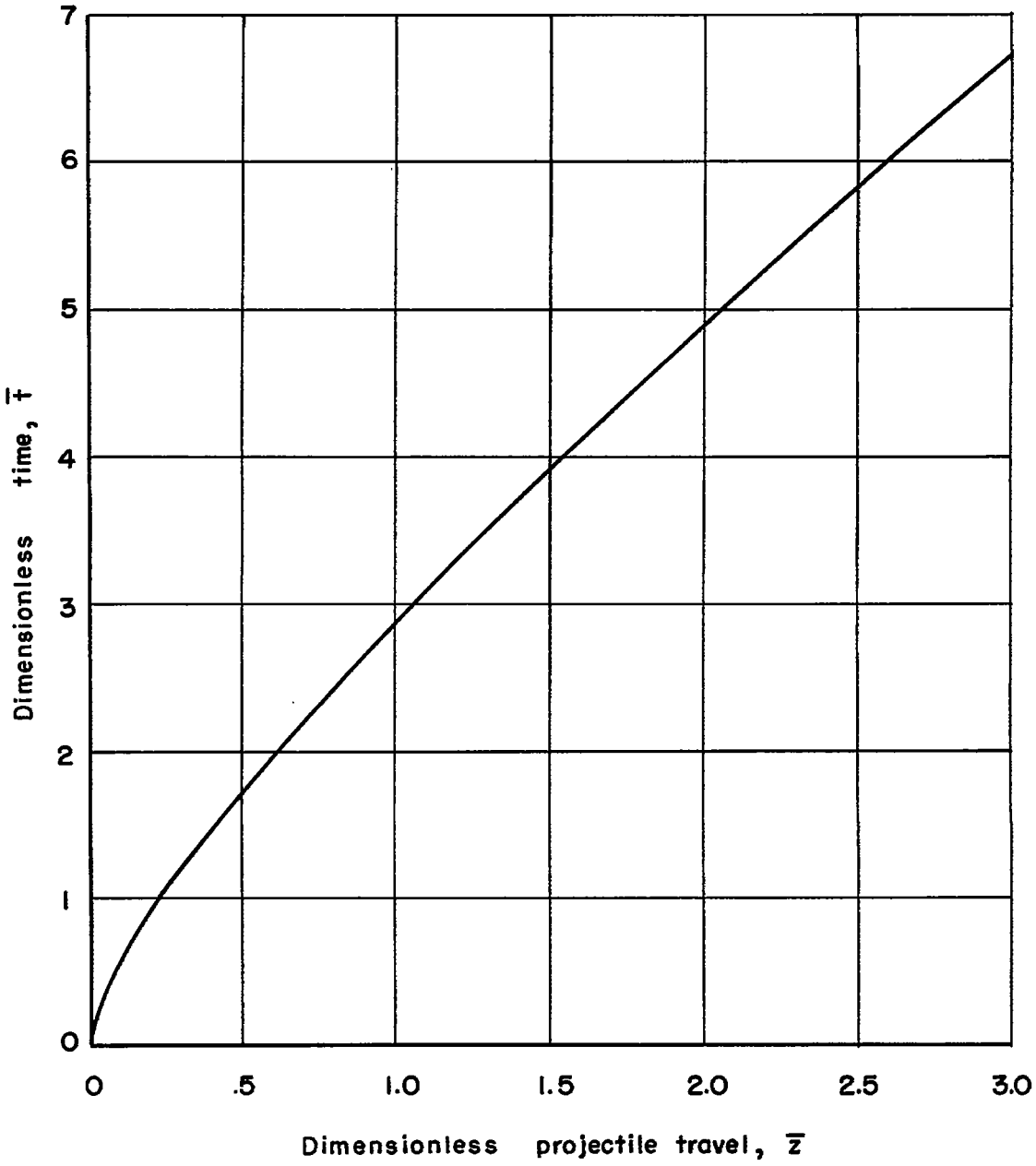

Figure 8.- Interior ballistic chart: variation of time with distance for $\gamma = 5/3$ (helium).

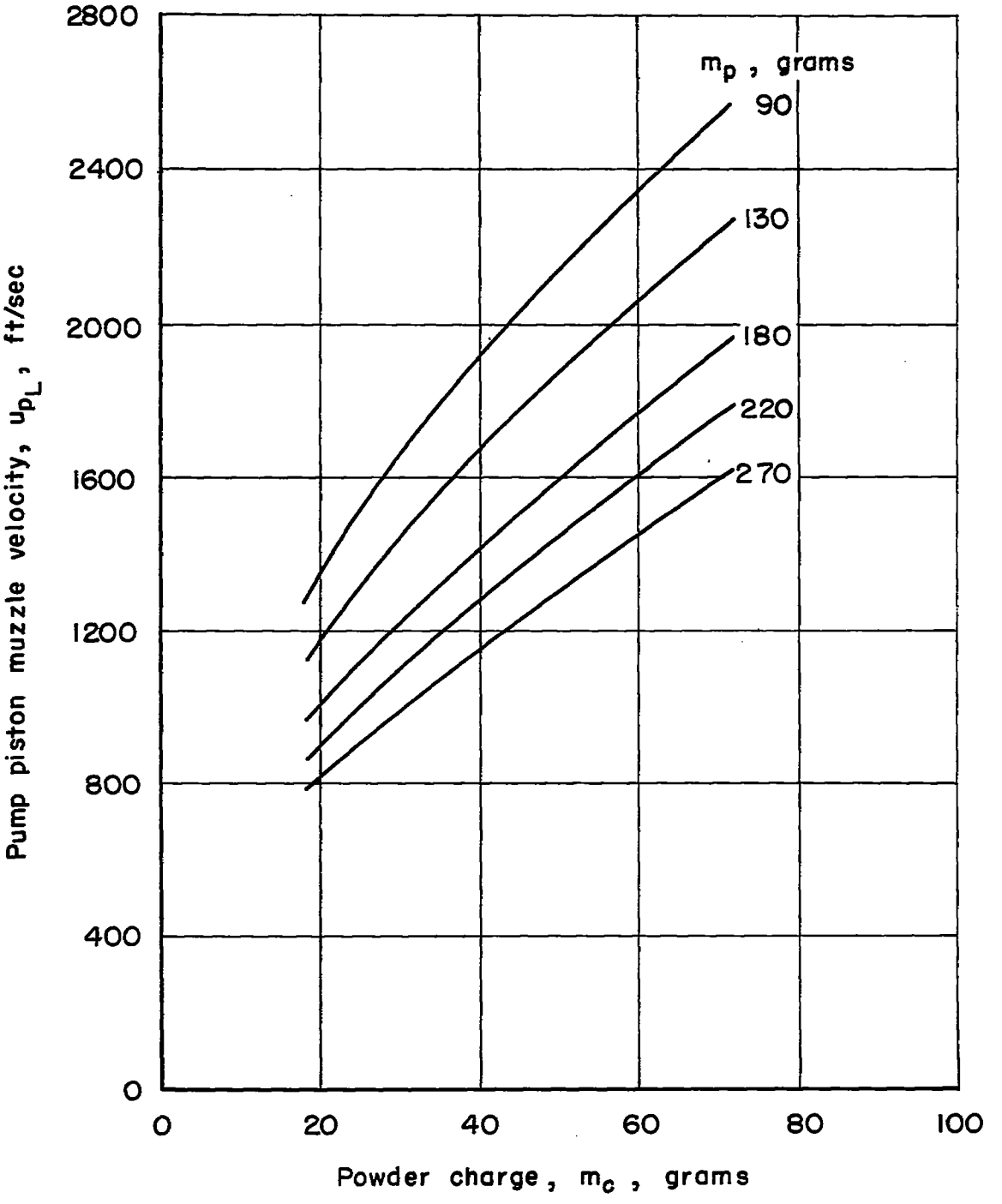

Figure 9.- Powder calibration chart.

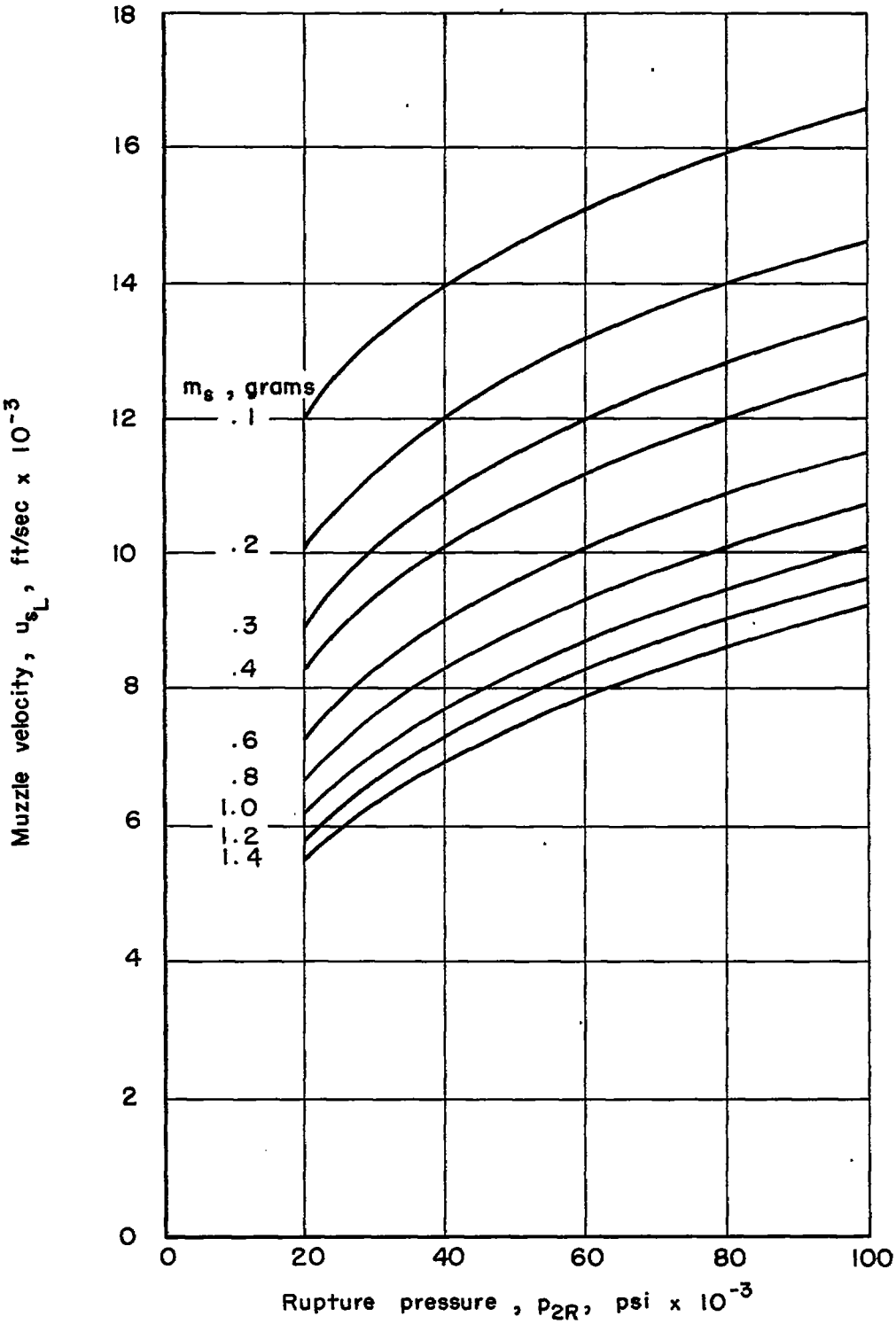

Figure 10.- Performance chart, muzzle velocity versus rupture pressure.

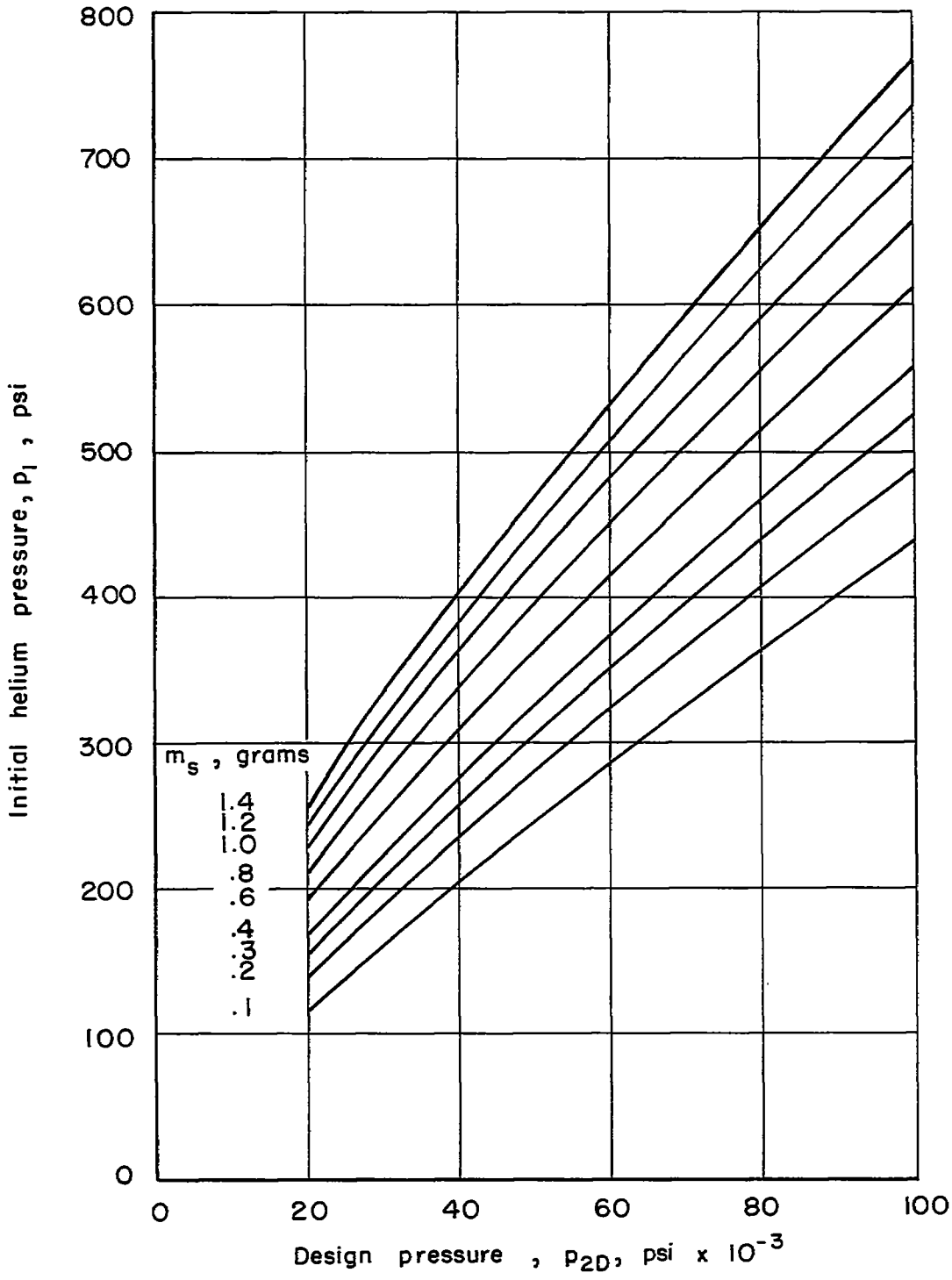

Figure 11.- Performance chart, initial helium pressure versus design pressure.

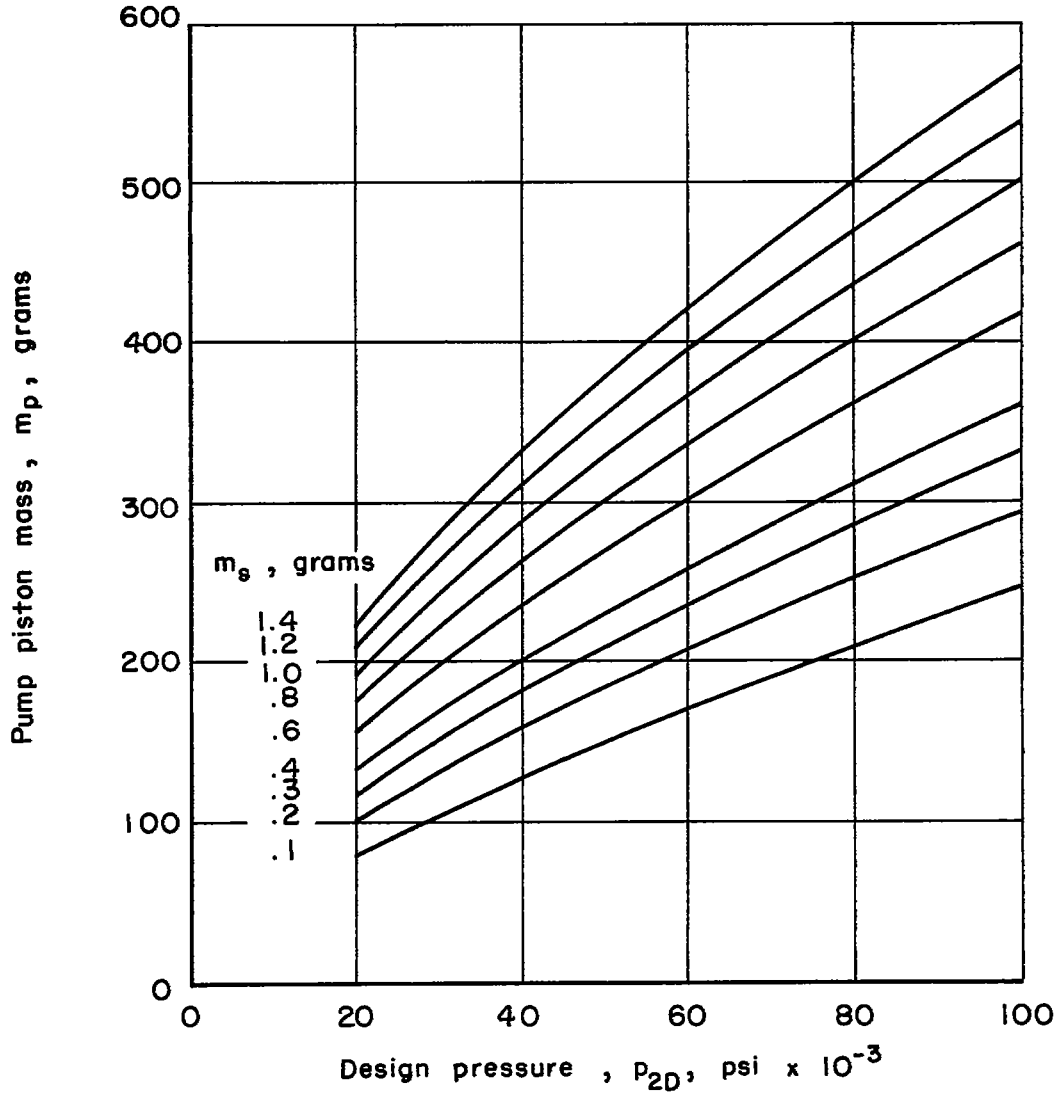

Figure 12.- Performance chart, pump piston mass versus design pressure.

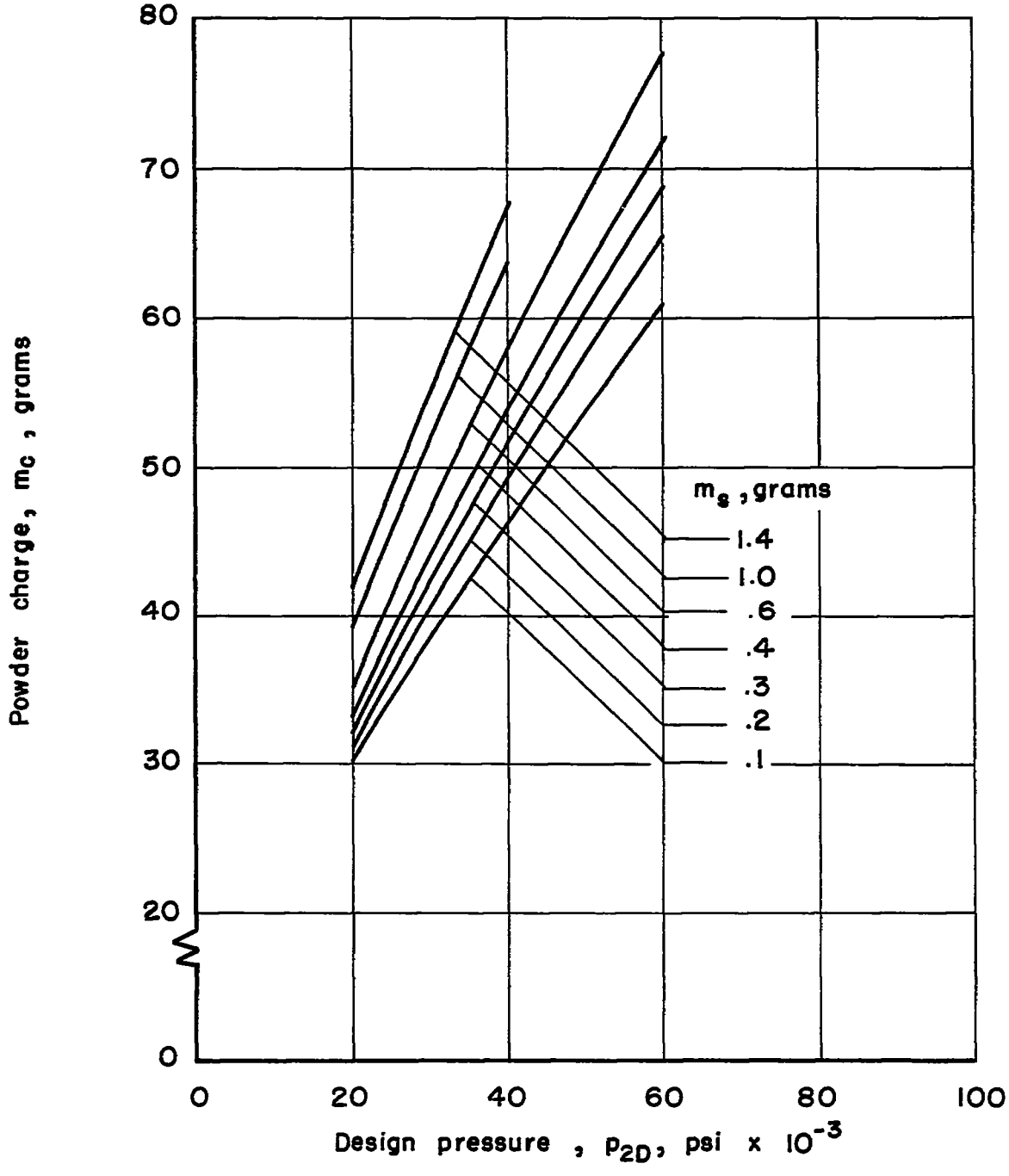

Figure 13.- Performance chart, powder charge versus design pressure.

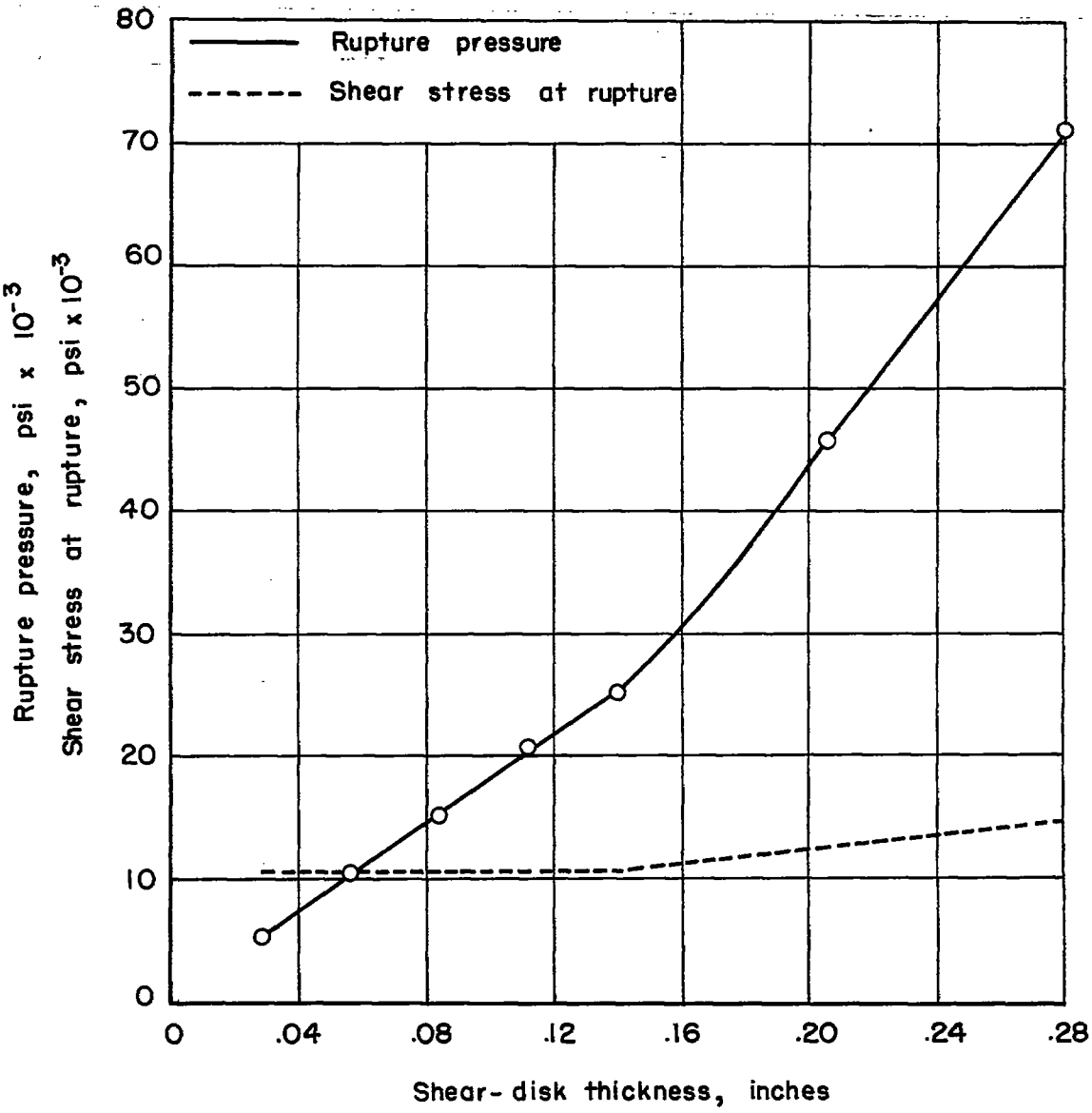

Figure 14.- Rupture pressure and shear stress at rupture of shear disks determined by hydraulic tests. (material: nylon)

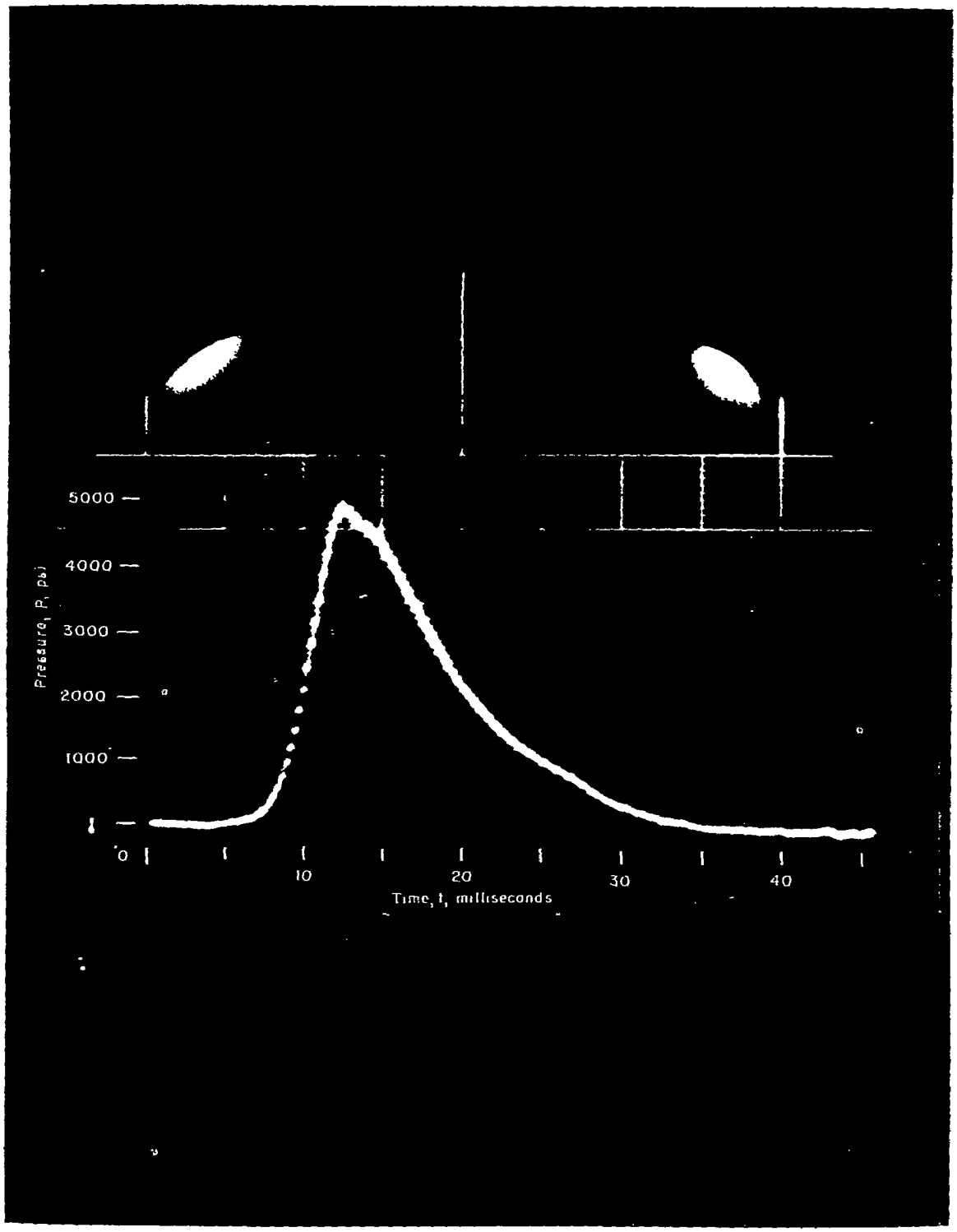

Figure 15.- Typical powder pressure record. A-20115

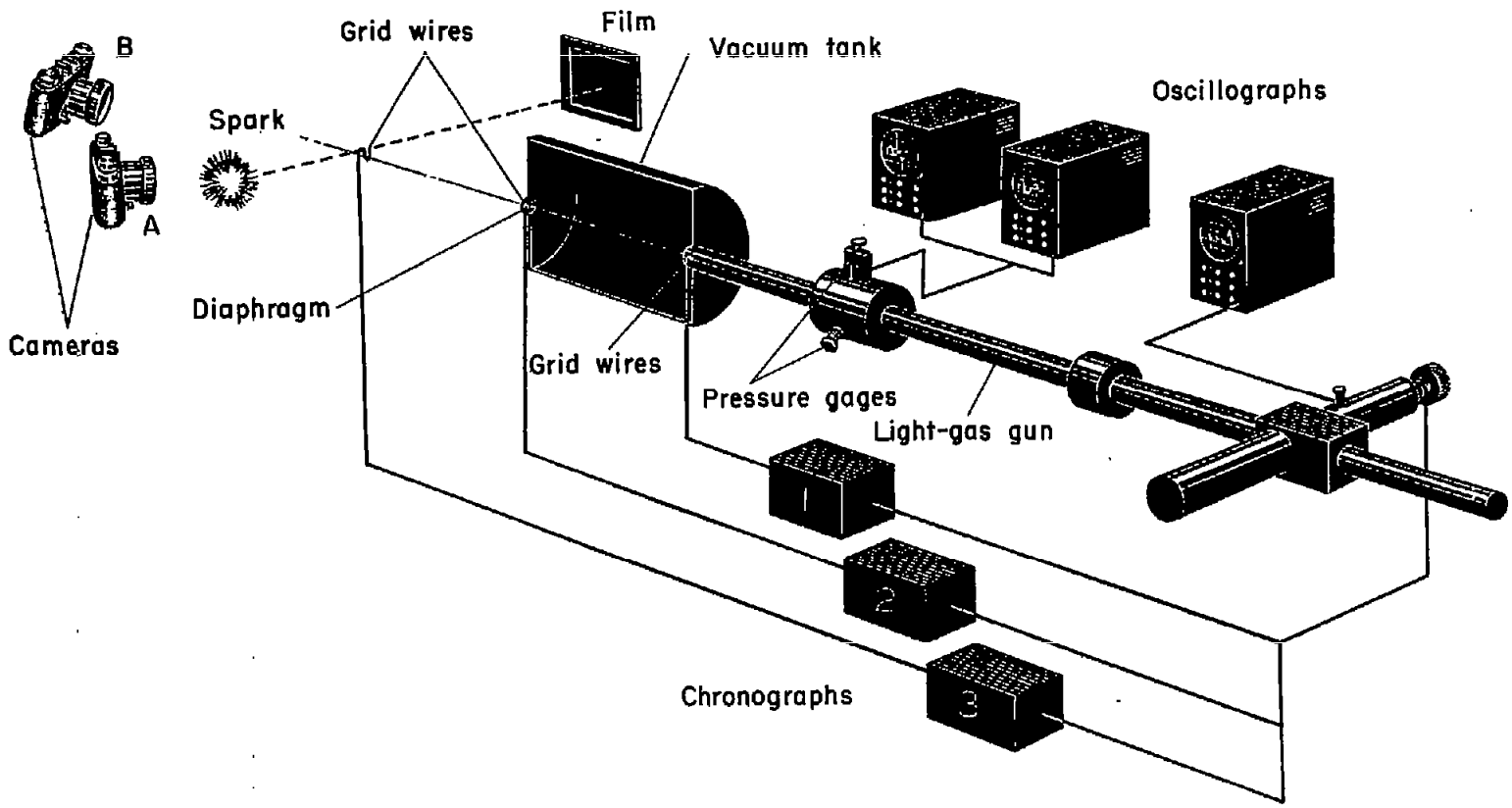

Figure 16.- Experimental setup

A-30025-7

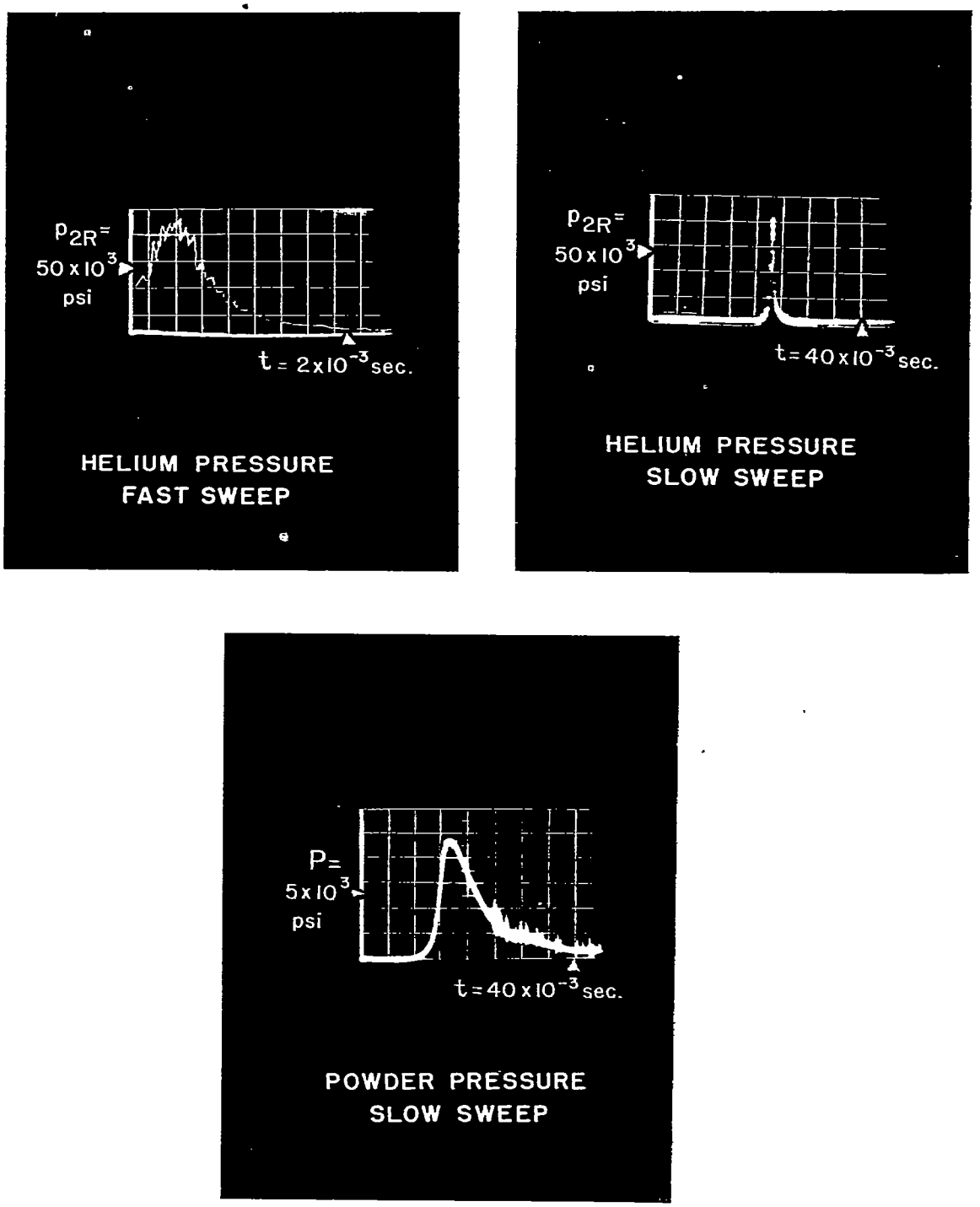

A-20375

Figure 17.– Pressure records of a typical round (round number 10).

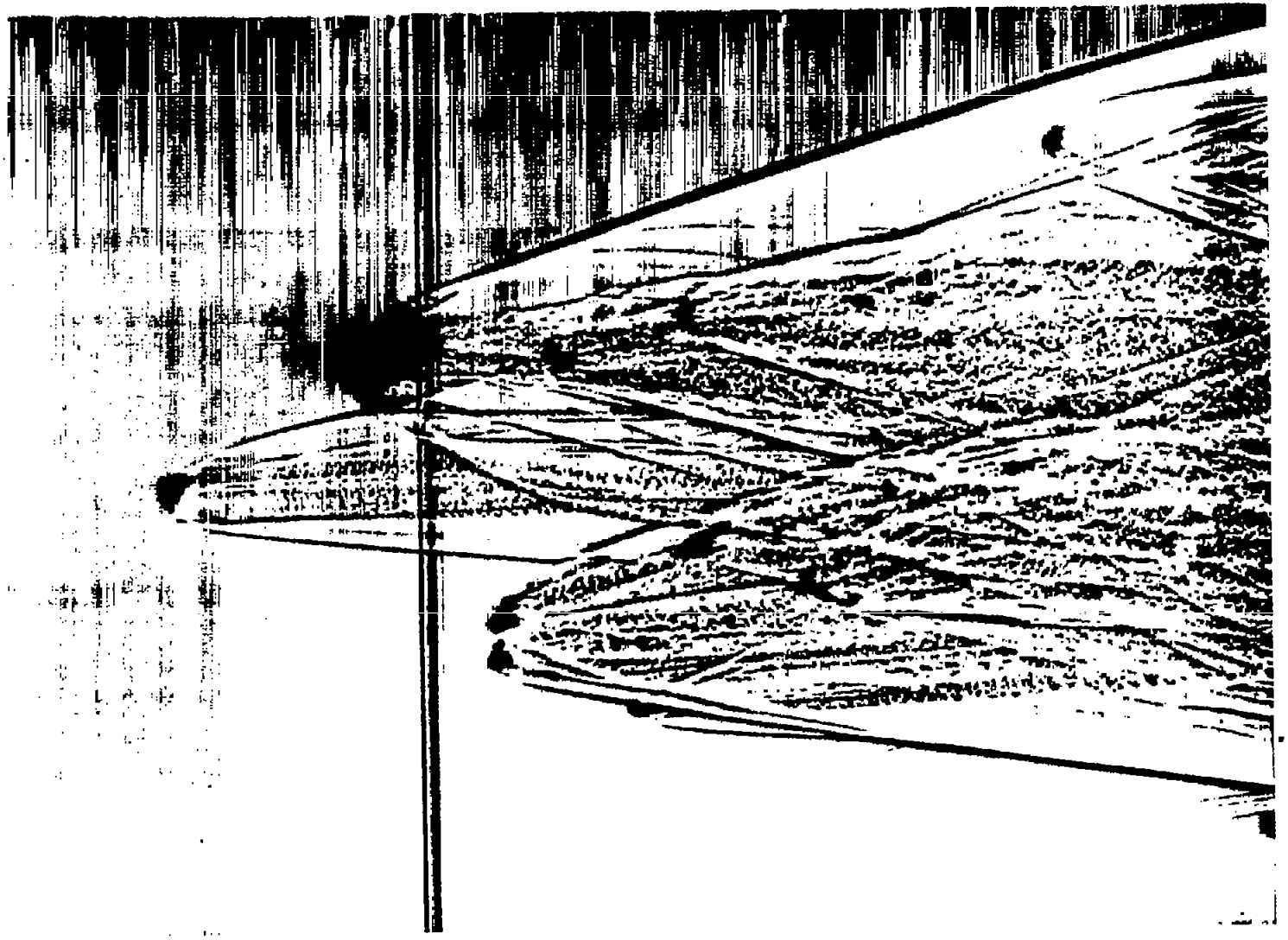

A-20361

Figure 18.- Spark photograph of round number 3.

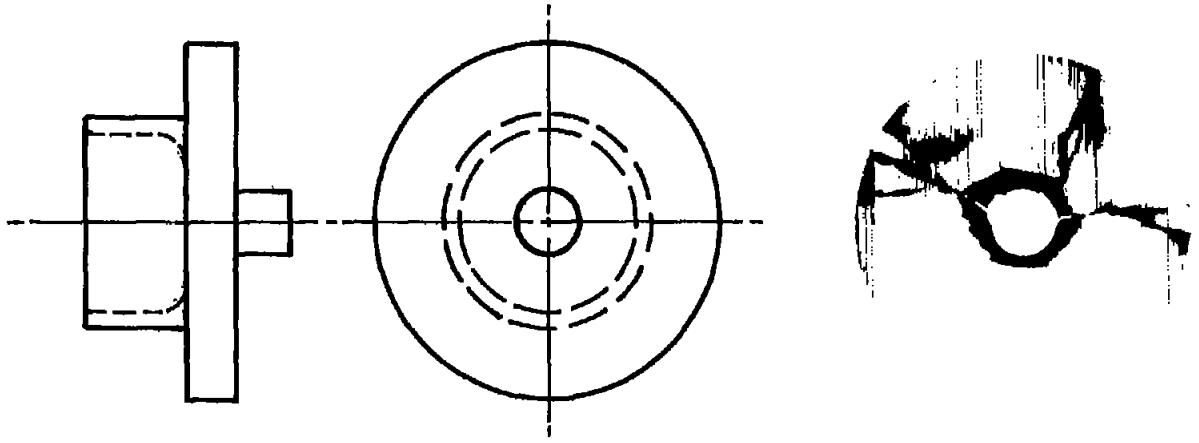

Ragged shear-disk break, round #3

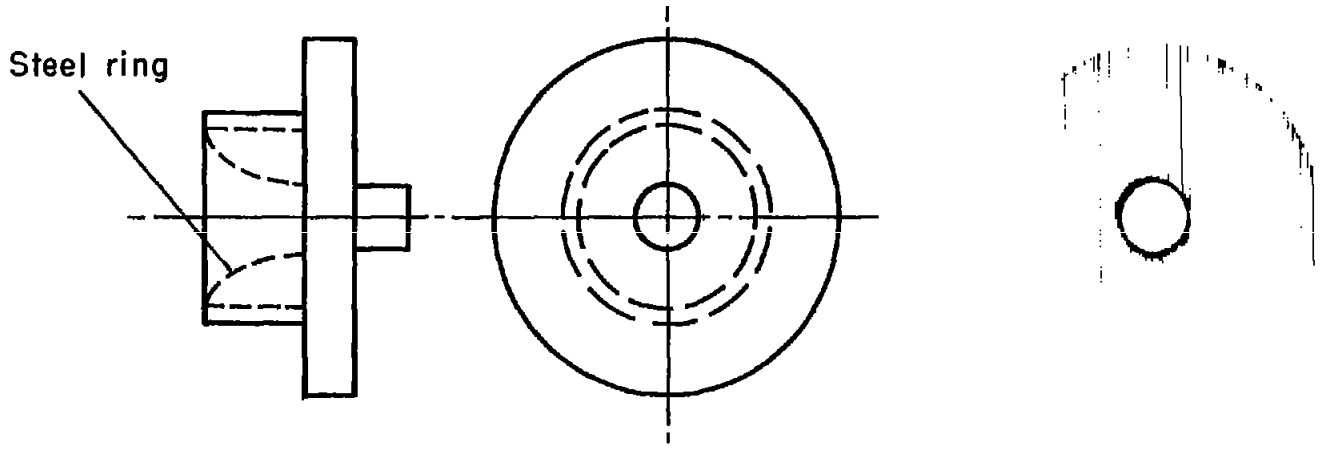

Clean shear-disk break, round #6

Figure 19.- Sketches and photographs showing development of shear disk designs.

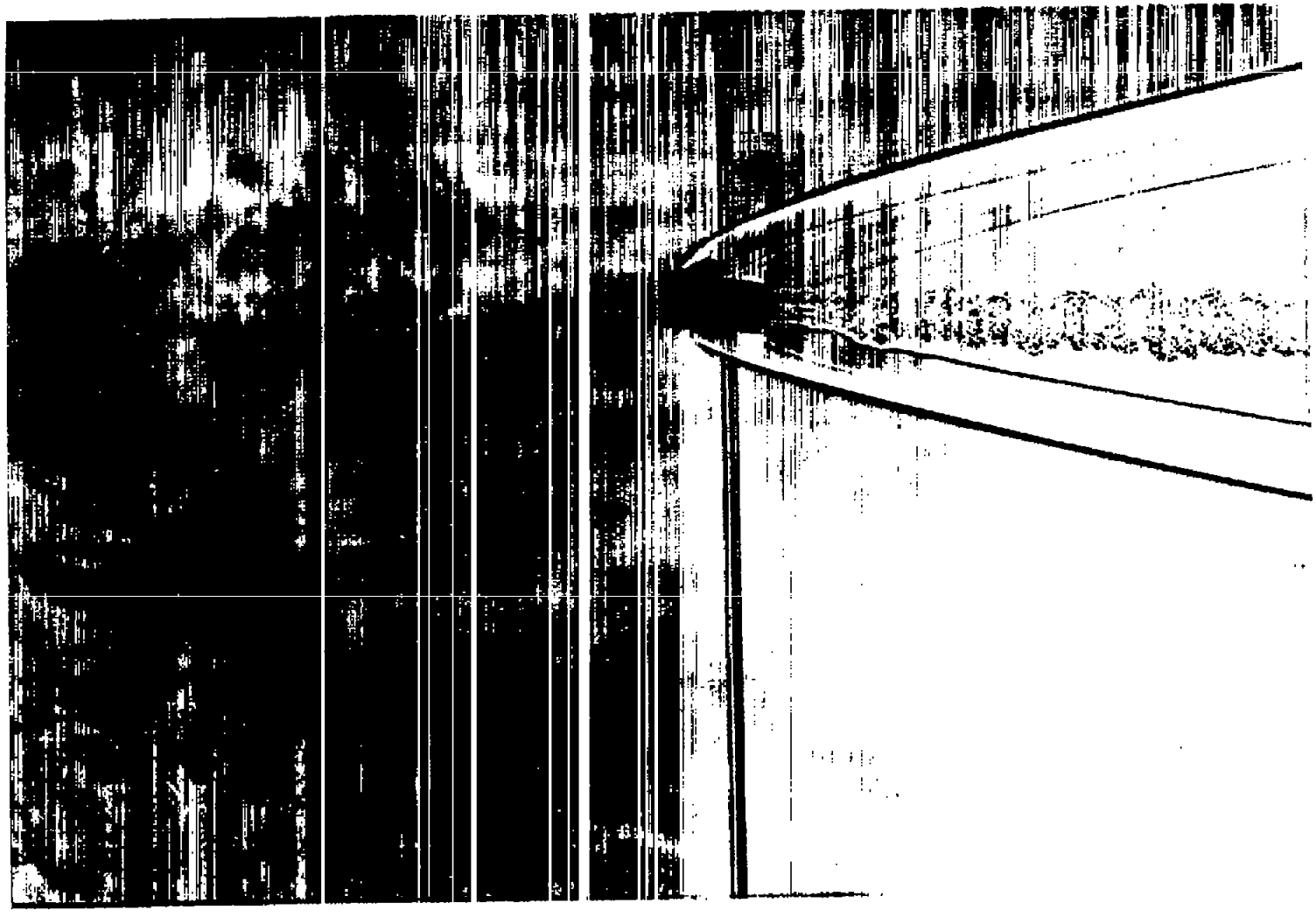

A-20362

Figure 20.- Spark photograph of round number 4.

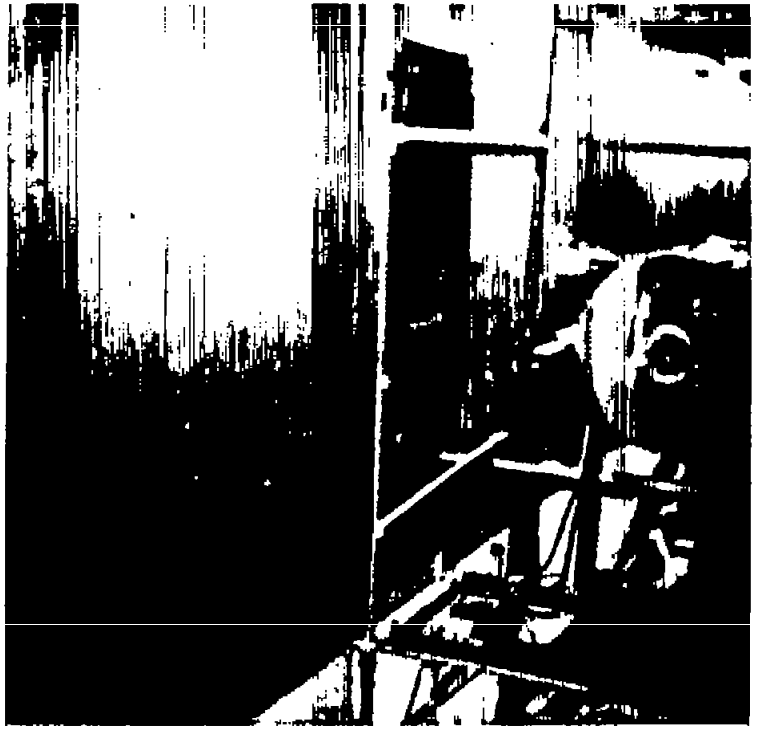

A-20370

(a) Experimental set-up before firing.

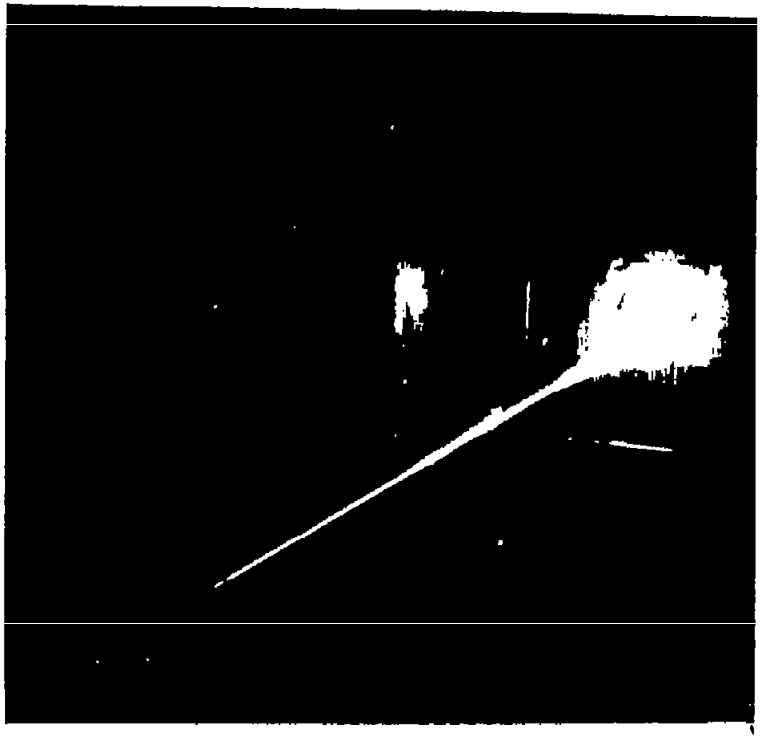

A-20371

(b) Streak photograph of projectile in flight.

Figure 21.- Streak photograph of round number 6: view from camera B. (Figure 16).

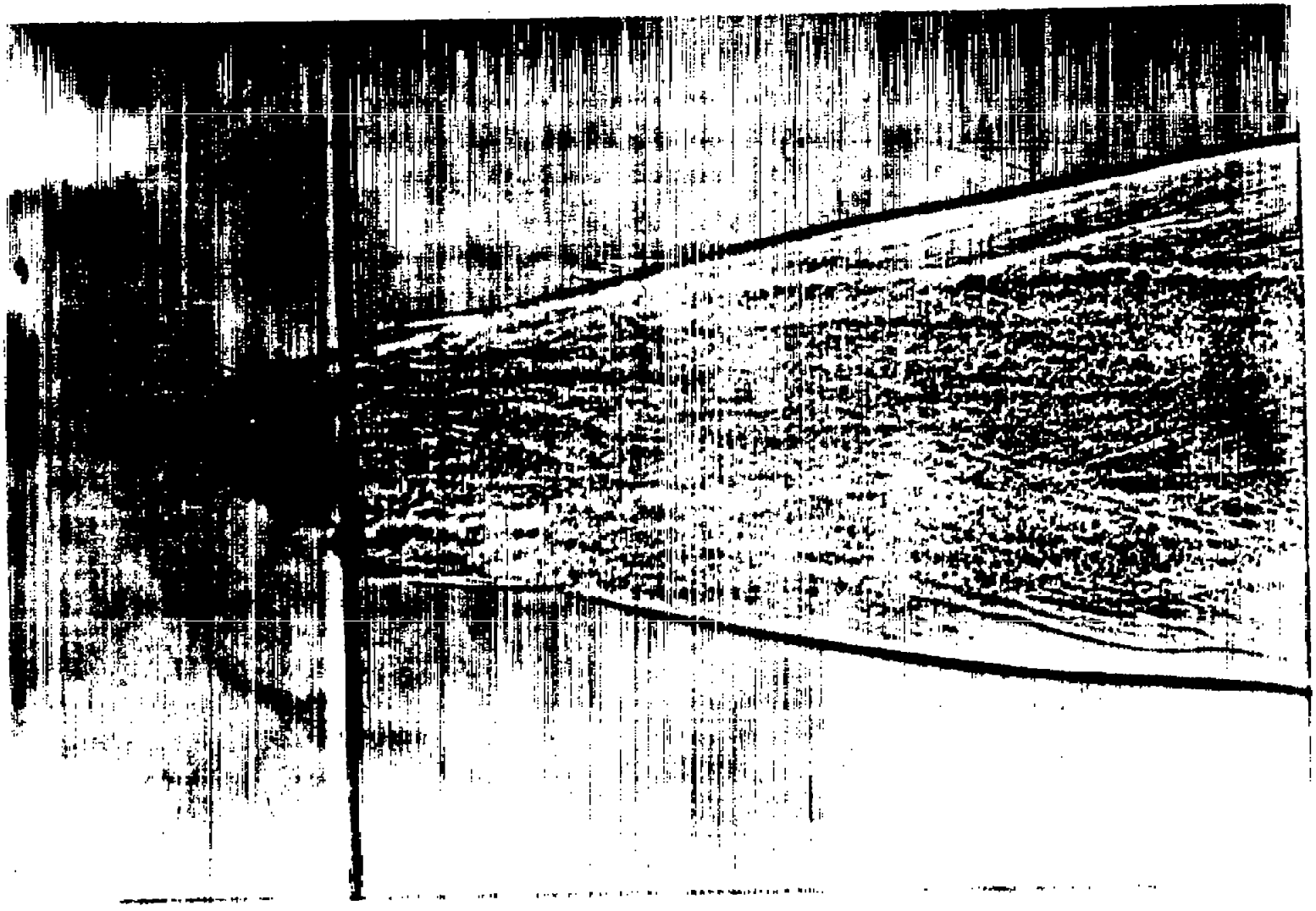

A-20363

Figure 22.– Spark photograph of round number 6.

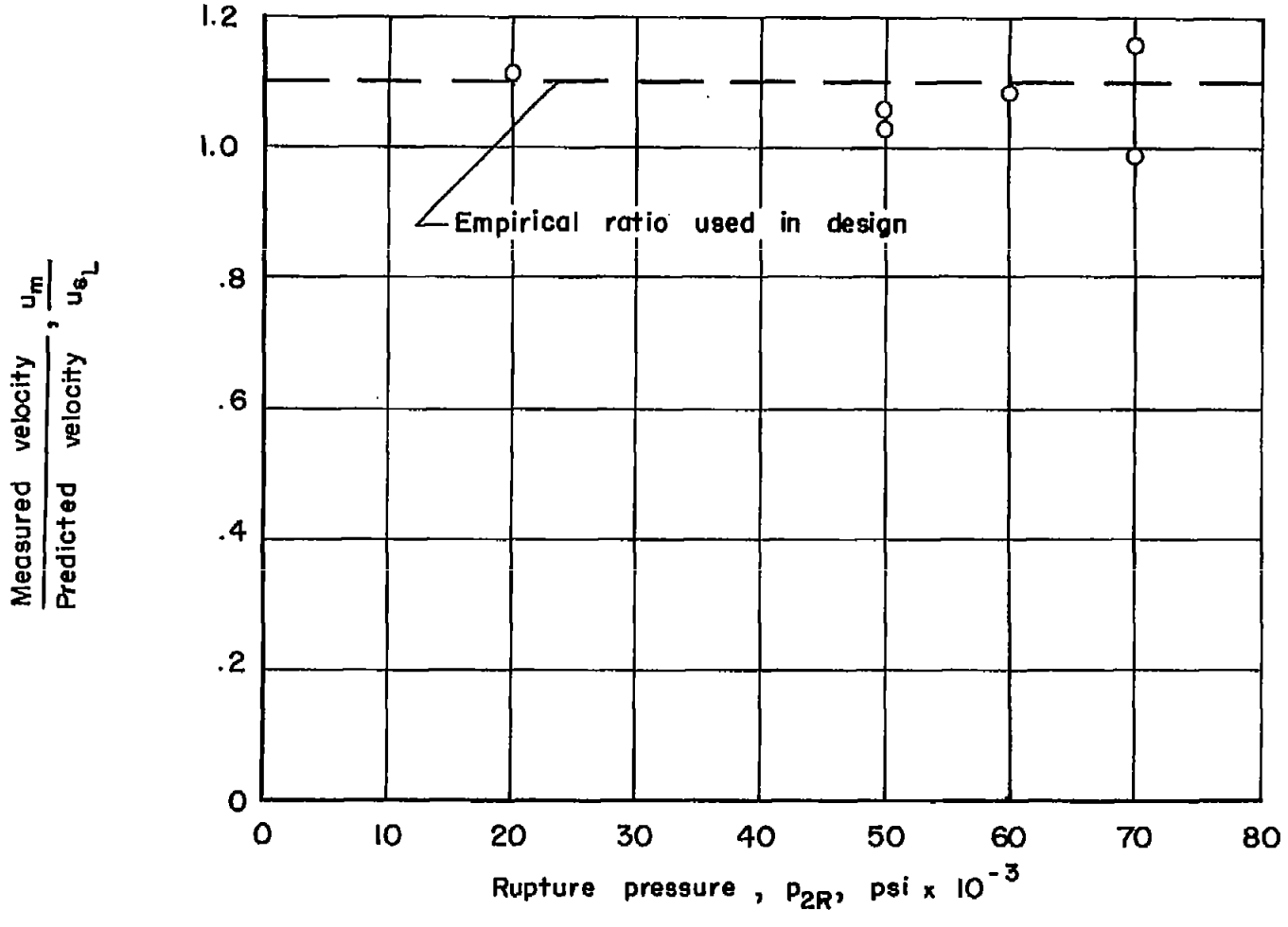

Figure 23.- Ratio of measured velocity to predicted velocity as a function of rupture pressure.

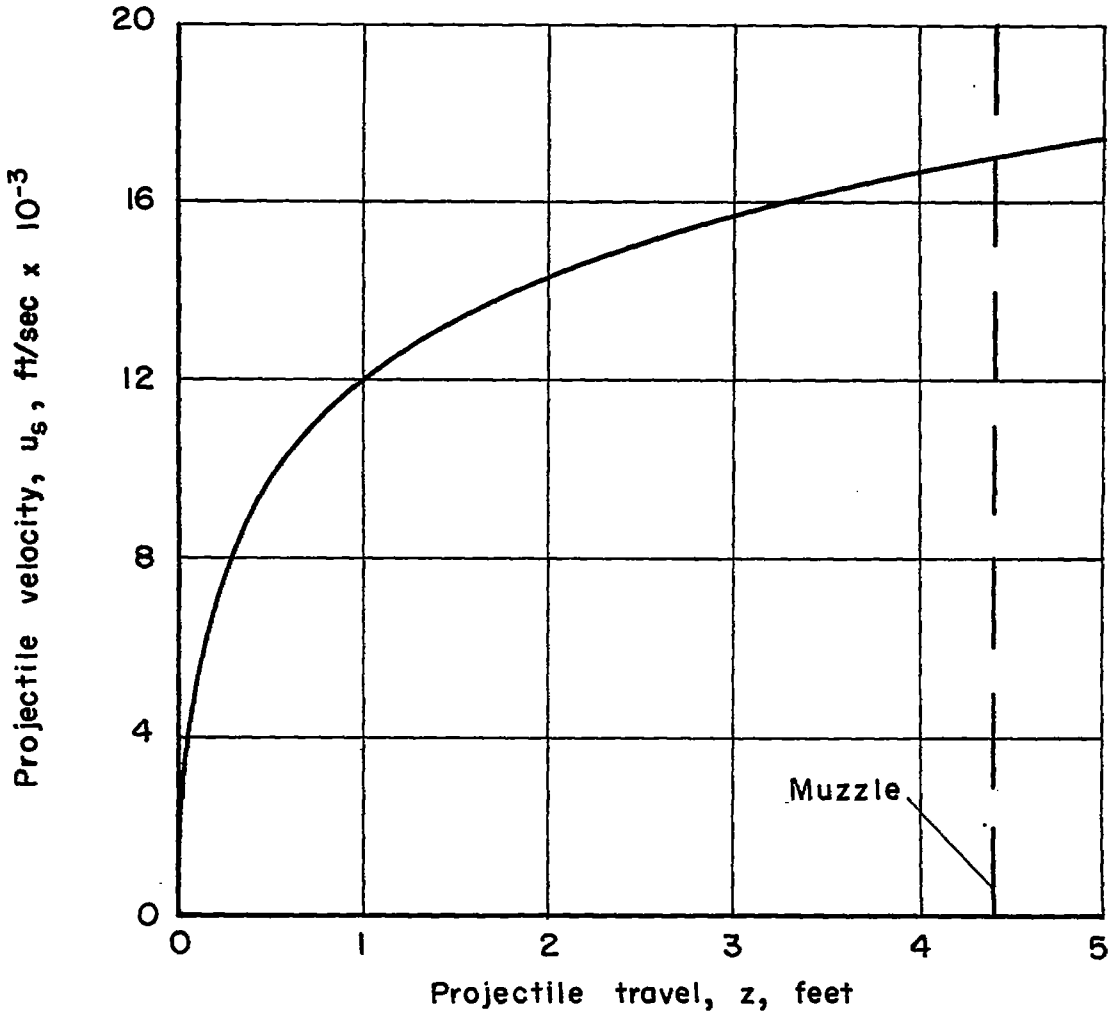

Figure 24.- Projectile velocity versus travel from method of characteristics, a_2 = 10,000 ft/sec, p_2 = 50,000 psi, m_s = 0.15 gram, γ = 5/3.

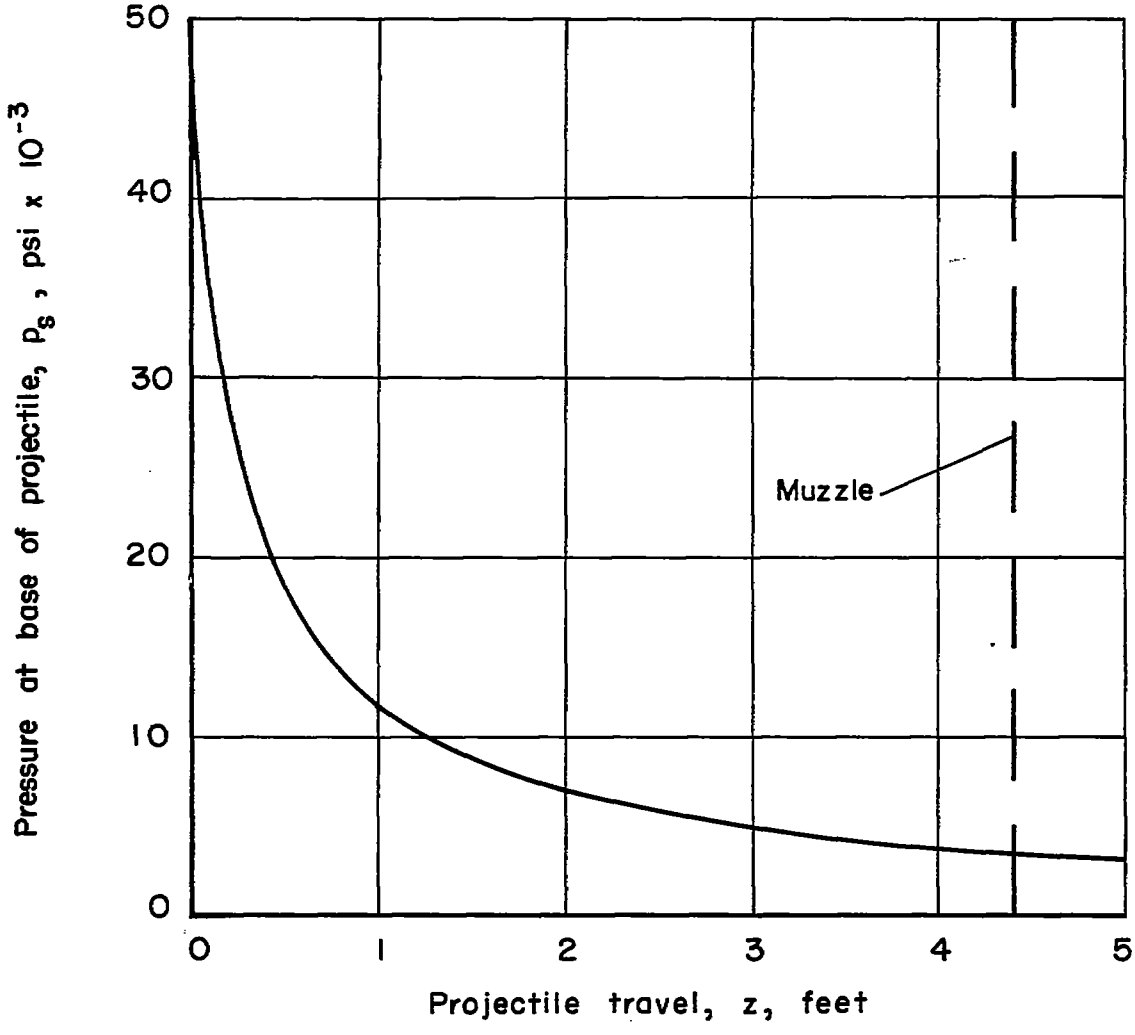

Figure 25.- Projectile base pressure versus travel from method of characteristics, a_2 = 10,000 ft/sec, p_2 = 50,000 psi, m_s = 0.15 gram, γ = 5/3.

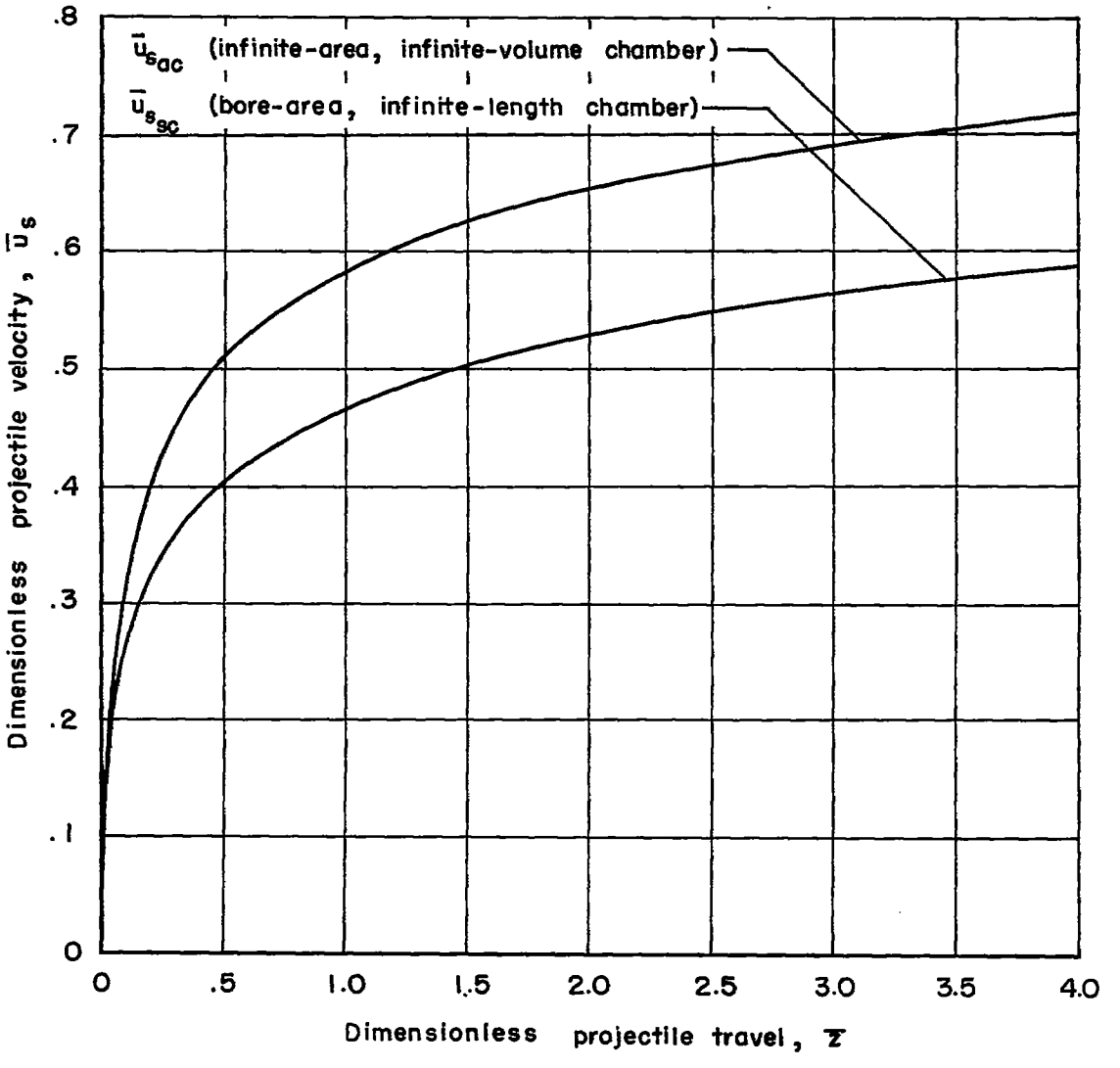

Figure 26.- Variation in velocity with distance for two conditions of chamberage.

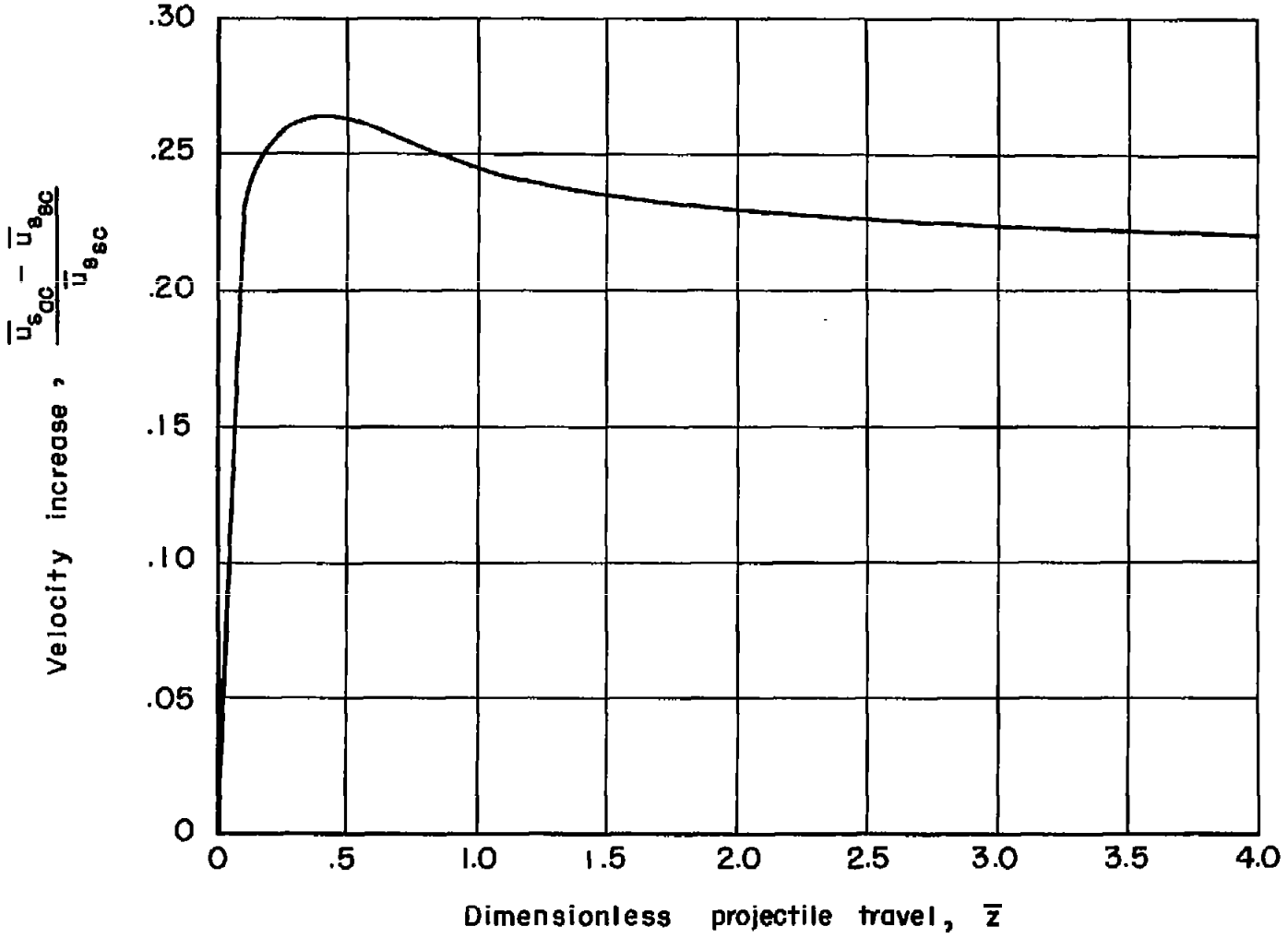

Figure 27.- Theoretical increase in velocity due to chamberage as a function of gun length.

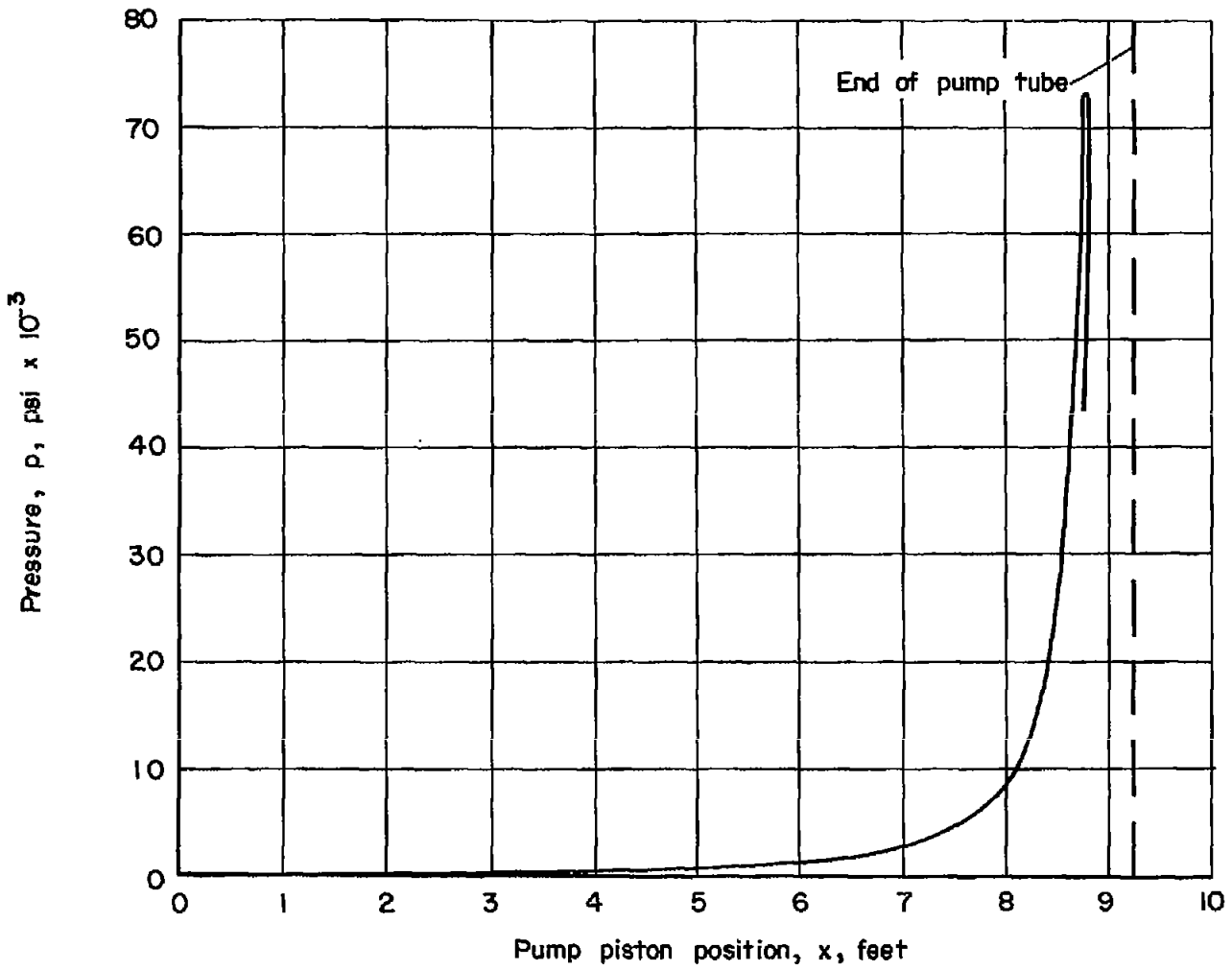

Figure 28.- Helium pressure in pump tube versus piston position from method of characteristics, $\gamma = 5/3$, $p_1 = 248$ psi, $a_1 = 3290$ ft/sec, $x_1 = 9.24$ ft, $p_{2R} = 50{,}000$ psi, $m_s = 0.15$ gram.

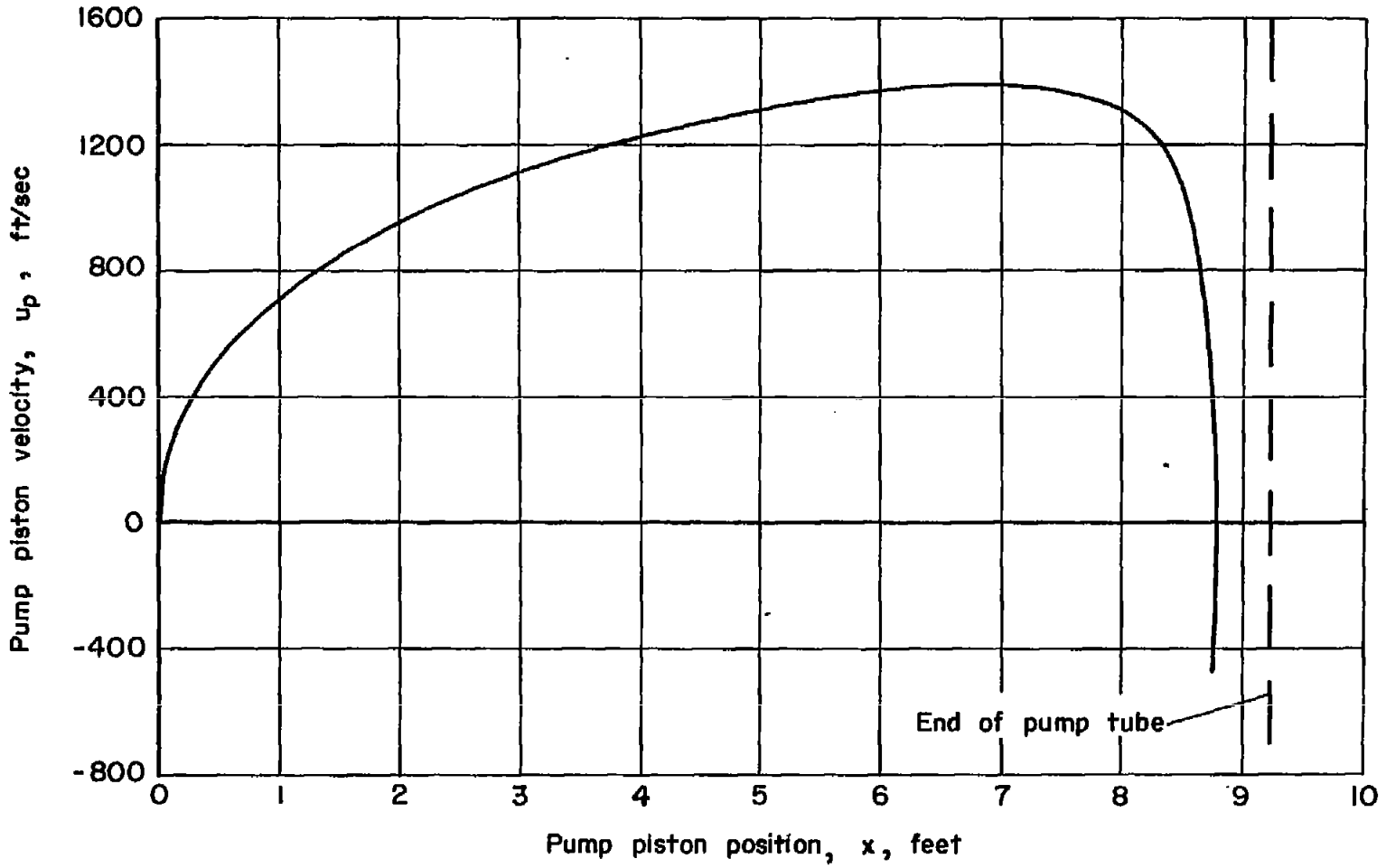

Figure 29.- Pump piston velocity versus position from method of characteristics, $\gamma = 5/3$, $p_1 = 248$ psi, $a_1 = 3290$ ft/sec, $x_1 = 9.24$ ft, $p_{2R} = 50{,}000$ psi, $m_s = 0.15$ gram.

NACA - Langley Field, Va.